Investigation of surfactant-drug pharmacokinetic interactions

L. Erasmus

orcid.org/0000-0003-2088-1979

***Baccalaureus Pharmaciae* 2015**

Dissertation submitted in partial fulfilment of the requirements for the degree *Magister Scientiae* in *Pharmaceutics* at the North-West University

Supervisor:	Dr. C. Gouws
Co-supervisor:	Dr. JD. Steyn
Assistant supervisor:	Prof. JH. Steenekamp

Graduation: May 2018

Student number: 22220429

“Fail early, fail often, but always fail forward”

- John C. Maxwell

ABSTRACT

The oral administration route is a non-invasive, cost-effective route that is associated with high patient compliance, especially among the elderly and children. Excipients are frequently added to the active ingredient to contribute to a pharmaceutical formulation that is stable, easy to formulate and has increased patient compliance. Ideally, excipients should be chemically inert. Surfactants, in particular, should not alter the permeability or transport of the active pharmaceutical ingredient. However, several studies relating to surfactant characterisation have proven that permeability of tissue could be affected by surfactants.

The aim of this study was to determine if selected surfactants had altering effects on intestinal drug permeation. For this purpose, membrane permeability of a model compound was evaluated across excised pig intestinal tissue mounted in a Sweetana-Grass diffusion apparatus.

The bidirectional transport of Rhodamine 123 (Rho123), a substrate of the P-glycoprotein (P-gp) efflux transporter with fluorescent properties, was measured in the presence of five surfactants and a bile salt, namely Brij® 58, Tween® 20, Span® 20, Cremophor® CO40 and sodium deoxycholate. The surfactants were added at three different concentrations, 0.1%, 0.5% and 1.0% (w/v), to investigate if the addition of these surfactants had any influence on the membrane permeability of Rho123 and if these effects were concentration dependent. The samples were withdrawn over a period of 120 min, from either the apical or the basolateral chambers, and fluorescence was measured with a microplate reader.

The results indicated that polyoxyl 20 cetyl ether (Brij® 58) mediated an increase in Rho123 transport in the apical to basolateral direction at concentrations of 0.5% and 1.0% (w/v), and a decrease in the basolateral to apical direction at concentrations of 0.5% and 1.0% (w/v) when compared to the Rho123 control group, indicating the inhibition of P-gp related efflux in a concentration dependent manner. Polyoxyl 40 hydrogenated castor oil (Cremophor® CO40) and Polysorbate 20 (Tween® 20) mediated no mentionable change in Rho123 transport in the apical to basolateral direction, while a decrease in the transport of the marker was seen in the basolateral to apical direction. This could indicate that P-gp related efflux was inhibited. Sorbitan monolaurate (Span® 20) mediated no effect on Rho123 transport in the apical to basolateral direction but mediated a significant decrease in the P-gp mediated efflux of Rho123. Sodium deoxycholate resulted in an increase in Rho123 transport in the apical to basolateral direction in a concentration dependent manner, and a decrease in transport in the basolateral to apical direction, in a concentration dependent manner when compared to the Rho123 control. P-gp was possibly inhibited and consequently efflux was decreased. The trans-epithelial electrical

resistance (TEER) values decreased in the presence of all the surfactants in both directions of transport, indicating that the surfactants possibly opened tight-junctions.

The results of the study confirmed that excipients, such as surfactants, can and do have altering effects on drug permeability by means of efflux inhibition and possible opening of tight junctions, which may lead to altered bioavailability of the co-administered drug.

Key words: Sweetana-Grass diffusion chambers, *in vitro*, Rhodamine 123, Brij®58, Cremophor®CO40, Tween® 20, Span® 20, Sodium deoxycholate, porcine jejunum tissue.

UITTREKSEL

Die orale toedieningsroete van geneesmiddels is ’n nie-indringende, koste-effektiewe roete wat normaalweg gekenmerk word deur ’n hoë mate van pasiëntmeewerkendheid, veral onder bejaardes en kinders. Hulpstowwe word gereeld in kombinasie met aktiewe bestanddele in farmaseutiese doseervorms ingesluit om onder andere stabiliteit en kwaliteit van die doseervorm te verseker of te verbeter. ’n Elegante doseervorm met aanvaarbare organoleptiese eienskappe word normaalweg deur pasiënte met kwaliteit geassosieer en dit lei tot beter aanvaarbaarheid en pasiëntmeewerkendheid. Tradisioneel word aanvaar dat hulpstowwe inert is maar hierdie siening is tans egter besig om drasties te verander aangesien toenemende bewyse daarop dui dat hulpstowwe wel die absorpsie van geneesmiddels kan beïnvloed. Verskeie studies wat verband hou met die karakterisering van oppervlakaktiewe stowwe het getoon dat die deurlaatbaarheid van biologiese weefsel deur oppervlakaktiewe stowwe beïnvloed word.

Die doel van hierdie studie was om vas te stel of geselekteerde surfaktante ’n invloed kan uitoefen op die omvang van geneesmiddeltransport deur dermwandweefsel. Vir hierdie doel is membraandeurlaatbaarheid van ’n modelverbinding geëvalueer oor uitgesnyde varkdermweefsel wat in ’n Sweetana-Grass diffusie-apparaat gemonteer is.

Die tweerigting-transport van Rhodamien 123 (Rho123), ’n fluoresserende substraat van die P-glikoproteïen (P-gp) effluks-transporteerder, is in die teenwoordigheid van vyf surfaktante en ’n galsout, naamlik Brij® 58, Tween® 20, Span® 20, Cremophor® CO40 en natriumdeoksiekolaat, bepaal. Die invloed van die surfaktante (galsout ingesluit) op die transport van Rho123 is by drie verskillende konsentrasies, 0.1%, 0.5% en 1.0% (m/v) ondersoek ten einde te bepaal of die effek (indien enige) konsentrasie afhanklik is. Monsters is oor ’n tydperk van 120 minute onttrek, van óf die apikale of basolaterale kamers, en die mate van fluoressensie van die monsters is met 'n mikroplaatleser gemeet.

Die resultate het getoon dat poli-oksiel-20-setieleter (Brij® 58) 'n toename in Rho123 transport in die apikale na basolaterale rigting by konsentrasies van 0.5% en 1.0% (m/v) en ’n afname in die basolaterale na apikale rigting by konsentrasies van 0.5% en 1.0% (m/v) in vergelyking met die Rho123 kontrolegroep veroorsaak het. Hierdie resultaat dui op ’n konsentrasie-afhanklike inhibisie van P-gp gemedieërde effluks. Poli-oksiel-40-gehidrogeneerde risinusolie (Cremophor® CO40) en Polisorbaat 20 (Tween® 20) het geen beduidende effek op die transport van Rho123 in die apikale na basolaterale rigting getoon nie, terwyl ’n afname in Rho123 transport in die basolaterale na apikale rigting waargeneem is. Dit dui op ’n moontlike inhibisie van P-gp gemedieërde effluks. Sorbitaanmonolauraat (Span® 20) het geen betekenisvolle effek op Rho123 transport in die apikale na basolaterale rigting gehad nie, maar het ’n beduidende afname in die

P-gp gemedieërde effluks van Rho123 veroorsaak. Natriumdeoksikolaat het ’n toename in Rho123 transport in die apikale na basolaterale rigting op ’n konsentrasie afhanklike wyse tot gevolg gehad, en in die basolaterale na apikale rigting is ’n konsentrasie afhanklike afname in Rho123 transport waargeneem wanneer dit vergelyk word met die Rho123 kontrolegroep. P-gp is moontlik geïnhibeer en effluks is gevolglik onderdruk. Die trans-epiteliale elektriese weerstand (TEEW) waardes het verlaag in die teenwoordigheid van al die surfaktante in albei transportrigtings, wat aandui dat die surfaktante moontlik intersellulêre-aansluitings oopgemaak het.

Die resultate van die studie het bevestig dat hulpstowwe, soos surfaktante, ’n invloed kan uitoefen op geneesmiddeldeurlaatbaarheid deur middel van effluksonderdrukking en moontlike opening van intersellulêre-aansluitings, wat kan lei tot ’n veranderde biobeskikbaarheid van die toegediende geneesmiddel.

Sleutelterme: Sweetana-Grass diffusie apparaat, *in vitro*, Rhodamien 123, Brij® 58, Cremophor® CO40, Tween® 20, Span® 20, Natriumdeoksikolaat, vark jejunum-weefsel.

ACKNOWLEDGEMENTS

"Commit everything you do to the Lord. Trust Him and He will help you" Psalm 37:5. First and foremost, I would like to thank God for blessing me in abundance and for giving me the opportunities in life that many can only dream of. All honour and glory be to God.

I would like to dedicate this dissertation to my grandmother *Eleonore du Plessis,* whom is unfortunately not here in person to celebrate this venture with me. I know that you are with me in heart and soul and that you are rejoicing. I miss you every day and I can only hope to be half the woman, mother, grandmother and wife that you were. You knew what was best for me, even when I did not know it yet. And you were right, I love being a pharmacist and I would like to thank you for sharing your 100s of stories of the pharmacy that inspired my career.

A big thank you to my parents, *Pieter and Leonie Erasmus*, for giving me the opportunity to further my studies. Thank you for the unconditional love, courage and support, and for always standing behind me with all the decisions I make. I can say that I am truly blessed to have you as my parents. *Mami,* thank you for always making time for me and for setting the best example of what it means to be a strong woman of God.

To my future husband, *Barry Smit*, thank you for the support, the love and the motivation. Thank you for giving me hope when it felt like there was none. I am privileged to have you in my life and I thank God for blessing me with the absolute best. You are my pillar of strength and I am excited to spend the rest of my life with you.

To my brother and sisters, *Louis Wolmarans*, *Angelique Wolmarans, and Melissa Erasmus*, thank you for always being there for me, for all the love, support and encouragement. Thank you for the example of hard work and determination that you have laid out for me.

Thank you to my mother-in-law *Mariana Hartslief*, and my sister-in-law *Annique Jordaan* for all the love and support. The motivational talks and thank you for pushing me to be the best version of myself! I am blessed to have you part of my family.

Dr. Chrisna Gouws, Dr. Dewald Steyn and Prof. Jan Steenekamp, my supervisor and co- supervisors, thank you for always being willing to assist me with so much knowledge and insight. Thank you for taking up this project and granting me the opportunity to expand my horizons. I am privileged to have learned from you. Thank you for the infinite patience and willingness to help. This is one of the greatest ventures I have done thus far in my life and I am thankful that you were there to guide me through it.

To my friends, *Wynand du Preez, Emsie Snydert- Lampbrechts, Rochelle Redelinghuys and Maruschka Redelinghuys*, *Aliana Duvenhage* and *Christelle Kemp* thank you for the help and support. Thank you for the motivational talks, it was not always an easy journey for but you made it better. I wish each of you a bright future ahead.

To *Prof. Sias Hamman*, thank you for the help with finalising the details of the project. Thank you for always being available to help or assist in whichever way possible.

Thank you to *Potch Abatoir*, and all the staff members for assisting in the collection of the porcine intestine and for always greeting me with kindness.

Thank you to *Dr. Suria Ellis* for the statistical analysis of my data and helping me with this section.

There are many that I have not mentioned, thank you to everyone who shared a cup of coffee or a kind word of encouragement, I can't thank you enough for the support.

TABLE OF CONTENTS

LIST OF ABBREVIATIONS

3R's	Replace, reduce, refine
ABC	ATP-binding cassettes
ADME	Absorption, distribution, metabolism, excretion
AP-BL	Apical to basolateral
ATP	Adenosine tri-phosphate
BBB	Blood brain barrier
BCRP	Breast cancer-resistant protein
BL-AP	Basolateral to apical
Caco-2	Human colorectal adenocarcinoma cells
Cl	Clearance
Cl_H	Hepatic clearance
Cl_R	Renal clearance
Cl_T	Total clearance
CMC	Critical micelle concentration
CO_2	Carbon dioxide
CRM CO40	Cremophor®CO40
CYP3A	Cytochrome P450 3A
e.g.	*Exempli gratia* (for example)
E_m	Emission wavelength
ER	Efflux ratio
E_x	Excitation wavelength
F	Bioavailability
GIT	Gastrointestinal Tract
HCO	Hydrogenated castor oil
HLB	Hydrophilic-lipophilic balance
HPLC	High-performance liquid chromatography
KRB	Krebs-Ringer bicarbonate

LOD	Limit of detection
LOQ	Limit of quantification
LY	Lucifer yellow
MDCK	Madin-Darby canine kidney
m/v	mass per volume (g/100 ml)
Na^+	Sodium
NaDC	Sodium deoxycholate
O_2	Oxygen
O/W	Oil in water
P_{app}	Apparent permeability coefficient
P-gp	P-glycoprotein
r^2	Regression coefficient
REC	Recovery
Rho123	Rhodamine 123
RSD	Relative standard deviation
S	Regression line slope
SD	Standard deviation
$t_{1/2}$	Elimination half life
TEER	Trans-epithelial electrical resistance
TEEW	Transepiteliale elektriese weerstand
V_D	Volume of distribution
W/O	Water in oil

LIST OF TABLES

LIST OF FIGURES

CHAPTER 1

INTRODUCTION

1.1 Background

The oral route of administration is one of the most popular, if not the most popular route of drug administration since it provides high patient compliance and convenience. Before a drug can become bioavailable after oral administration, it must be absorbed across the intestinal epithelia and into the blood circulation. Situated primarily in the apical membrane, P-glycoprotein (P-gp) has an important role of clearing the lipid bilayer of the membrane by means of a drug efflux pump and thereby limiting the absorption of lipophilic drugs and foreign molecules. Therefore, for drugs to be transported across the intestinal epithelia by means of the transcellular route, the drug should have certain physicochemical properties to overcome the obstacles of drug absorption across the intestinal barriers.

Excipients are substances which are included in pharmaceutical formulations in addition to active ingredients, to aid in the manufacturing of a medicinal product with suitable weight, volume, consistency and drug release characteristics. Traditionally, excipients were claimed to be pharmacologically inert but various studies have reported that the addition of some excipients to pharmaceutical formulations may alter the pharmacokinetics of the active ingredients (Pifferi *et al*., 1999:1; Garcia-Arieta, 2014: 89-97). Furthermore, excipients may also have physical and/or chemical interactions with the active ingredients. These interactions can modify the rate of dissolution or the uniformity of the dosage form. On the other hand, some materials can adsorb drug particles on their surfaces, which will increase the active surface area and improve rate of dissolution and wettability (Pifferi & Restani, 2003:541). Absorption enhancing excipients can improve the permeation of therapeutic agents either across the apical cell membrane or by altering the tight junctions between cells (Lee & Yamamoto, 1990:171-207; Aungst, 2012:10-18). These mechanisms used to alter the permeation of therapeutic agents may include altering the mucus rheology, a change in fluidity of the cell membrane, proteins leaking through the membrane and increasing paracellular transport through the opening of tight junctions. Surfactants may also affect P-gp function and therefore influence drug absorption (Hamman *et al*., 2005:165-171; Mahato *et al*., 2003:153-214).

The inclusion of surfactants into dosage forms may promote drug permeability across biological barriers, which in turn may improve drug bioavailability and treatment efficacy (Junginger & Verhoef, 1998:370). The permeability altering effects of the selected surfactants should be investigated by employing a suitable *in vitro* method, which is cost and time effective and with as few ethical considerations as possible (Le Ferrec *et al*., 2001:649-668).

Various *in vitro* models were assessed, and the Sweetana-Grass diffusion chambers were chosen for bidirectional transport studies. Porcine intestinal tissue, a by-product of meat production, was chosen since it complies with the 3R's principle of more ethical research.

1.1.1 Rhodamine 123 as model compound

Rhodamine 123 (Rho123) (Figure 1.1) is a cationic, lipophilic, fluorescent dye with a molecular weight of 380.82 g/mol, and a melting point of 235˚C (Al-Mohizea *et al.,* 2015:618). Being a P-gp substrate, Rho123 has been used as a selective marker for studying the activity of P-gp and to assess P-gp related drug interactions (Pavek *et al*. 2003:1239). This xanthene derivate has become an ideal compound to use as a P-gp substrate, seeing that it is not a substrate for Cytochrome P450 3A (CYP3A), a metabolizing enzyme, which may influence the investigation into P-gp mediated reactions (Al-Mohizea *et al.,* 2015:618). Due to its fluorescent activity, dye levels can easily be detected in cell extracts and accumulation can be seen in intact cells, such as tumour cells. Rho123 accumulation in, or efflux from, cells is often used as a measure of P-gp transport activity (Pavek *et al*., 2003:1239-1250). First introduced in 1988 by Neyfakh (1988:168), Rho123 was used in mitochondrial studies to investigate multidrug resistance. Neyfakh proved that Rho123 was a definite substrate for P-gp, and it has since been used by various investigators as a probe for investigating P-gp functional activity (Zhao *et al*., 2016:1526-1534).

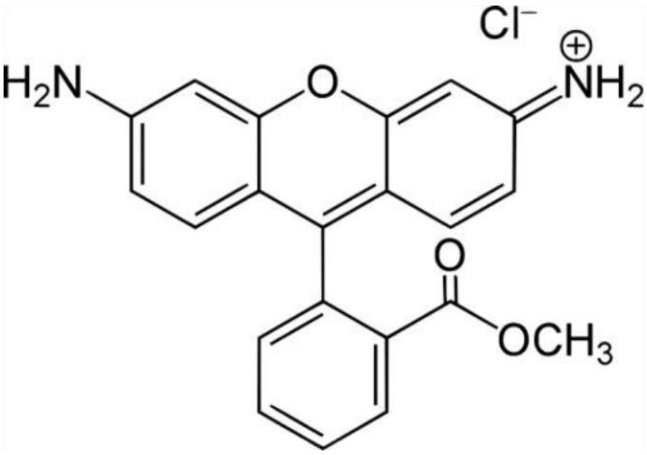

Figure 1.1: Chemical structure of Rhodamine 123

1.1.2 Models for evaluating drug absorption

Permeability studies can be performed using various models to evaluate drug transport. The most commonly used models are *in vitro* models which include cell cultures (e.g. human colon adenocarcinoma cells (Caco-2) and Madin-Darby canine kidney (MDCK) cell lines), *ex vivo* models (e.g. excised animal intestinal tissues in Sweetana-Grass diffusion chambers) and *in situ* perfusion models (e.g. segments of intestine as part of live animals). The use of *in vitro* / *ex vivo* models has recently become more popular due to the exclusion of the use of live animals. These models therefore comply with the 3R's concept (Alqahtani *et al.*, 2013:1-14). The 3R's concept has been introduced to limit research on animal models due to ethical issues. The first R refers to "Replace", where live animals should be substituted with other alternatives such as *in vitro* models. The second R refers to "Reduce" in the sense that more suitable methods should be considered where fewer animals are used. The third R represents "Refinement", which refers to development of techniques to reduce the pain animals feel and distress they experience during experimentation (Zurlo *et al*., 1996:878, Törnqvist *et al*., 2014:1).

In vitro permeation studies are routinely performed to evaluate drug permeation across biological membranes. This approach is relatively cost and time effective and can be used to screen new drug entities to ensure that they have favourable pharmacokinetic properties before costly clinical trials are performed (Panchagnula & Thomas, 2000:132). The excised tissue approach will be used in this study (i.e. excised porcine jejunum tissues in the Sweetana-Grass diffusion chamber

apparatus) to evaluate the influence of selected pharmaceutical surfactants on the membrane permeation characteristics of Rho123.

1.2 Research problem

Traditionally excipients were considered to be inert, however, recent research indicates that excipients (such as surfactants) are not inert and may have permeation altering effects on drugs. It is therefore evident that the extent to which some commonly used surfactants may alter the pharmacokinetics of the active ingredients in pharmaceutical formulations necessitates investigation.

1.3 Aims and objectives

1.3.1 General aim and objective

The aim of this study was to determine if selected surfactants had altering effects on intestinal drug permeation. For this purpose, membrane permeability of a model compound was evaluated across excised pig intestinal tissues mounted in a Sweetana-Grass diffusion apparatus

1.3.2 Specific aims and objectives

- To select surfactants that represents the different types of surfactants with different Hydrophilic-lipophilic balance (HLB) values.
- To conduct bidirectional transport studies with the model compound in the presence and absence of selected surfactants (at different concentrations) across excised porcine intestinal tissue.
- To conduct trans-epithelial electrical resistance (TEER) measurements in the presence and absence of selected surfactants across excised porcine intestinal tissue.
- To calculate % TEER reduction, apparent permeability coefficient (P_{app}) and efflux ratio (ER) values.
- To modify and validate a published fluorescence method for analysis of the model compound by microplate reader.

1.4 Ethical considerations

In this study, porcine intestinal tissue was collected from a local abattoir where pigs were slaughtered solely for meat production purposes. Animals were not sacrificed for the purpose of this study; therefore, it complied with the 3R's principle. The only aspects that required ethical consideration were the site of tissue collection (it should be an authorised abattoir that applies disease control) and proper disposal of animal tissue after the transport studies had been conducted. All the tissue samples were disposed of according to guidelines applicable to bio-hazardous waste disposal. An ethics application for the use of excised porcine intestinal tissue was submitted to the Ethics committee (AnimCare) of the North-West University, which was approved (NWU00025-15-A), as indicated in Addendum A.

1.5 Structure of dissertation

The structure of this dissertation consists of an introduction (Chapter 1), which provides general aims and objectives along with the motivation and rationale for the study. A literature review is presented in Chapter 2, giving more insight into the study. Chapter 3 describes methods and materials used, along with the validation of the analytical method. Results and statistical analysis will be presented and discussed in Chapter 4, followed by concluding remarks and future recommendations in Chapter 5.

CHAPTER 2

A LITERATURE REVIEW ON INTESTINAL DRUG ABSORPTION AND SURFACTANTS

The oral route is considered as the most convenient for drug administration as it is associated with the best patient compliance. This route is non-invasive, easy to use and less painful, and most drugs are well absorbed from the gastrointestinal tract (GIT) (Pelkonen *et al.,* 2001:621; Chan *et al*., 2004:27). A drug must be absorbed from the GIT and into the systemic circulation while remaining intact (no significant first-pass metabolism) in order to be considered bioavailable and therapeutically active (Pang, 2003:1507). The most common factors which influence drug absorption after oral administration include the physicochemical properties of the compound and the physiological attributes of the GIT at the region of absorption (DeSesso *et al*., 2001:210). The main site of absorption of any ingested compound is the small intestine, and permeation efficiency across the intestinal membrane is one of the most important factors which govern oral drug absorption (Balimane *et al.,* 2000:301, Chan *et al*., 2004:27). Permeation is a two-way process which is comprised of absorption (from the lumen into the bloodstream), and efflux (active transport of the absorbed compound back into the lumen).

2.1 Anatomy and physiology of the gastrointestinal tract

The GIT is located in the abdominal region of the body and is responsible for primary bodily functions including secretion, absorption and elimination (Balimane *et al*., 2000:302). All needed nutrients and vitamins, excluding oxygen, should be taken in orally, and then be digested by the GIT prior to absorption into the bloodstream. An important function of the GIT is to serve as an effective barrier against ingested toxins and bacteria from the intestinal lumen (Nunes *et al*., 2015:203). The body's natural defence mechanism to get rid of unwanted substances that manage to infiltrate the GIT is vomiting and diarrhoea and is often the result of poisoning and irritation caused by unwanted bacteria in the stomach and small intestine. The organs responsible for aiding in digestion by secreting hormones and bile salts are the liver, gallbladder and pancreas.

The small intestine, consisting of the duodenum, jejunum and ileum, is responsible for most of the absorptive function of the GIT and makes up 60% of the GIT (Mayershon, 2009:23). Approximately 90% of drug absorption takes place in the small intestine with the remaining 10% being absorbed by the large intestine (Balimane *et al*., 2000:301; Renukuntla *et al*., 2013:75-93). Without taking into consideration the 1-2 L fluid ingested with food or as water daily, the GIT and associated organs secrete up to 8 L of fluid daily of which only 100 ml – 200 ml is lost as water in stool. This indicates that there is very efficient absorption of water throughout the GIT (Mayershon, 2009:23). The entire GIT consists of four consecutive layers; from the luminal surface these are the mucosa, submucosa, muscularis mucosa and the serosa. The outer three layers are similar throughout the entire GIT, whereas the mucosa has structural and functional differences in the various areas of the GIT (Rozehnal *et al*., 2012:367-373).

2.1.1 Comparison of the gastrointestinal anatomy and physiology of humans and pigs

The digestive system and related processes of pigs are very similar to that of humans due to their extensive omnivorous nature, making the pig a superior model for intestinal drug absorption studies compared to other non-primate models (Patterson *et al*., 2008:651; Westerhout *et al*., 2014:176) This comparison is illustrated in Figure 2.1.

Despite the noticeable differences in intestinal length and structural layout, there are microscopic similarities between the intestinal villi and epithelial cell type. The metabolic processes and digestive transit times of humans are similar to those of pigs, making the pig an ideal model to investigate influences on drug absorption and bioavailability in humans (Patterson *et al*., 2008:651).

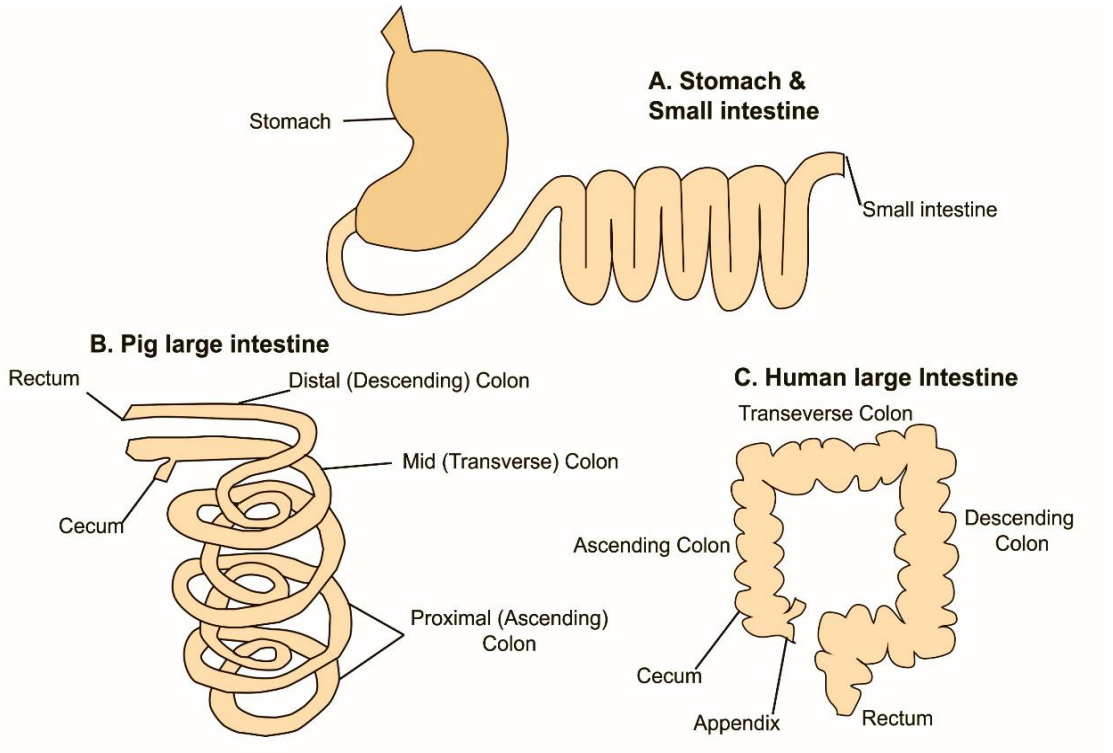

Figure 2.1: Illustration of the structure of (A) human and pig stomach and small intestine which have the same structure, compared to (B) pig large intestine and (C) human large intestine which differs in structure (adapted from Patterson *et al*., 2008:653)

2.1.1.1 Stomach

After oral ingestion, materials encounter the stomach, which main function is to store and mix food, and secrete digestive fluids to reduce the components into a lubricated mass that can be emptied in a controlled manner into the upper small intestine (Mayershon, 2009:23). The stomach consists of three parts: *fundus*, *antrum* and body, which has no significant anatomical differences except for the fundus and the body that secretes acid and is responsible for storing components while the *antrum* secretes gastrin and is mostly responsible for mixing the components (Dos Santos *et al*., 2015:41; Sjögren *et al*., 2014:104). Lining the mucosal surface of the stomach is an epithelial layer consisting of columnar cells that secretes mucus which forms a layer of approximately 1 – 1.5 cm thick. The main function of this mucus layer is to protect the stomach from enzymes, pathogens and ulceration from acid (DeSesso *et al*., 2001:210).

The stomach of a pig is similar to that of a human with the exception for a muscular outpouching with no significant function near the pyloric region of the stomach and it is called the *torus pyloricus* (Patterson *et al*., 2008:651).

2.1.1.2 Small intestine

The main difference between the GIT of humans and pigs is the length and layout of the small and large intestines. The small intestine of humans is 5.5 m – 7 m in comparison to the much longer pig small intestine, with an average length of 15 m – 22 m (Patterson *et al*., 2008:653). The small intestine consists of a lumen with convulsed mucosa to enhance the surface area available for absorption and digestive functions, these folds are known as the folds of Kerckring as seen in Figure 2.2. Finger-like projections line the intestinal epithelial, known as villi, ranging from a length of 0.5 mm - 1.5 mm and reaching a density of approximately 10 to 40 villi/mm^2 (DeSesso *et al*., 2001:217). Microvilli projects from the villi to further enlarge the absorption surface area, up to 600 microvilli per villi. The villi in the intestinal epithelia can enhance the absorption surface area by a factor of three and the microvilli by a factor of ten (Mayershon, 2009:26). Although present in both humans and pigs, the different regions of the duodenum, jejunum and ileum are not as prominently defined in humans as it is in pigs. In humans, the small intestine is situated behind the large intestine, in comparison to pigs where the small intestine is situated slightly to the right of the abdomen.

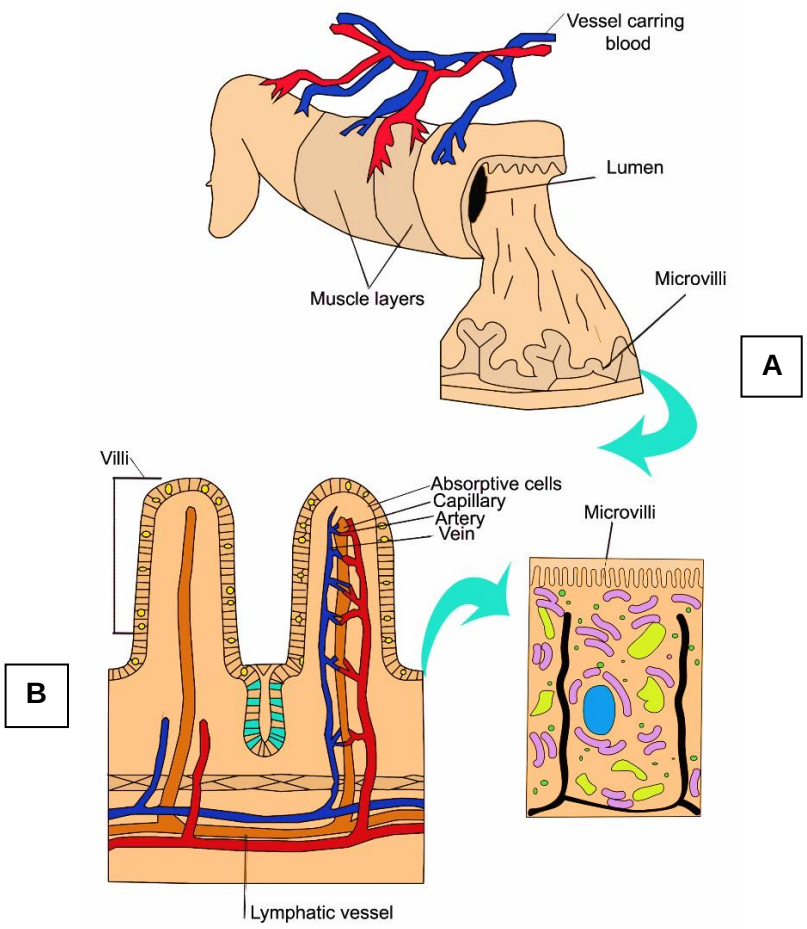

Figure 2.2: Illustration of (A) finger like projections, villi, emerging from the small intestine into the lumen and (B) anatomical structure of a single villus (Adapted from Mayershon, 2009:23)

2.1.1.3 Large intestine

The large intestine consists of the colon (with three main regions namely the transvers-, ascending and descending colon), the rectum and the anus (Ashford, 2013:298-306). In humans, the large intestine is arranged square-like and is located in the centre and lower region of the abdomen, whereas the large intestine of pigs is spiral-like, beginning from the mid-abdomen and spiralling into the upper-left quadrant of the abdomen (see Figure 2.1) (Patterson *et al,.*2008:651-664). The function of the colon is to store and eliminate faecal matter and to absorb water and electrolytes (Mayershon, 2009:29).

2.2 Pharmacokinetics

The term pharmacokinetics describes processes such as absorption, distribution, metabolism and excretion (ADME) that a drug may undergo after administration to a living organism (Loftsson, 2015:48). Absorption refers to the kinetic process whereby drug molecules traverse from the site of administration, across biological membranes, to reach the systemic circulation and consequently the site of action. This process, mostly mediated by passive diffusion, relies on a concentration gradient across the membranes (Rowland *et al*., 2011:839).

2.2.1 Absorption mechanisms in the gastrointestinal tract

The GIT wall has a bilayer structure and separates the lumen of the stomach and intestines from the blood circulatory system. The bilayer structure of the membrane consists of lipids, proteins, lipoproteins and polysaccharides. The membrane is semi-permeable allowing some compounds to rapidly transport across the barrier, and at the same time preventing other compounds to cross the barrier (Ashford, 2007:279).

Drugs can be absorbed across the intestinal epithelium by transport across the cells (*transcellular transport),* or by moving between the cells (*paracellular transport)* (Ward *et al*., 2000:346) as illustrated in Figure 2.3.

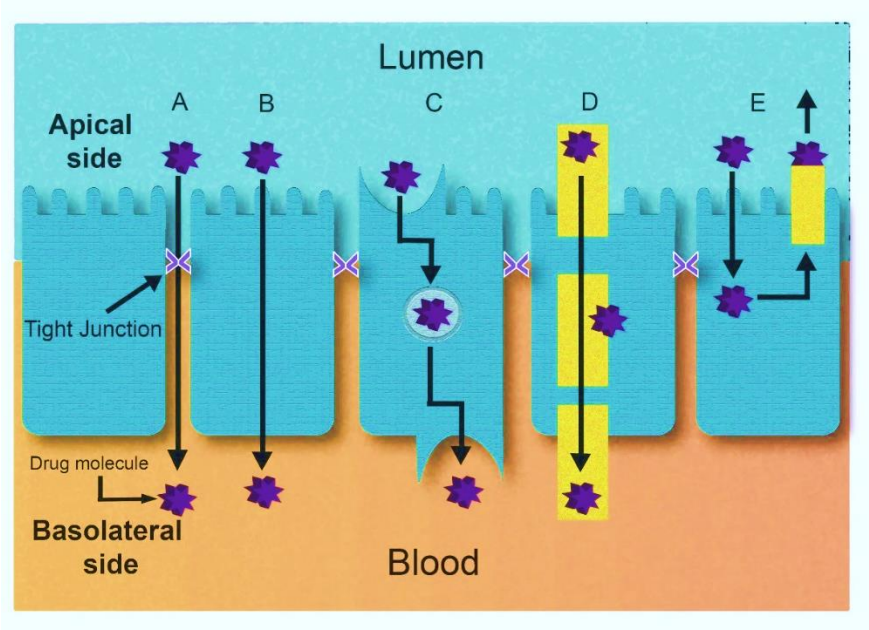

Figure 2.3 Schematic illustration of compounds crossing the intestinal epithelia by means of: (A) passive paracellular transport through tight junctions, (B) passive transcellular transport (diffusion) along the concentration gradient. (C) Vesicular transport (transcytosis) depicting endocytosis on the apical side and exocytosis on the basolateral side. (D) Carrier-mediated transport. (E) Efflux transport, where a drug molecule or foreign substance is effluxed out of the cell (Adapted from Chan *et al.,* 2004:26; Balimane *et al*., 2006: F2)

2.2.1.1 Transcellular pathway

Transcellular absorption across intestinal epithelia can be divided into three sub-groups namely 1) passive diffusion, 2) carrier-mediated transport and 3) vesicular transport (Figure 2.3) (Shargel *et al*., 2005:303-354; Ashford, 2007:279).

2.2.1.1.1 Passive diffusion

Small lipophilic molecules are usually absorbed via passive diffusion where the molecules diffuse from the mucosal side of the intestinal membrane with a high concentration of the drug across the membrane into the bloodstream where a low concentration of molecules is found. The blood flow transports the absorbed molecules, therefore maintaining the concentration gradient (Shargel *et al*., 2005:303-354). According to Ashford (2007:279) the factors that are limiting to the transport of molecules across the membrane are the physiological properties of the

membrane, the nature of the membrane, the concentration gradient across the membrane and the physicochemical properties of the drug.

2.2.1.1.2 Carrier-mediated transport

Although the majority of compounds are transported via passive diffusion, there are compounds that are absorbed transcellularly by means of one of two carrier-mediated pathways namely, active transport and facilitated transport (Renukuntla *et al*., 2013:78).

When a drug molecule traverses across the intestinal membrane, bound to a carrier, in the direction of the concentration gradient it is known as facilitated transport. Drug molecules move from a high concentration to a low concentration and the process is not energy dependant (Shargel *et al*., 2005:303-354; Ashford, 2013:298-306).

Active transport is where a carrier binds to a drug that can be transported across the intestinal epithelia, to move from a region with a lower concentration to a region with a higher concentration. This transport mechanism is an energy dependant process and once the molecule is moved across the intestinal membrane, the carrier will return to the apical side and wait for other molecules or ions to carry across the membrane (Ashford, 2007:281, Mayershon, 2009:44). The carrier molecule is highly selective and therefore drug molecules will compete for binding sites on the carrier (Shargel *et al.*, 2005:303-354).

2.2.1.2 Endocytosis, pinocytosis & transcytosis

The term endocytosis refers to the process where the cell membrane engulfs a molecule and becomes pinched off to form a small intracellular vesicle that is membrane bound. Being membrane-bound allows material to be transferred into the cell. After engulfment in the cell, the material is often transferred to other vesicles or lysosomes to be digested and removed from the membrane (Ashford, 2013:298-306).

Pinocytosis is also known as fluid-phase endocytosis and involves the engulfment of extracellular fluid into a membrane vesicle. The cell will engulf molecules irrespective of the metabolic importance of the material to the cell, although the efficacy of this process is rather low (Ashford, 2013:298-306).

Phagocytosis is the process where a cell membrane engulfs particles larger than 500 nm. The process of engulfment is important for the absorption of multiple vaccines, like the polio vaccine, from the GIT (Ashford, 2013:298-306).

Transcytosis involves the process where the material internalised by the membrane and surrounding area is secreted on the opposite side after transport through the cell (Shargel *et al*., 2005:303-354).

2.2.2 Paracellular transport

Drug molecules are transported via the passive paracellular route when they move or diffuse through the aqueous spaces located between the cells. The molecules usually diffuse from high to low concentrations. The paracellular transport is dependent on the chemical structure of the molecule being transported, with the anatomical structure of the cell and spaces between the cells also influencing the rate of transport according to the physiological function. (Ward *et al.,* 2000*:*346; Linnankoski *et al*., 2010:2167*).*

Hydrophilic drugs are not transported via passive diffusion due to the hydrophilic nature of the drugs but can be transported across the cell membrane by means of paracellular transport. This can be restricted by the presence of tight junctions (Barthe *et al*., 1999:154; Ward *et al*., 2000:346).

Tight junctions seal the pathway in-between neighbouring cells, which regulate the movement of hydrophilic molecules between the epithelial cells. The epithelial barrier serves a dual purpose, namely keeping potentially harmful and toxic molecules from crossing the epithelial membrane and entering the body, while allowing beneficial substances such as water and ions into the body (Ward *et al*., 2000:346). Tight junctions can be manipulated to 'open' by using an absorption enhancer which leads to higher levels of transport, and consequently more absorption of molecules. Approximately 0.1% of the intestinal surface area consists of tight junctions. The scarcity of tight junctions validates the need to investigate other/novel approaches which could be used to improve intestinal membrane permeation of drug molecules (Nellans, 1991:339; DeSesso *et al.*, 2001:209).

2.2.3 Efflux transport mediated by P-glycoprotein

Since the membrane glycoprotein was discovered in 1976 by Juliano and Ling, and named P-glycoprotein (P-gp), it has become an important aspect to consider in the development of orally

administrated drugs (Werle, 2008:500). Located in the apical membranes of epithelial cells, P-gp is a 170kDa molecule that belongs to the transporter proteins known as efflux pumps. This transporter protein is synthesised in the endoplasmic reticulum and modified in the Golgi apparatus before being transported to the cell surface (Silva *et al*., 2015:2). Apart from the high expression levels of P-gp in cancerous cells, this molecule can be found in healthy tissue like the liver, placenta, capillary endothelial cells of the brain and testis, proximal tube in the kidney and the epithelial cells of the intestine (Zhao *et al*., 2013:430). P-gp together with other mechanisms e.g. Cytochrome P450 3A (CYP3A), forms part of the natural detoxification system of the body and has a direct effect on drug pharmacokinetics namely, absorption, distribution metabolism and excretion (ADME) (Werle, 2008:500). The above-mentioned transporters, including other efflux pumps such as multidrug resistant protein (MRP) one and two and breast cancer resistant protein (BCRP), belong to the ATP Binding Cassette (ABC) family (Werle, 2008:500).

P-gp is responsible for the efflux of a large number of drugs out of cells and tissues, and may in some instances lead to a significant reduction in the bioavailability and therapeutic effectiveness of drugs. Efflux is an energy dependent process, mediated by the availability of adenosine tri-phosphate (ATP) (Barthe, *et al.,* 1999:154, Wang *et al*., 2004:2755). By acting as a drug-efflux pump, P-gp only allows compounds with specific structural properties to permeate the intestinal epithelia and therefore it could decrease/reduce drug bioavailability (Barthe *et al.,* 1999:154, Werle *et al*., 2008:500). For a drug/compound to have higher oral bioavailability, P-gp could be inhibited thus the compound's absorption across the intestine may be more efficient (Cornaire *et al.*, 2004:119). The structure of the P-gp molecule is illustrated in Figure 2.4.

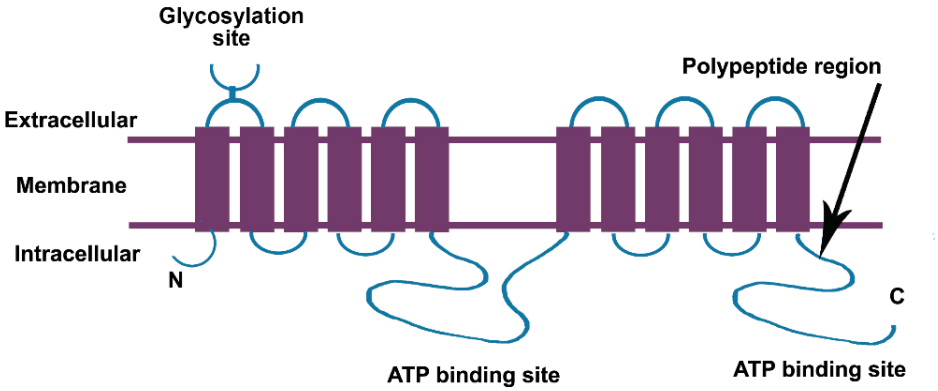

Figure 2.4: Illustration of P-glycoprotein (P-gp) structure (Adapted from Bansal *et al*., 2009:46)

2.2.4 Distribution, Metabolism and Excretion

Orally administrated drugs that reach the bloodstream after absorption from the GIT are eliminated as a metabolite after metabolism, or as intact drug molecules in the urine. The pharmacokinetic factors that characterise ADME are volume of distribution (V_D), elimination half-life ($t_{1/2}$), bioavailability (F) and clearance (Cl) (Shargel *et al*., 2005:303-354). The V_D describes how a drug is distributed through the body whether it be low, for instance V_D<0.2L/kg where the drug will only be located in the blood or be it high where the V_D is more than the total body volume and the drug is then tissue bound (Loftsson, 2015:49). The elimination half-life ($t_{1/2}$) is reached once the concentration of drug in the blood circulation is reduced by 50%. After a drug is absorbed from the gut, it usually undergoes first pass metabolism which influences the bioavailability of the drug. Bioavailability is the term used to describe the fraction of administered drug that reaches the systemic circulation unchanged after oral intake, where F≈1 indicates high bioavailability where close to 100% absorption is reached, and when F<1 it indicates lower bioavailability. Lower bioavailability may be the result of incomplete absorption, first pass metabolism or excretion of unchanged drug in the faeces (Shargel *et al*., 2005:303-354; Loftsson, 2015:49). Clearance (Cl) is a parameter that is used to describe how fast a drug is removed from the body, and can consist of hepatic clearance (Cl_H) and renal clearance (Cl_R).

During hepatic clearance (Cl_H) the drug is metabolised by the liver while renal clearance (Cl_R) describes the process of elimination of the drug via the kidneys. The total clearance (Cl_T) is the sum of hepatic clearance (Cl_H) and renal clearance (Cl_R) (Loftsson, 2015:49).

2.3 Excipients

Active ingredients are rarely administered alone and are usually combined with excipients to improve different characteristics such as the stability, organoleptic properties and dissolution of the active ingredient. Formulation of the active ingredient with excipients to render a dosage form improves patient compliance seeing that the active drug in formulation is easier to administer than the active ingredient alone and the taste of the active ingredient can be manipulated by adding excipients (Jackson *et al*., 2000: 336, Garcia-Arieta, 2014:89). Excipients was thought to be inert and have no influence on the bioavailability of pharmaceutical formulations, but studies have shown that the excipients added to the active ingredient may have drug-excipient interactions, and consequently could influence the bioavailability and absorption of the drug (Jackson *et al*., 2000: 336).

The excipients used in pharmaceutical formulations can be used solely for the purpose of improving handling and uniform dosing (e.g. diluents and fillers), to improve taste (such as sweeteners, coating agents and colouring agents), or to improve the manufacturing process such as lubricants and binders, while some help to release the drug from the dosage form for example disintegrants. Drugs with low aqueous solubility, for instance lipophilic drugs, are formulated with surfactants or wetting agents to improve their absorption and consequently the bioavailability of the drug (Garcia-Arieta, 2014: 89).

2.3.1 Surfactants

Surfactants are excipients used in pharmaceutical formulations to enhance the dissolution of poorly soluble drugs and to stabilise suspensions and emulsions. Due to their broad spectrum of pharmaceutical applications, surfactants are also known as wetting agents, solubilising agents and dissolution enhancers. Surfactants are used to prevent aggregation between particles caused by shaking or agitation, by lowering the surface tension between the hydrophilic and hydrophobic regions of a molecule (Goole *et al*., 2010:17; Kamerzell *et al*., 2011:1118). Surfactants are known to interfere with P-gp and alter the absorption and bioavailability of P-gp substrates (Cornaire *et al*., 2004:119, Al-Saraf *et al*., 2016:66-69).

Amphiphilic or amphipathic compounds consist of a clear lyophilic and lyophobic region, lyophilic being solvent-liking and lyophobic being solvent-hating region. In compounds where the solvent is water the regions are then named the hydrophilic (water-loving) or hydrophobic (water-hating) region. The specific polarity of a molecule will differ in different solvents, for example a polar group will act as a lyophilic molecule in a polar solvent and as a lyophobic molecule in a non-polar solvent (Billany, 2005:395). Because the molecules have a dual nature it can lower surface tension by accumulating at the interface and allowing the hydrophobic region to be removed from the aqueous solvent, hence surfactant's alternative description as surface-active agents (Attwood, 2009:423). Surfactants are classified per the nature of the hydrophilic head of the molecule and can be anionic, cationic, zwitterionic and non-ionic, where the hydrophobic tail of the molecule is usually unsaturated or saturated hydrocarbon chains. In less common situations the hydrophobic tail of the surfactant can have heterocyclic or aromatic rings (Goole *et al*., 2010:22).

2.3.1.1 HLB-system

The Hydrophilic-Lipophilic Balance (HLB) value refers to the balance between the lipophilic and hydrophilic properties of a surfactant and is illustrated in Figure 2.5 (Fernandes *et al*., 2013:109). Surfactants with HLB values that range between 4 and 6 are used as water in oil (W/O) emulsifiers, while surfactants with HLB values between 7 and 9 are used as wetting agents. Surfactants with HLB values between 8 and 18 are used as oil in water (O/W) emulsifiers and those with HLB values ranging between 13 and 15 are used as detergents, while those with HLB values of 15 to 18 are used as solubilising agents (Al-Sabagh, 2002:73, Attwood, 2009:430).

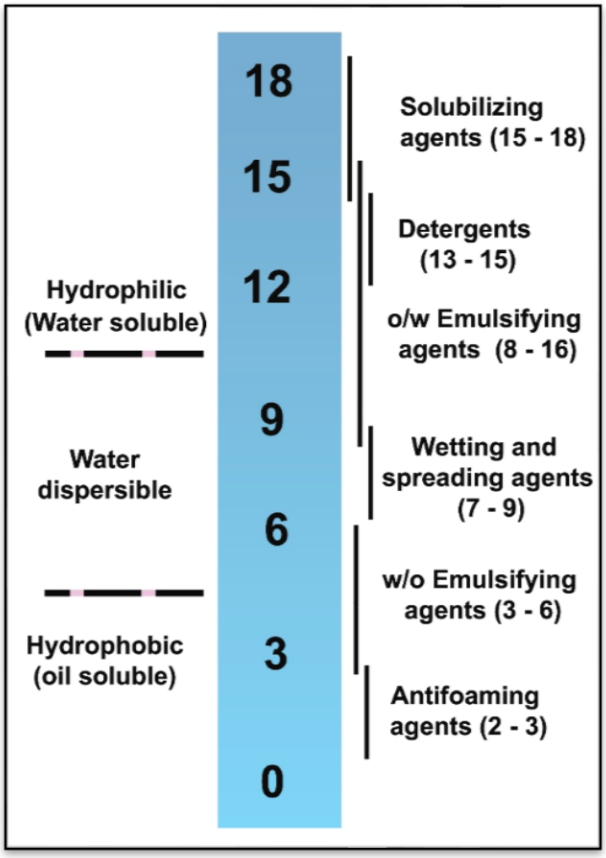

Figure.2.5: Illustration of the HLB balance system (Attwood, 2009:430)

2.3.1.2 Anionic surfactants

When an anionic surfactant is added to an aqueous solution the compound dissociates to form anions that is negatively charged, which can be used as an emulsifying agent (Billany, 2005:383-396). This group of surfactants consists of a polar group (e.g. sulphate, sulfonate and phosphate) and a non-polar part (hydrocarbon chain such as found in long-chain fatty acids) and is widely used due to their low cost (Attwood, 2009:423). Anionic surfactants are used in preparations like preoperative skin cleansers and medicated shampoos because of their bacteriostatic nature against gram (-) bacteria, these surfactants should only be used externally because of their toxicity (Billany, 2005:395; Attwood, 2009:424).

2.3.1.3 Cationic surfactants

Quaternary ammonium and amine surfactants such as cetrimide and benzalkonium chloride are typical examples of the cationic surfactant group because the charge is carried on the nitrogen ion (Billany, 2005:396). The amine-based compounds function only in a protonated state and can therefore not be used in high pH regions like the small intestine, whereas the quaternary ammonium compounds can be used at a wide pH range (Attwood, 2009:424). The cationic surfactants have great importance because of their gram (-) and gram (+) bactericidal activity and are used as wound cleansers, and as antiseptic aqueous solutions to clean contaminated utensils (Attwood, 2009:424). The antiseptic properties of emulgents can be attributed to the cationic nature of the surfactant (Billany, 2005:396).

2.3.1.4 Zwitterionic surfactants

These surfactants can have a positive or a negative charge depending on the ionization of the polar head of the group. In the case of an ammonium group the charge is almost always positive, and a negative charge is often the result of a carboxylate group. Should the ammonium group be quaternary the molecule will be permanently charged and exist as a zwitterion over a wide pH range. If the molecule does not have a quaternary group the surfactant will be amphoteric, where the molecule changes from cationic to zwitterionic to anionic as the pH rises and therefore these surfactants will only be zwitterionic surfactants over a certain pH range (Attwood, 2009:431).

2.3.1.5 Non-ionic surfactants

These surfactants are commonly used in formulations to increase the water solubility of the active ingredient, which in turn may also increase the oral bioavailability of the active ingredient. Non-ionic surfactants are also known to be less toxic to biological membranes than ionic surfactants, which usually make them a more popular choice for inclusion in pharmaceutical formulations (Rege *et al.*, 2002:237; Christiansen *et al*., 2011:167). One of the non-ionic surfactants that is widely used in pharmaceutical formulations is the surfactant with a poly (oxyethelene) chain as the polar head. This group is more commonly known as the Brij® range, with various chain lengths. Cremophor® EL is also a polyoxyelated castor oil with 35 oxyethelene groups and is used as a solubilising agent in intravenous preparations. Cremophor® CO40 is similar, but has 40 oxyethelene groups (Attwood, 2009:426). The widely used sorbitan esters (Span®) are mixtures of sorbitol esters and its mono- and de-anhydrides of oleic acid that is used as a water in oil emulsifier. Span® is not only used as a wetting agent but is also used as emulsifying agent in

topical preparations (Attwood, 2009:426). Tween®, on the other hand is a complex mixture of partial sorbitol esters and its mono- and di-anhydrites condensed with appropriate amounts of ethylene oxide is used as oil in water emulsifiers and wetting agents in the preparation of suspensions (Attwood, 2009:426; Shen *et al*., 2011:494).

Polyoxyl 20 cetyl ether (Brij® 58)

Polyoxyl 20 cetyl ether (Brij® 58) is a type of non-ionic surfactant, which contains a hydrophilic head and a distinctive hydrophobic tail. It has attracted researchers' attention due to its potential use as an extended drug-release system for hydrophobic drugs in hydrogels (Sowmiya *et al.*, 2010:97). The formation of surfactant molecule aggregates inside the hydrogel can mediate sustained release of the drug from the dosage form. The interactions between the solutes such as the drug and the hydrogels can also influence the rate of drug release (Kapoor *et al.*, 2008:624). Brijs® are known to inhibit P-gp and is used in pharmaceutical formulations as emulsifiers and solubilisers to improve dissolution of poorly soluble compounds and consequently enhance absorption (Zhao *et al*., 2016:1527). Polyoxyethylene alkyl ethers are used in suppositories to increase drug release from the pharmaceutical formulation. Other uses of Brijs® include being used as solubilising agents for drugs of low water solubility, such as griseofulvin and cortisone acetate, and as solubilising agents for vitamin oils and essential oils. Polyoxyl 20 cetyl ether has a HLB value of 15.7 (Gupta *et al*., 2013541-549:).

Polyoxyl 40 hydrogenated castor oil (Cremophor® CO40/RH40)

Polyoxyethylene castor oils are non-ionic solubilising agents used in parenteral, topical and oral pharmaceutical formulations, and are prepared when one mol of hydrogenated castor oil is reacted with 40 mol of ethylene oxide. Polyoxyl 40 hydrogenated castor oil (Cremophor® CO40) may be used instead of polyoxyl 35 hydrogenated castor oil (Cremophor® EL) in preparations for fat soluble vitamins, or other hydrophobic pharmaceutical formulations because it has little to no taste or odour (Singh, 2009:543). This commonly used pharmaceutical surfactant have been identified as an inhibitor of P-gp and/or cytochrome P450 3A (CYP3A) (Zhao *et al*., 2013:429). Cremophor®CO40 and other hydrogenated castor oil (HCO) derivatives have been used as surfactants in experimental studies and have according to Singh (2009:543) shown to prolong the plasma circulation times of menatetrenone. This excipient is also used in suppositories which causes enhanced drug released. The HLB value of this surfactant is 14 - 16 (Singh, 2009: 545).

Polysorbate 20 (Tween® 20)

Polysorbates, also commonly known as Tween®, are non-ionic surfactants that have a two-way structure consisting of a hydrophobic alkyl tail and a hydrophilic ethylene glycol tail (Shen *et al*., 2011:494). Being homologous polysorbates, Tweens®, can have various length tails, for example Tween® 40 will have a longer alkyl tail than Tween® 20, as seen in Figure 2.6 (Ćirin *et al*., 2012:3670).

This group of bio suitable surfactants was known as inert pharmaceutical surfactants, but it has been shown that amongst others, Tween® 20 have permeation enhancing effects across biological tissue (Dimitrijevic *et al.,* 2000:157, Ćirin *et al*., 2012:3670).

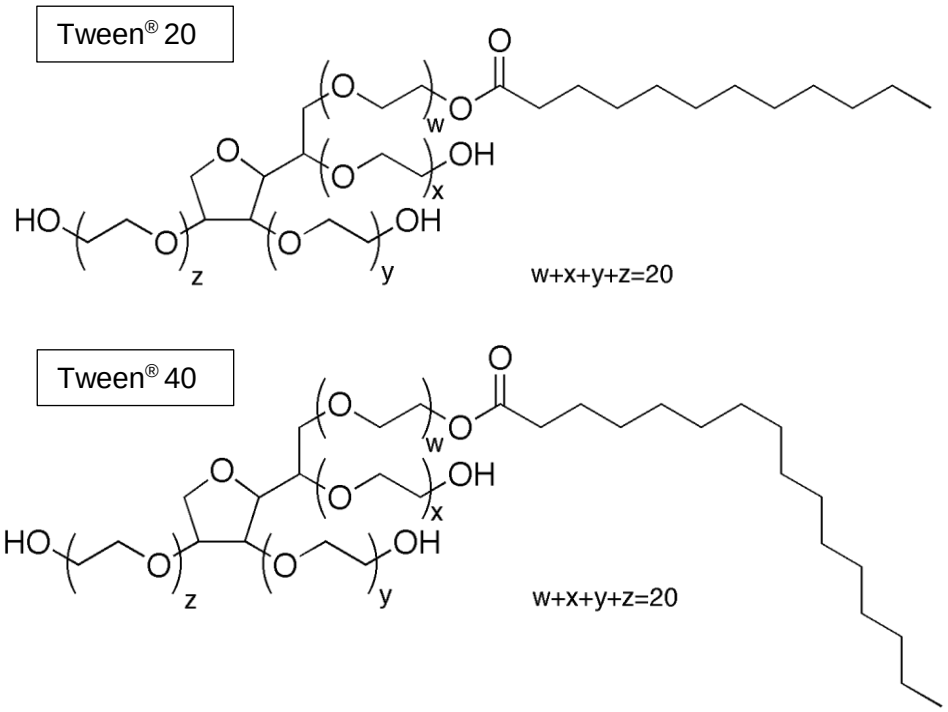

Figure 2.6: Chemical structure of Tween® 20 and Tween® 40 illustrating the different lengths of alkyl tails (Shen *et al*., 2011:495)

Polysorbates are used as solubilising agents in essential oils and vitamin-oils and can be used as wetting agents in the formulation of O/W emulsions. This surfactant has been used in recent studies to evaluate the effect on permeation, making Tween® 20 an ideal surfactant for investigating permeability effects (Al-Saraf *et al*., 2016:66-69). According to Zhang (2009:550) Tweens® have been known to improve the bioavailability of drugs known as P-gp substrates.

Polysorbate 20 has a HLB value of 16.7 (Zhang, 2009:551). Table 2.1 below lists the uses of the polysorbates.

Table 2-1: Various uses of polysorbates (adapted from Zhang, 2009:676)

	Uses	**Concentration % m/v**
Emulsifying agent	Used alone in oil-in-water emulsions	1-15
	Used in combination with hydrophilic emulsifiers in oil-in-water emulsions	1-10
	Used to increase the water-holding properties of ointments	1-10
Solubilising agent	For poorly soluble active constituents in lipophilic bases	1-15
Wetting agent	For insoluble active constituents in lipophilic bases	0.1-3

Sorbitan monolaurate (Span® 20)

According to Zhang (2009:676), sorbitan monoesters consist of a mixture of partial esters of sorbital and its mono- and dianhydrides with fatty acids. Spans® are commonly used in cosmetics and in topical creams and ointments of varying consistencies. It is often used on its own to stabilise water-in-oil emulsions or in combination with polysorbates to produce oil-in-water and water-in-oil emulsions (Zhang, 2009:676). Another important use of sorbitan esters is self-emulsifying drug delivery systems for poorly soluble drugs. Table 2.2 describes the uses and concentrations of sorbitan esters. Sorbitan monolaurate has a HLB value of 8.6 (Zhang, 2009:676).

Table 2-2 Various uses of sorbitan esters (adapted from Zhang, 2009:676

	Uses	**Concentration % m/v**
Emulsifying agent	Used alone in water-in-oil emulsions	1-15
	Used in combination with hydrophilic emulsifiers in oil-in-water emulsions	1-10
	Used to increase the water-holding properties of ointments.	1-10
Solubilising agent	For poorly soluble, active constituents in lipophilic bases	1-10
Wetting agent	For insoluble, active constituents in lipophilic bases	0.1-3

Sodium deoxycholate

Bile salts are natural solubilising agents that are of amphipathic nature. The bile salts are synthesised as a product of cholesterol elimination from the body (Yang *et al*., 2011:1516-1524). These bio-surfactants are used as absorption enhancers across biological membranes like the blood brain barrier (BBB), skin, mucosa, buccal, corneal, pulmonary and intestinal membranes, they enhance the absorption by either making hydrophobic compounds more soluble or by making the apical and basolateral membranes more permeable (Malik, 2016:179-201).

The liver eliminates cholesterol through biotransformation into bile alcohols and bile acids, which are further eliminated by sulfation or amidation to form bile salts that are secreted into bile. There are two groups of bile acids namely primary and secondary bile acids.

The primary group can be divided into cholic acid and chenodeoxycholic acid, and the secondary group into deoxycholic acid and lithocholic acid (Moghimipour *et al*., 2015:14452).

The bile acids in the primary group can be synthesized via two different pathways; the classic or alternative pathway as illustrated in Figure 2.7. Large quantities of bile acids are synthesised by means of the classical pathway, while the alternative pathway is only responsible for the production of 10% of bile acids (Monte *et al*., 2009:804-816). In the primary route, a cytochrome P450 enzyme, 7α-hydroxylase, is responsible for converting cholesterol to 7α-hydroxycholesterol that is further converted to chenodeoxycholic acid or cholic acid by the 12α-hydroxylase enzyme. This route is also known as the neutral route and the rate limiting step in this process of bile acid formation is the conversion of cholesterol to 7α-hydroxycholesterol.

The alternative pathway includes the hydroxylation of cholesterol on position 27 by an enzyme of mitochondrial origin, sterol 27-hydroxylase. The hydrophobicity of bile acids is reduced by conjugating the bile acids with glycine and taurine prior to secretion (Moghimipour *et al*., 2015:14452, Malik, 2016:179-201).

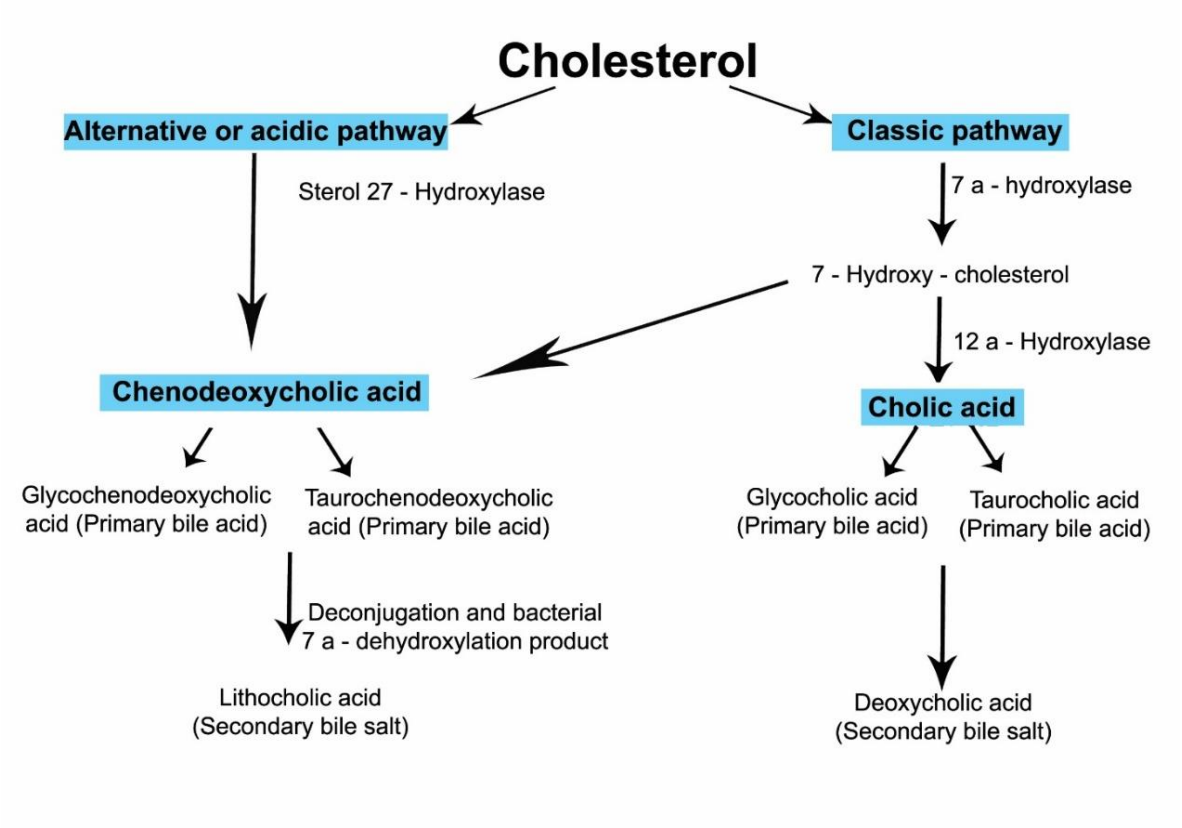

Figure 2.7: Image illustrating the transformation of cholesterol into secondary bile acids, through the classic or alternative pathway (Adapted from Monghimipour *et al*., 2015:14456)

Bile salts and their micellar properties have been well studied because of the physiological properties they possess. When a bile salt is added to an aqueous solution above its critical micelle concentration (CMC), the bile salt will form micelles. By binding the bile salts with Na^+ ions, or after conjugation with taurine or glycine, the CMC is lowered (Moghimipour *et al*., 2015:14456). Because bile salts are biocompatible, it has become popular as a permeation enhancer. By interacting with the phospholipids in biological membranes, it is able to enhance drug absorption (Moghimipour *et al*., 2015:14456). Sodium deoxycholate has been successfully used as a permeation enhancer in various studies (Lo *et al*., 2000; Jain *et al*., 2016) making it an ideal surfactant to use in permeation studies.

2.4 Models used for drug permeability studies

2.4.1 *In vivo* models to study drug absorption

In vivo models are widely used for drug absorption and bioavailability studies after oral administration of a drug. These models allow an intact system with a mesenteric blood flow, a lymphatic system and an intact digestive system (Gamboa *et al*., 2013:805). There are physiological and anatomical differences between various species, for example gastric emptying rate, pH, gastric motility, transport proteins and metabolic enzymes which play an important role in bioavailability and need careful consideration before using these models (Alqathani *et al*., 2013:4).

Advantages of *in vivo* models include:

- An intact digestive system with peristalsis, intact blood flow and a mucosal layer present in the intestine gives more accurate results than excised intestinal tissue.
- A better representation of pharmacological properties of the administered therapeutic drug can be seen in *in vivo* models (Hildalgo, 2001:389).

Disadvantages of *in vivo* models:

- Larger amounts of test compound are used in comparison to *in vitro* models
- It may be problematic to identify the rate limiting step of absorption.
- The exact mechanisms of absorption are not easily identifiable (Hildalgo, 2001:389).

2.4.2 *In situ* model to study drug absorption

In situ models utilise small intestinal segments where the intestine is still part of an anesthetised animal to study pharmacokinetics (Alqathani *et al*., 2013:4). This model resembles the *in vivo* model closely because it mimics the functions of the blood circulation, metabolism and nervous system as well as the higher expression of transporter proteins than in the *in vitro* model. A better correlation can be made between data obtained from animal *in situ* tests and the effective permeability of drugs in humans (Lennernäs, 1998). The important role of regional differences of intestinal drug transport and dose dependant pharmacokinetics can be evaluated with this model (Alqathani *et al*., 2013:5).

In situ models require a minimum amount of pre-experimental organ preparation thus minimising potential organ damage (Zhang *et al*., 2012:554). The expression of transporters found in the small intestine of rats are very similar to that of humans, consequently this model can be used to predict the active uptake of compounds (Antunes *et al*., 2013:12). A drawback of these models is the use of an anaesthetic to sedate the animal. This can have potential effects on the intestinal drug absorption of the chosen compound and therefore the type of anaesthetic should be selected with care (Le Ferrec *et al*., 2001:653).

2.4.3 *In vitro* / *Ex vivo* models to study drug absorption

The Ussing diffusion chamber with *ex vivo* tissue is a widely used *in vitro* model, and provides a good representation of drug absorption and the effect of drug influx and efflux transporters across the epithelial tissue (Nunes, 2015:209). An excised segment of intestinal tissue from pig, dog, monkey, rat, mouse, rabbit or human is placed on the spikes of diffusion half-cells. The compartments are usually then filled with Krebs Ringer bicarbonate buffer (KRB) and a mixture of 95% O_2 and 5% CO_2 is pumped through the compartments to maintain tissue viability. The drug is added to the apical side to test drug absorption or to the basolateral side to measure drug efflux (Alqahtani *et al*., 2013:3). This model has successfully been used in various studies to evaluate drug absorption and efflux and the effect of region specific absorption (Lennernäs, 2007:1104-1120; Bergmann *et al*., 2009:1211-1225; Rozehnal *et al*., 2012:367-373).

2.5 Animal tissue-based *in vitro* models for permeability studies

2.5.1 Sweetana-Grass diffusion chambers

Ussing type diffusion chambers were first introduced in the 1950's by the Danish physiologist Hans Ussing. Ussing diffusion chambers are used to determine the movement of electrolytes, non-electrolytes and water across any membrane inserted between the half-cells of the diffusion chamber (Hoffmann, 2001:321).

The original method and apparatus had several shortcomings that were recognised and addressed by the researchers George Grass and Stephanie Sweetana. Grass and Sweetana introduced a new apparatus and method which are commonly known today as the Sweetana-

Grass diffusion chamber apparatus/method (Grass & Sweetana, 1988:372). One of the changes they incorporated in the Sweetana-Grass diffusion half-cells was that only one material type (acrylic) was in contact with drug-containing fluids. This improvement was made after un-identified peaks were found during High-performance liquid chromatography (HPLC) sample analysis, which later were traced back to compounds which were found in the tubing used in the Ussing diffusion chamber. Although this was addressed, the Ussing diffusion chamber could still not be used for permeability studies with very lipophilic drugs due to the adsorption of the drugs to the tubing (Hoffman, 2001:321).

The Sweetana-Grass diffusion chambers are more practical to use than the original Ussing chamber design due to various improvements. In the revised apparatus, only the fluid reservoir is heated and not the diffusion cells itself, which ensures better temperature control and makes cleaning of the apparatus easier (Grass & Sweetana, 1988:372). The surface area was also doubled from the Ussing chamber design in order to accommodate tissue from a wide variety of species. This apparatus can be used to evaluate transport of compounds across mucosal/epithelial barriers such as gastrointestinal tissue, buccal tissue, tongue tissue and skin (Nunes *et al.*, 2009:203). An illustration of the Sweetana-Grass diffusion chamber apparatus is shown in Figure 2.8

Figure 2.8: Sweetana-Grass diffusion apparatus used for transport studies

The apparatus consists of six cell blocks where each cell block includes two half-cells clamped together, holding the excised tissue sample in between. A circulation system by means of gas flow has been added to each half-cell, preventing stagnant layer formation and to ensure that the membrane has maximum exposure to the fluid on both sides, as illustrated in Figure 2.9. The cell blocks are positioned linearly in a unit with a front and back plate which are heated to biological temperature (37°C), to assure tissue viability and to mimic biological conditions (Sweetana *et al*., 1993:9).

Figure 2.9: Sweetana-Grass diffusion cell. Tissue is mounted between the half-cells and the Kreb's Ringer bicarbonate buffer is circulated by the gas (O_2/CO_2) inlet, circulating it in the direction of the arrows

2.5.1.1 Porcine intestinal tissue

The 3R's principle has been introduced to limit studies on animal models due to ethical considerations (Cabrera-Pèrez *et al*., 2016:3). The first R in the 3R's principle refers to "replace", where live animals should be substituted with other alternatives, such as *in vitro* models. The

second R is “reduce”, in the sense that more suitable methods should be considered where fewer animals are used. “Refinement” refers to development of techniques to reduce the pain animals feel and distress they experience during experimentation (Zurlo *et al.*, 1996:878; Törnqvist *et al*., 2014:1; Cabrera-Pèrez *et al*., 2016:3). The porcine intestinal tissue is easily obtainable and complies with the 3R’s principle. There are advantages and disadvantages to this model as listed below.

Advantages of porcine intestinal tissue as model for pharmacokinetic studies

- The pig’s anatomy, physiology and environment of the GIT are similar to that of humans, making it an ideal model for drug absorption studies (Westerhout *et al*., 2014:174).
- High availability and low cost of the porcine intestinal tissue.
- The omnivorous nature and similar eating behaviour is an advantage above other animal models.
- In a study conducted by Nedjfors *et al* (2000:501-507), the regional intestinal mucosal permeation of marker molecules was tested using Ussing diffusion chambers with various animal tissues. The results showed that although the rat showed higher permeability than human tissue, the porcine intestinal tissue showed a better correlation with human intestinal tissue than any other animal model (Nedjfors *et al*., 2000:501-507). This was later confirmed by Westerhout *et al*., (2014:174).

Disadvantages of porcine intestinal tissue as model for pharmacokinetic studies

- The variety of intestinal tissue used for the study may influence the absorption of the model compound.
- It is of utmost importance to keep the tissue fresh and viable, which is not an easy task when working with excised tissue that requires transportation (Pietzonka *et al*., 2002).
- Tissue damage can occur when stripping off the serosa and muscle layers, leading to loss of viability (Westerhout *et al*., 2014:174).

2.5.1.1.1 Murine intestinal tissue

Due to the similarities between human and rat membranes the intestinal absorption of drugs in humans can be predicted using rodent intestinal tissue, regardless of the bioavailability of the drug and the metabolism variation in the two species (Cao *et al*., 2006:1676). When low solubility

drugs are used, it has been shown that the Ussing chambers are more effective when using rat intestinal tissue than Caco-2 cells to predict the human fraction absorbed (Watanabe *et al*., 2004:659).

Advantages of rat intestinal tissue as a model for pharmacokinetic studies

- Despite the various differences between humans and rats, DeSesso *et al.* (2001:209) found a correlation between human and rat intestine of $R^2 = 0.8$.
- Permeability data gathered from rat intestinal permeation studies correlate well with data obtained from human permeability studies (Lennernäs, 2014:338)
- There is a higher availability of rats for experimental purposes than other animal models such as dogs and monkeys.
- Rats can be used for *in vivo* pharmacokinetic and toxicokinetic studies, *in vitro* for Ussing diffusion chambers and by means of the everted sac method to conduct permeability studies.
- In a study conducted by Miyake *et al.* (2017:373-380) it was determined that although dogs have the closest correlation in regard to permeability, there is a better correlation between the intestinal physiology of rats and humans, making the rat model a more reliable model in terms of physiological correctness.

Disadvantages of rat intestinal tissue as a model for pharmacokinetic studies

- Rats are nocturnal animals, meaning they function at night and not during the day like humans. This means that the circadian rhythm of humans and rats are different leading to different times of drug absorption.
- The re-uptake of faecal matter, resulting in the uptake of metabolised drugs which can influence drug-plasma levels (Sjögren *et al*., 2014:99).
- The intestinal length of rats is five times smaller than that of humans, and the surface area of the human intestine is 200 times larger than that of a rat, thus a correlation cannot as easily be made between humans and rats (DeSesso *et al*., 2001:217).
- Rats need to be bred specifically for research purposes, leading to ethical considerations.

2.5.1.1.2 Everted sac

The other model frequently used in *in vitro* studies is the everted sac model. This model is used to study intestinal drug absorption and metabolism. The model uses fresh isolated segments of

animal intestinal tissue that are flushed with cleansing medium and everted. The everted intestine is filled with oxygenated medium and submerged in drug containing medium. This model has been used to test the effect of drug absorption at various concentrations and to evaluate the effect of P-gp related efflux on the extent of absorption (Balimane *et al*., 2000; Dixit *et al*., 2012:13-17; Alqahtani *et al*., 2013:4).

2.5.2 Cell culture-based *in vitro* models for permeability studies

2.5.2.1 Colorectal adenocarcinoma cell line (Caco-2)

The Caco-2 cell line is derived from human colorectal adenocarcinoma cells, and is one of the most popular cellular models for drug transport research due to its physiological properties and human origin. The cells take three weeks to grow into polarised cells, which closely resemble that of intestinal enterocytes consisting of an apical brush border and defined tight junctions between the cells. Despite their colonic origin, they show similarity to small intestine absorptive cells (Le Ferrec *et al*., 2001:649-655).

Advantages of the Caco-2 cell line as a model for pharmacokinetic studies

- Relatively low maintenance.
- Good representation of functional properties of human intestinal cells.
- No inter-species variation.
- Transport studies can be performed in both the apical to basolateral, or basolateral to apical direction.
- It mimics the diffusion properties found in the human body and also contains tight junctions, microvilli and active transporters.

Disadvantages of Caco-2 cell lines as model for pharmacokinetic studies

- The absence of mucus secreting goblet cells.
- Caco-2 cells cannot be used to quantitatively predict human absorption *in vivo.*
- It is a cancer derived cell line, and therefore may have different properties than normal human epithelial cells.
- Intestinal motility cannot be mimicked when using cell cultures.
- The preparation time may vary between 2-4 weeks and the cells can easily become infected.

- Although the Caco-2 cells are from human origin, there can be tissue variation due to morphology changes and genetic drift.
- Relatively high cost of production and maintenance of cells.
- Inaccuracies with regards to permeability of poorly soluble drugs and the calculation of the apparent permeability coefficient (P_{app}) values can occur (Buckley *et al*., 2012:235).

2.5.2.2 Madin Darby canine kidney (MDCK) cells

Madin Darby canine kidney (MDCK) cells were isolated from the kidney of a dog by Madin & Darby, and have since been cultured for research purposes (Gaush *et al*., 1966:931). This cell line can differentiate into columnar epithelial cells or form T-junctions when cultured on semi-permeable membranes.

Advantages of the MDCK cell line as a model for pharmacokinetic studies

- This cell line has a culturing period of three to five days that is a shorter period than most cell lines, for instance the Caco-2 cell line which takes up to three weeks to culture (Le Ferrec *et al*., 2011:649; Alqahtani *et al*., 2013:3).
- The cells are easily maintained which is more convenient for the researcher.

Disadvantages of MDCK cell line as a model for pharmacokinetic studies:

- Production and maintenance of the cells is costly.
- Unlike Caco-2 cells, MDCK cells do not express P-gp, which is necessary to facilitate transport (efflux) from the basolateral to apical side and therefore bidirectional studies are not possible.
- Intestinal motility cannot be mimicked when using cultured cells.
- Mucus secreting goblet cells are absent in cell cultures (Le Ferrec *et al*., 2011:649).
- The model is of canine origin that will add to the disadvantage of inter-species variation (Alqahtani, *et al*., 2013:3).

2.6 Conclusion

Based on the evidence in the literature, it is evident that pharmaceutical excipients, especially surfactants are not inert as previously thought, but may have altering (pharmacokinetic) effects on the properties of the model compound Rho123. The altering effects may primarily be the result of P-gp inhibition or the increased solubilisation of phospholipids in the membrane. These interactions can be clinically important if it leads to higher plasma levels and longer elimination

times of the active ingredient. In the event that the surfactant causes drug efflux it can possibly lead to sub-therapeutic plasma levels of the active ingredient. Although the permeation effect of surfactants on *in vitro* models have been performed, there is a need for further studies on porcine intestinal tissue seeing that the data obtained from previous studies shows a better correlation between excised human and porcine intestinal tissue than other excised animal models (Nedjfors *et al*., 2000:501-507; Westerhout *et al*., 2014:167-177)

CHAPTER 3

EXPERIMENTAL METHODS

Pharmaceutical excipients have been known to be inert and to have no effect on the active ingredient of a formulation, except for initiating the release of the active ingredient out of the pharmaceutical formulation to be absorbed through the gastrointestinal tract (GIT) (Goole *et al*., 2010:17-31). However, more evidence has come to light suggesting excipients are not inert and may have direct or indirect effects on the membrane-spanning transporter proteins (Zhang *et al*., 2016:831). Such effects could potentially alter the ADME (Absorption, Distribution, Metabolism and Excretion) properties of a drug, and thereby influence the therapeutic efficacy and/or possible side effects of the formulation (Goole *et al*., 2010:17-31).

The potential permeation altering effects of five surfactants, namely Brij® 58, Tween® 20, Span® 20, Sodium deoxycholate and Cremophor® CO40, on the intestinal permeation of a known P-glycoprotein (P-gp) substrate, Rhodamine 123 (Rho123) was investigated. Various *in vitro* and *in vivo* models were assessed and the most suitable model, namely excised porcine intestinal tissue mounted in Sweetana-Grass diffusion chambers, were chosen to perform bidirectional transport studies. This model is attractive because it closely represents the anatomy and physiological characteristics of human tissue without using live animals, since the tissue is obtained as a by-product of meat production (Patterson *et al*., 2008:652).

To validate that the integrity of the intestinal tissue was maintained, the permeability of Lucifer yellow (LY), a paracellular permeability fluorescent marker, was determined. Trans epithelial electric resistant (TEER) was also measured to ensure the excised intestinal tissue segments remained viable during the transport studies (Pietzonka *et al*., 2002:39-47).

All transport experiments were performed in triplicate and analysed by a validated fluorescence detection method to analyse samples for their Rho123 content.

3.1 Materials

Rhodamine 123, Lucifer yellow, Kreb's Ringer bicarbonate buffer, Brij® 58 and sodium deoxycholate were purchased from Sigma-Aldrich (Johannesburg, RSA). The remaining

surfactants, namely Tween® 20, Span® 20 and Cremophor® CO40 was donated by Prof. Jan Steenekamp from the North-West University (Potchefstroom, RSA).

3.2 Preparation of materials

Krebs Ringer bicarbonate buffer (KRB) was prepared once a week and refrigerated until needed. If any signs of precipitation occurred, a new buffer was prepared. A 1312.96 µM stock solution of Rho123 was prepared and kept frozen at -80ºC. Prior to each transport study the Rho123 aliquot was thawed in a refrigerator and diluted in KRB to a working solution of 5 µM. The surfactant solutions were prepared fresh prior to each experiment by dissolving it in a 37ºC pre-heated solution of Rho123 (5 µM) for the apical to basolateral studies, or KRB buffer for the basolateral to apical transport studies. The permeation studies were conducted at surfactant concentrations of 0.1% (w/v), 0.5% (w/v) and 1.0% (w/v) (Rege *et al*., 2002:240; Cornaire *et al*., 2004:121; Buggins *et al*., 2007:1493).

3.3 Tissue preparation

Porcine jejunum tissue was collected at a local abattoir in Potchefstroom where the pigs were slaughtered solely for meat production and the intestines is gathered as a by-product thereof. Immediately after slaughter, roughly 30 cm of the jejunum was removed. The excised jejunum segment was flushed and rinsed and subsequently submerged in freshly prepared ice cold KRB, adjusted to pH 7.4, and transported to the laboratory in a cooler box filled with ice (Barthe *et al*., 1999:154-168).

Figure 3.1 Image illustrating preparation of porcine intestinal tissue by taking the selected section of the jejunum and flushing it with Kreb's Ringer bicarbonate buffer

As shown in Figure 3.1, the intestinal tissue was thoroughly rinsed with KRB. The jejunum was pulled over a glass tube (Figure 3.2 (A)) and the serosal layer, longitudinal muscle and circular muscle were removed using blunt dissection with the aid of tweezers to prevent damage to the underlying tissue (Figure 3.2 (B)). During the preparation, the excised tissue was constantly rinsed with ice cold KRB and kept indirectly on ice to keep the tissue viable.

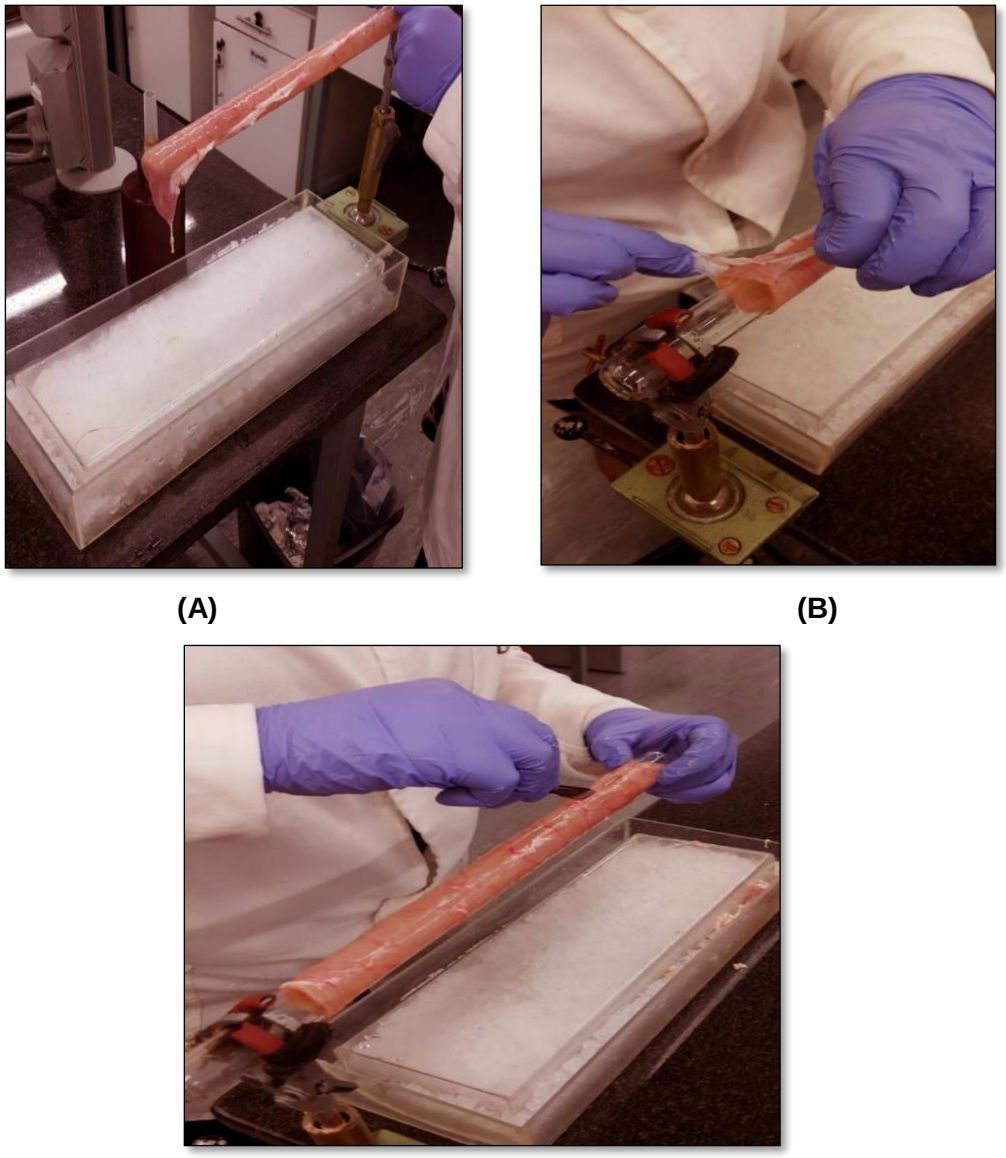

Figure 3.2: Images illustrating (A) intestinal tissue on a wetted glass rod. (B) The serosa is removed. (C) Intestinal tissue mounted on a glass rod was cut along the mesenteric border.

The prepared intestinal tissue was cut along the mesenteric border with a scalpel (Figure 3.2 (C)) and the resultant jejunum tissue sheet was rinsed with KRB buffer and placed onto pre-wetted filter paper in a clean glass dish to ensure that the smooth surface texture was maintained (Legen *et al.*, 2005:183). The jejunum sheet was then cut into equal smaller pieces excluding pieces that contained Peyer's patches, and mounted onto the Sweetana-Grass diffusion chamber half-cells as demonstrated in Figure 3.3.

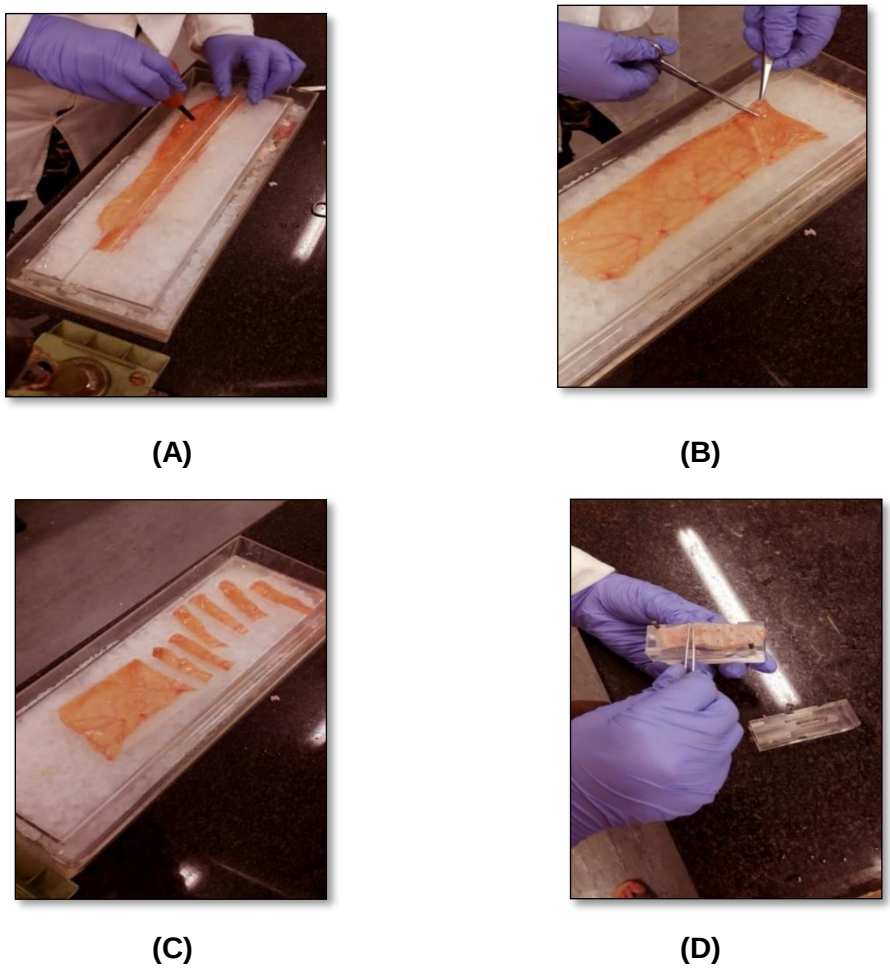

Figure 3.3 Images illustrating (A) intestinal tissue rinsed onto pre-wetted filter paper. (B) Intestinal sheet obtained after cutting segment along the mesenteric border. (C) The intestinal tissue sheet is cut into smaller segments. (D) The segments of intestinal tissue are mounted onto the half-cells with the filter paper facing upward

Each of the assembled half-cells were clamped into the diffusion manifold (Figure 3.4) and connected to an carbogen supply (95% O_2 and 5% CO_2), while kept at a temperature of 37°C for the duration of the study.

Figure 3.4 Image illustrating Sweetana-Grass diffusion chambers with mounted porcine intestinal tissue in half-cells

3.4 Membrane viability evaluation

Sjögren (2016:361) raised the issue that the process of removing the serosal during the pre-experimental preparation process is a technically challenging process which may subsequently lead to tissue damage and reduced viability of the intestinal segments. To ensure that the tissue was still viable, LY was used as a paracellular permeability marker, and the TEER was also measured.

3.4.1 Trans-epithelial electrical resistance (TEER)

The trans-epithelial electrical resistance (TEER) measures the resistance per unit area (Pereira *et al*., 2015:75). The TEER values indicates whether the intestinal mucosa mounted in Sweetana-Grass diffusion chambers is still viable during and after the transport study (Pietzonka *et al*., 2002). A decrease in TEER is not necessarily a sign of compromised integrity of the intestinal tissue, but may also indicate the opening of tight junctions (Borchard *et al*., 1996:131-138).

After the equilibration period (15 min initial KRB circulation) the TEER was measured before the start of the transport study and at intervals of 20 min during the study to ensure that the integrity of the intestinal tissue was not lost during the 120 min study. A Dual Channel Epithelial Voltage Clamp (Warner Instruments, Hamden, Connecticut, USA) was used to measure the TEER.

3.4.2 Evaluation of intestinal integrity by Lucifer Yellow.

Lucifer yellow (LY) is a non-toxic impermeant fluorescent dye, introduced in 1978 it is still one of the most widely used tracer molecules (Hanani, 2012:22). This paracellular permeability marker has also been used previously to evaluate the integrity of *in vitro* models (Rozehnal *et al*., 2012:367). A 50 µM solution of LY in KRB was prepared and an apical to basolateral transport study was conducted in the same way as the Rho123 studies (see section 3.5). The samples were analysed by means of fluorescence detection and consequently measured at wavelength of E_x = 485nm and E_m = 535nm. (See Section 4.1 for results).

3.5 Bidirectional transport across porcine intestinal tissue

The transport of Rho123 in two directions, apical to basolateral (AP-BL) and basolateral to apical (BL-AP), across excised porcine jejunum tissue was measured in the Sweetana-Grass diffusion apparatus (Legen *et al.*, 2005:183). The diffusion chambers containing the mounted intestinal tissue were filled with 7 ml KRB and left to equilibrate for 15 min. Thereafter, the KRB was removed from the donor chamber and replaced with an equal volume of 5 µM Rho123 solution in KRB with or without the appropriate concentration of surfactant (Tang *et al*., 2004:1185). Samples of 180 µl were withdrawn at 20 min intervals from the acceptor chamber (either the basolateral or apical side, depending on the direction of the transport study) over a period of 2 hours. The volume of the withdrawn samples was replaced with an equal volume of transport medium used in the specific chamber. The concentration of Rho123 in each transport sample was determined by means of a validated fluorescence method (see Section 3.6 and Section 3.7) (Tang *et al*., 2004:1185, Hoffmann, 2001:321).

The results obtained from the transport studies was corrected for dilution and expressed as cumulative drug transport (% of initial dose) and the apparent permeability coefficients (P_{app}) for the test compound was calculated from the transport data according to the following equation (Wempe *et al.*, 2009:93, Zhao *et al*., 2016: 1528):

$$P_{app} = \frac{dC}{dt}\left(\frac{1}{A.60.C_0}\right)$$ ***Equation 1***

Where P_{app} is the apparent permeability coefficient ($cm.s^{-1}$), $\frac{dC}{dt}$ is the permeability rate (amount of Rho123 permeated per minute), A is the diffusion area of the diffusion chamber (cm^2) and C_0 is the initial concentration (mg/ml) of Rho123.

The efflux ratio (ER) was calculated according to the following equation (Wempe *et al.*, 2009:93, Zhao *et al*., 2016:1528).

$$ER = \frac{P_{app}(B\text{-}A)}{P_{app}(A\text{-}B)}$$ ***Equation 2***

Where P_{app} (B-A) is the apparent permeability coefficient for the permeation in the basolateral to the apical direction and P_{app} (A-B) the same variable in the apical to basolateral direction.

3.6 Florescence detection

A SpectraMax® Paradigm® Multi-Mode Detection Platform multi-plate reader (Separations, Johannesburg, RSA) was used to analyse the samples taken during the bidirectional transport studies. An opaque Co-Star® 96-well plate (The Scientific Group, Randburg, RSA) was prepared according to the requirements of the experiment. For Rho123, 2 linear ranges consisting of 6 concentrations, a KRB group blank, a standard range and a time zero sample (Rho123 5 µM) were prepared and inserted into the plate. After all transport samples were inserted, the plate was placed on a shaker (Bibby Scientific Limited, Staffordshire, UK) for 30 min at 300 rpm and a constant temperature of 21˚C to ensure all samples on the microplate was the same temperature and thoroughly mixed. The wavelengths used to measure Rho123 was E_x = 480 nm and E_m =520 nm. For LY, the plate setup was done in the exact same manner as for Rho123 except for the time zero sample that was prepared at a concentration of 50 µM. The wavelengths used to measure LY was E_x =485nm and E_m =535nm.

3.7 Validation of analytical method for measuring Rho123

The purpose of the validation process is to determine whether the process can deliver adequate results, and when practically applied to the study, relevant results can then be recorded and successfully interpreted within the framework of the study.

Parameters that were deemed crucial regarding the validation of the analytical method for Rho123 was narrowed down to the following: specificity, linearity, accuracy and precision (Ou *et al*., 2001:4620, Kumar *et al*., 2012:4). To minimalise variability, the apparatus, method and storage conditions of the components where kept unchanged.

3.7.1 Linearity

The linearity refers to the ability of an analytical method to obtain tests results that is directly proportionate to the concentration of the analyte in the sample (Ou *et al*., 2001:4620, Kumar *et al*., 2012:4). A solution of 5 µM Rho123 was prepared and 5 ml thereof was diluted to a final concentration of 2.5 µM. A Rho123 concentration series, ranging from 5 µM to 0.0025 µM, was subsequently prepared and transferred to a black 96-well plate, and KRB was included as a background control. The linearity data obtained for Rho123 following fluorescence analysis, are summarised in Table 3.1, with the linear regression graph for Rho123 illustrated in Figure 3.5.

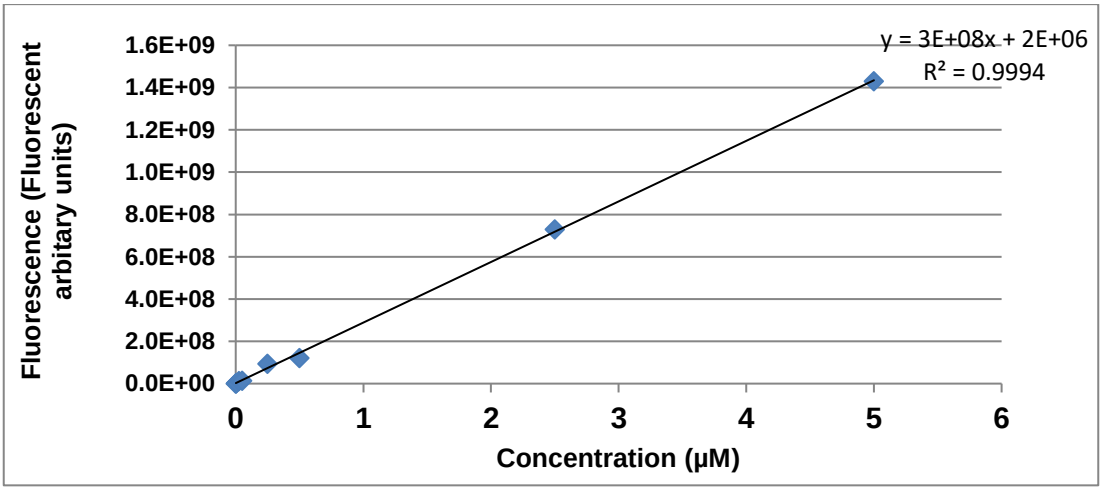

Figure 3.5: Linear regression graph obtained for Rhodamine 123 fluorescence plotted as a function of Rhodamine 123 concentration

The fluorescence data obtained for the concentration series were plotted and linear regression was performed. Linear regression should yield a regression coefficient (R^2) of ≥ 0.99 (Kumar *et al*., 2012:4). This method showed a high level of linearity based on the R^2 value of 0.9996.

Table 3-1: Linearity data obtained for Rhodamine 123

Concentration (µM)	Fluorescence (Fluorescent arbitrary units)
0.0005	33974
0.0025	665733.5
0.005	1526642.5
0.025	6882073
0.05	9879708
0.25	65934535.5
0.5	135877095.5
2.5	745497179.5
5	1549289276
$R^2 = 0.9996$	
Y-intercept = 0	

3.7.2 Accuracy

The accuracy (also known as trueness) of an analytical procedure expresses the familiarity of agreement between the value which is accepted as theoretical and the experimental value. (Ou *et al*., 2001:4620, Kumar *et al*., 2012:4). This also indicates repeatability due to the reliability of the results that were obtained. Rho123 was prepared at a concentration of 5 µM and diluted into concentrations of 3.75 µM, 2.5 µM, and 1.25 µM. The ranges inserted into the 96-well plate were analysed at 11:00 am, 14:00 pm and 18:00 pm. The percentage recovery (%REC) was calculated by means of Equation 3 and subsequently the percentage relative standard deviation (% RSD) was calculated by means of Equation 4.

$$\%\text{REC} = \frac{(\text{experimental concentration})}{(\text{theoretical concentration})} \text{ x } 100 \qquad \textit{Equation 3}$$

$$\%\text{RSD} = \frac{(\text{ SD})}{(\text{ Average \%REC})} \times 100 \qquad \textit{Equation 4}$$

Table 3.2 shows that the method yielded a mean % REC of 100.80% (see Addendum B for the data obtained) with a %RSD of 1.12% across the samples. These %REC values are within the acceptable limits recorded by Singh (2013:26-33) which states that the %REC should be between the limits of 98 to 102%.

It has been accepted as usable if the %RSD ≤ 2% (Ou *et al*., 2001:4619-4626). Since this method resulted in a %RSD of 1.12%, it was accepted as reliable and repeatable.

Table 3-2 Rhodamine 123 recovery from spiked samples

Time	% Recovery						Mean	SD	%RSD
11:00	101.28	100.35	100.30	101.61	101.48	100.13	100.86	0.61	0.60
14:00	99.86	101.84	100.47	100.53	98.70	103.15	100.76	1.42	1.41
18:00	100.17	103.56	100.03	101.30	99.64	99.93	100.77	1.35	1.34
				Between Readings			**100.80**	**1.13**	**1.12**

3.7.3 Specificity

Specificity is the ability to accurately test for a substance in the presence of other components which may or may not influence the substance itself (Ou *et al*., 2001:4620, Kumar *et al*., 2012:4). To accomplish this, Rho123 was analysed separately as well as in the presence of each of the surfactants to determine the possible effects they could have on the analytical method. Rho123 (5 µM) and KRB were respectively pipetted into an opaque 96-well plate six-fold to serve as control groups. Furthermore, surfactants combined with Rho123 at a concentration of 1.0% (w/v) was pipetted into the plate. This was once more done in six-fold and represented the highest concentration of surfactant used in the transport studies.

The surfactants were diluted in KRB to a concentration of 1.0% (w/v) was pipetted into the plate in six-fold. Two replicates of a standard range were added to the plate to estimate linearity, subsequently a linear regression analysis was done, and the data obtained was used to determine the %RSD of the respective surfactants as seen in Table 3.3.

Table 3-3: Rhodamine 123 recovery from spiked samples

	Theoretical concentration (µM)	**Mean Fluorescence (fluorescent arbitrary units)**	**Experimental concentration (µM)**	**Accuracy (%)**
Rho123	5	1370756158	5.01	100.21
Rho123/Brij® 58	4.98	1394472254	5.10	101.94
Rho123/Tween® 20	4.98	1348161872	4.89	98.35
Rho123/Span® 20	4.98	1402411966	5.13	102.52
Rho123/Cremophor® CO40	4.98	1382511356	5.02	100.85
Rho123/NaDC	4.98	1365923149	4.96	99.65

3.7.4 Precision

The precision of an analytical procedure expresses the closeness of agreement (also known as repeatability) between a series of measurements obtained from multiple sampling of the same homogeneous sample under the prescribed conditions (USP, 2014; Kumar *et al.,* 2012:3-11). The results obtained from this procedure are expressed as %RSD or standard deviation (SD) of a series of samples (USP, 2014). Precision can be divided into two categories namely intra-day and inter-day precision (Kumar *et al.,* 2012:3-11).

3.7.4.1 Intra-day precision (repeatability)

The intra-day precision test is conducted through multiple sampling under consistent operating conditions over a short period of time (ICH, 2005). Rho123 samples were analysed at concentrations of 5 µM, 3.75 µM, 2.5 µM, 1.25 µM, 0.5 µM and 0.05 µM directly after each other as seen in Section 3.7.2. The samples were pipetted into the 96-well plate in triplicate.

Table 3.2 shows that the intra-day precision was achieved with a %RSD value of 1.12%. For the intra-day precision (repeatability) to be compliant the %RSD must be lower than 2.0% (USP, 2014).

3.7.4.2 Inter-day precision

Rho123 solutions were prepared containing 5 µM, 2.5 µM and 0.0125 µM Rho123 respectively. The samples were analysed over three consecutive days to subsequently determine the inter-day variability of the analysis method. The samples were pipetted into a 96-well microplate in triplicate. Two standard ranges were prepared in the plate. For the inter-day precision to be acceptable the %RSD must be lower than 5% (USP, 2014).

As seen in Table 3.4, the fluorescence analysis method for Rho123 was acceptable since the %RSD is 0.81% (as seen in Addendum B) which is lower than the required %RSD of 5%.

Table 3-4: Inter-day precision obtained for Rhodamine 123

	% Recovery			**Mean**	**SD**	**%RSD**
Day 1	101.77	99.69	102.64	101.37	1.24	1.22
Day 2	99.62	100.61	100.20	100.14	0.41	0.41
Day 3	100.04	99.39	101.31	100.25	0.80	0.80
		Between days		**100.58**	**0.81**	**0.81**

3.7.5 Limits of detection and quantification

Limit of detection (LOD) is a term that describes the lowest concentration of an analyte that can be accurately detected, but not necessarily quantified (Ou *et al*.,2001 :4619-4626, Kumar *et al*.,2012:3-11). Samples or ranges with known concentrations were analysed and the level of variability was assessed to establish the minimum level where the analyte can be reliably detected (Ou *et al*., 2001:4619-4626, Kumar *et al.,* 2012:3-11). The LOD was determined using Equation 5 as seen below (ICH, 2005). The LOD for Rho123 is 0.0002 µM (See Addendum B for calculations).

$$\mathrm{LOD} = (3.3\ \sigma)/S \qquad \textit{Equation 5}$$

Where 3.3 in equation 5 is the factor constant representing the signal-to-noise ratio, σ**,**represents the standard deviation (SD) of the KRB blanks and S represents the slope of the standard regression line.

According to Kumar *et al.,* (2012:7) the limit of quantification (LOQ) is known as the concentration level above which the concentration can be precisely and accurately determined, usually with a %RSD < 3% (Singh, 2013:31). The LOQ was determined by using Equation 6 (ICH, 2005). The LOQ of Rho123 is 0.0005 µM. The %RSD was determined as 1.62% which is acceptable (See Addendum B for calculations).

$$\mathrm{LOQ} = (10\ \sigma)/S \qquad \textit{Equation 6}$$

Where 10 in equation 6 represents the factor constant representing the signal-to-noise ratio,σ**,** represents the standard deviation (SD) of the KRB blanks and S represents the slope of the standard regression line.

3.8 Conclusion of validation

After carefully accessing the accuracy, precision, limits of detection and quantification, specificity and linearity of the model drug Rho123, the method was deemed acceptable. Lucifer yellow showed no transport across the porcine intestinal tissue, indicating that the intestinal tissue was still viable after the 120 min transport study was completed.

CHAPTER 4

RESULTS AND DISCUSSION

The potential of five selected surfactants was investigated to evaluate if they had the ability to alter the transport of Rhodamine 123 (Rho123) across porcine intestinal epithelia. *In vitro* transport studies were conducted in the apical to basolateral (AP-BL) direction, as well as the basolateral to apical (BL-AP) direction, across excised segments of porcine jejunum tissue using the Sweetana-Grass diffusion apparatus.

The model was validated by evaluating the integrity of the excised porcine intestinal jejunum tissue using a 50 µM Lucifer yellow (LY) to ensure cumulative transport (%) of Rho123 was not the result of leaky tissue. In addition to LY exclusion, trans-epithelial electrical resistance (TEER) was measured at 20 min intervals to insure the integrity of the jejunum tissue was maintained throughout the transport study.

Permeation of Rho123 (5 µM) alone was used as the control, and transport of Rho123 in combination with the various surfactants was compared to transport obtained with the control study to determine if the surfactants had altering effects on the permeation, and to what extent. Samples were collected at 20 min intervals, and were analysed by means of a validated fluorescence detection method (see Section 3.7). The cumulative Rho123 transport (%) was measured, and the apparent permeability coefficients (P_{app}) and efflux ratios (ER) were subsequently calculated. Statistical analysis of the results consisted of ANOVA analyses with a suitable *post hoc* test (Dunnett t-tests) to determine if the results from the test groups (with surfactant) differed statistically significant relative to that of the control group (Rho123 only). Statistical significance was demonstrated if $p < 0.05$ and is indicated by an asterisk (*). If $p < 0.01$, the result is indicated by a double asterisk (**).

4.1 *In vitro* transport of Lucifer Yellow

The apical to basolateral transport of a 50 µM Lucifer yellow (LY) solution was measured to assess the membrane integrity of the porcine intestinal tissue gathered from the local abattoir. The results were plotted as a function of time and is presented in Figure 4.1.

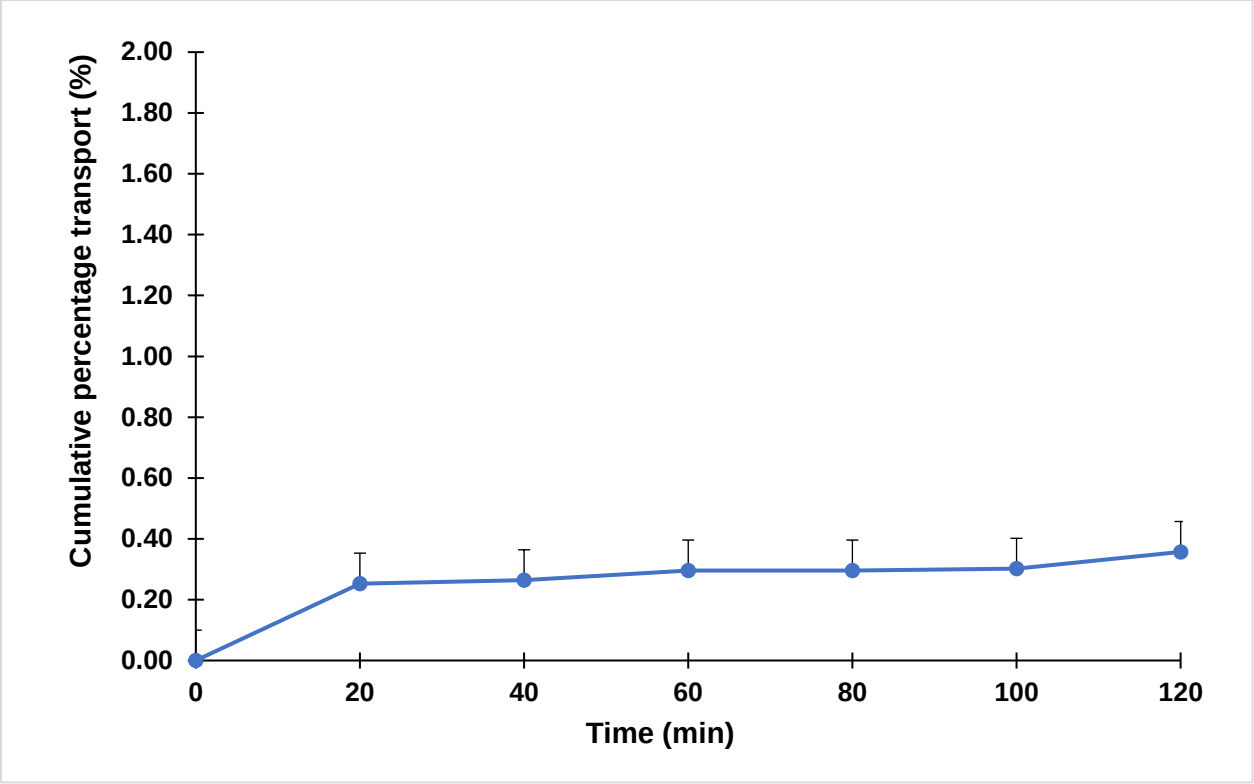

Figure 4.1: The cumulative percentage transport of Lucifer yellow across excised porcine jejunum tissue in the apical to basolateral direction, plotted as a function of time

The maximum cumulative percentage transport of LY was 0.36% (see Addendum C for data collected). This percentage transport obtained is well within the allowable 2.0%, and indicates that the tissue remained intact and viable for the duration of the study (Wahlang *et al.*, 2011:275-282). These results indicate that the procedure used to prepare and mount the tissue in the Sweetana-Grass diffusion chambers as well as the model is suitable for the proposed studies for the extent of time proposed.

4.2 *In vitro* transport of Rhodamine 123 (control group)

The bidirectional transport of Rho123 across excised porcine intestinal jejunum tissue was measured to serve as a control for this study. Samples were collected at 20 min intervals for a duration of 120 min, and the data obtained were expressed as the percentage cumulative transport (%) of Rho123 (5 µM) from the donor chamber.

The cumulative percentage Rho123 transported across the excised porcine jejunum tissue is presented as a function of time in Figure 4.2 (data can be seen in Addendum C).

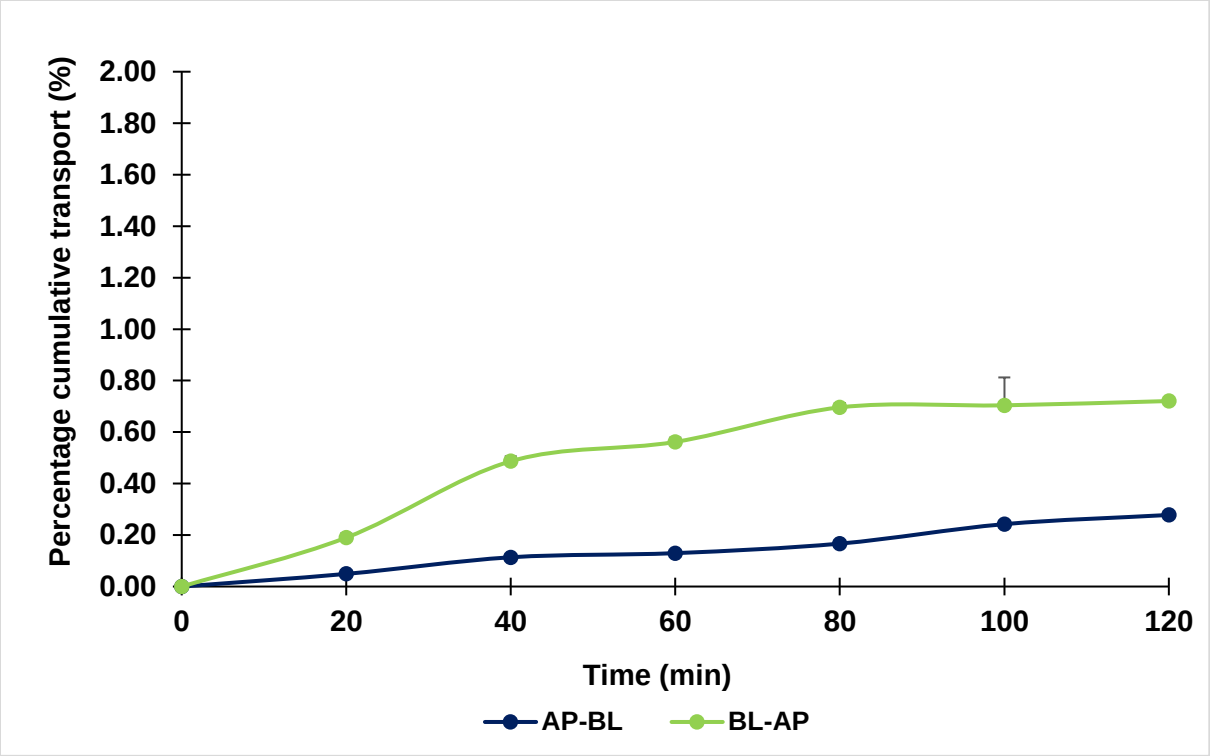

Figure 4.2: The cumulative percentage bidirectional transport of Rho123 across excised porcine jejunum tissue, plotted as a function of time.

Efflux transporters like P-glycoprotein (P-gp) found in the apical epithelial tissue of the intestine, favours the transport of substances out of the cell and into the lumen, thus favouring secretory transport (Silva *et al*., 2015:1-2). From Figure 4.2 it can be observed that for the model compound, Rho123, a higher percentage transport was measured in the BL-AP direction with a maximum percentage transport of 0.72%, whereas transport in the AP-BL direction yielded a maximum percentage transport of 0.28%. This suggests that Rho123 was subjected to P-gp related efflux transport to some extent.

The cumulative percentage transport data was subsequently used to calculate the apparent permeability coefficient (P_{app}) values and the efflux ratio (ER) values for Rho123, as shown in Table 4.1.

Table 4-1 The apparent permeability coefficient values and efflux ratio values for Rho123 transport across excised porcine jejunum tissue

Cell	P_{app} ($\times 10^{-7}$)		ER
	AP-BL	BL-AP	
1	2.197	6.499	2.958
2	2.031	4.916	2.420
3	2.162	5.634	2.606
Mean	**2.130**	**5.683**	**2.662**
SD	**0.088**	**0.793**	**0.273**

As shown in Table 4.1, the mean P_{app} values calculated for Rho123 were 2.130 ± 0.088 and 5.683 ± 0.793 for the AP-BL and BL-AP directions, respectively. The mean ER value representing the efflux ratio for Rho123 was calculated as 2.662 ± 0.273. The mean P_{app} values for the bidirectional transport of Rho123 across excised porcine intestinal tissue, in the absence of any surfactants are illustrated in Figure 4.3.

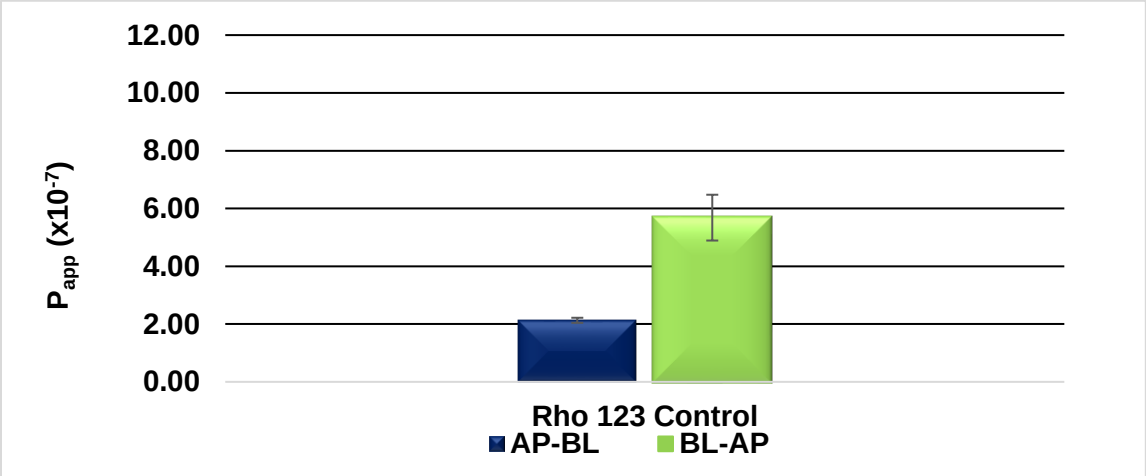

Figure 4.3: The mean P_{app} values for Rho123 transport across excised porcine jejunum segments.

The standard deviation (SD) values for the mean P_{app} and ER values for the transport of Rho123, the model compound, was relatively low as indicated in Table 4.1. This demonstrates that the extent of transport and P-gp related efflux of Rho123 had suistainable repeatability in the porcine jejunum model. The data obtained from the Rho123 transport study also confirms that it is a suitable and reliable model compound to investigate the potential pharmacokinetic interactions of co-administrated surfactants, and their possible effects on the permeation of Rho123 across intestinal epithelia. Studies by Al-Mohizea (2015:617) and Tang (2004:1185) also showed that Rho123 is a substrate for the efflux transporter P-gp, and therefore has limited intestinal absorption. This was demonstrated in the results of this study as well.

4.3 *In vitro* bidirectional transport of Rho123 in the presence of Brij® 58

Polyoxyl 20 cetyl ether (Brij® 58) is a known P-gp inhibitor and could, therefore, potentially improve the absorption of a P-gp substrate like Rho123 across intestinal epithelium through suppression of efflux mediated by the P-gp transporter (Zhao *et al*., 2016:1527). The bidirectional transport of Rho123 in the presence of three concentrations of Brij® 58 (0.1% (w/v), 0.5% (w/v) and 1% (w/v)) over a period of 120 min is presented in Figure 4.4 and Figure 4.5.

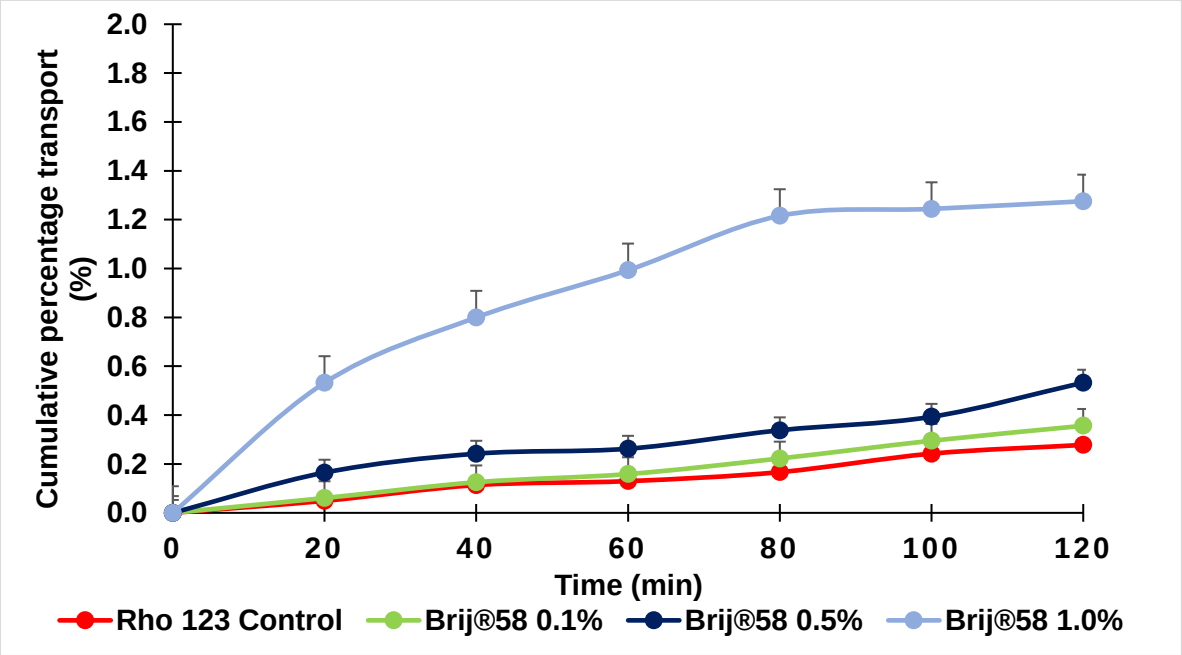

Figure 4.4: The cumulative percentage transport of Rho123 across excised porcine jejunum tissue in the apical to basolateral direction, plotted as a function of time, in the presence of 0.1% (w/v), 0.5% (w/v) and 1.0% (w/v) Brij® 58

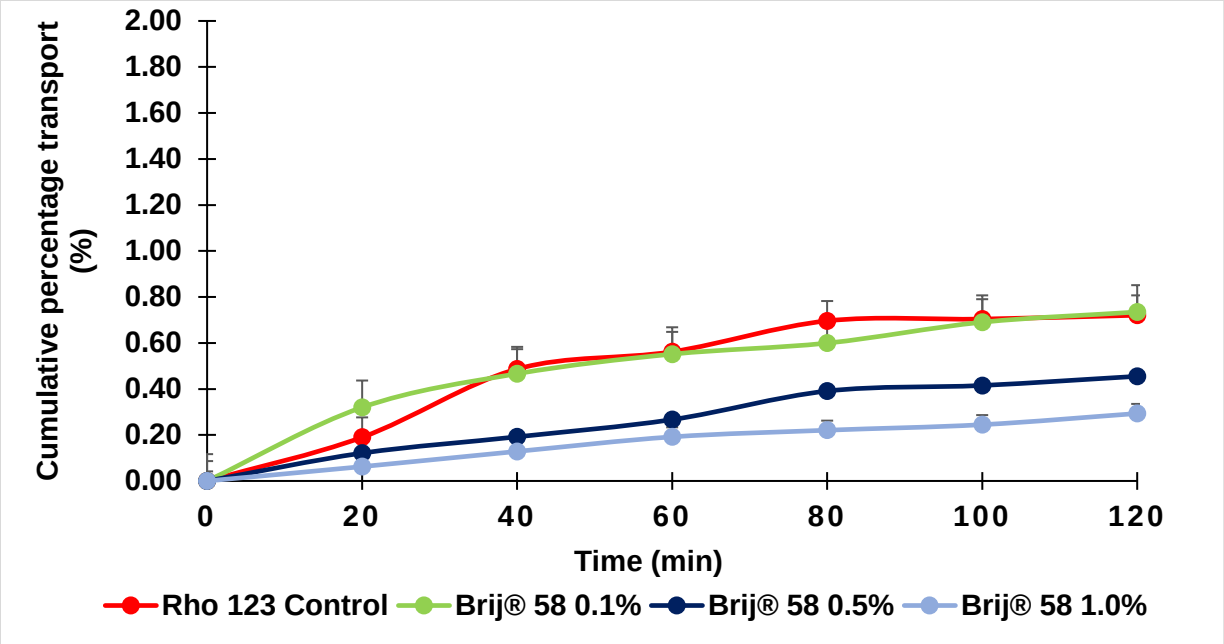

Figure 4.5: The cumulative percentage transport of Rho123 across excised porcine jejunum tissue in the basolateral to apical direction, plotted as a function of time, in the presence of 0.1% (w/v), 0.5% (w/v) and 1.0% (w/v) Brij® 58

When compared with the cumulative percentage transport of the control sample (Rho123 with no Brij® 58), a concentration of 0.1% Brij®58 mediated no significant increase in Rho123 transport ($p > 0.05$). However, when the concentration Brij®58 present was increased to 0.5% (w/v) and 1% (w/v), a statistically significant increase in Rho123 transport was observed ($p < 0.05$ and $p < 0.01$). The secretory (BL-AP) transport of Rho123 in the presence of 0.5% (w/v) and 1% (w/v) Brij®58 decreased in comparison to the Rho123 control group as seen in Figure 4.5, with a statistical significance of $p < 0.01$ for both concentrations. No statistically significant change in P -gp related efflux of Rho123 was observed in the presence of a Brij® 58 concentration of 0.1% (w/v) ($p > 0.05$).

The P_{app} values for the Rho123 transport in the presence of the various concentrations of Brij®58 were calculated (as seen in Addendum C), and is presented in Figure 4.6.

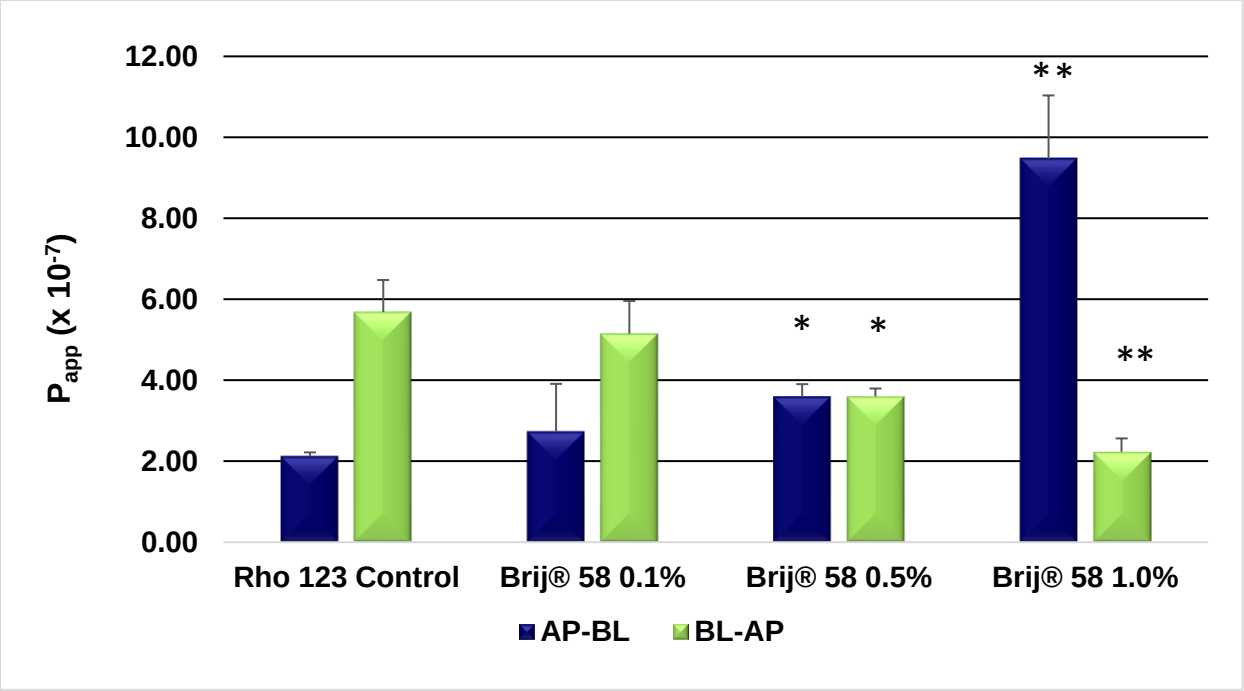

Figure 4.6: The mean P_{app} values of Rho123 transport in the presence of 0.1%, 0.5% and 1.0% (w/v) Brij® 58 in the apical to basolateral and basolateral to apical direction. Statistically significant differences (compared to the control samples) are indicated with an asterisk (*) where $p < 0.05$ and with a double asterisk (**) where $p \leq 0.01$

Although 0.1% (w/v) Brij® 58 mediated no statistically significant increase in Rho123 transport in the apical to basolateral direction, it can be observed in Figure 4.4 and 4.6 that transport was slightly increased from 0.278% to 0.356%. The increase in the P_{app} for 0.5% (w/v) Brij® 58 was 1.91-fold and 4.57-fold for 1% (w/v) Brij® 58 ($p < 0.05$ and $p < 0.01$ respectively).

In the BL-AP direction a statistically significant decrease in P_{app} of Rho 123 can be seen in the presence of 0.5% (w/v) Brij® 58 ($p < 0.01$) and 1.0% (w/v) Brij® 58 ($p < 0.01$), while no statistically significant decrease was observed at a concentration of 0.1% (w/v) Brij®58 ($p=0.532$), as shown in Figures 4.5 and 4.6.

Although Brij® 58 is a known P-gp inhibitor, a reduction in TEER over the course of 120 mins was recorded for 0.5% (w/v) Brij® 58, and 1.0% (w/v) Brij® 58. These results can possibly indicate the opening of tight junctions, which would also result in higher levels of transport for P-gp substrates, like Rho123, as seen in a previous *in vitro* study (Zhao *et al*., 2016:1527). Brij® 58 presented a concentration dependant increase of cumulative Rho123 transport in the absorptive (AP-BL) direction.

The P_{app} values were subsequently used to calculate the ER for Rho123 in the presence of Brij® 58 (by means of Equation 2 in Chapter 3). The ER values of Rho123 in the presence of selected Brij® 58 concentrations was compared to that of Rho123 alone, and is illustrated in Figure 4.7.

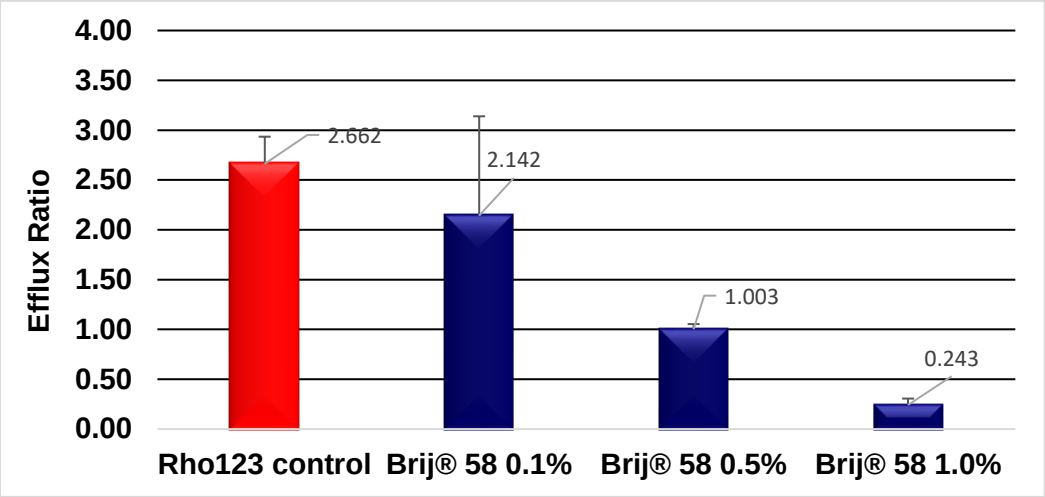

Figure 4.7: The efflux ratio values for Rho123 transport in the absence and presence of 0.1%, 0.5% and 1.0% (w/v) Brij® 58

At a concentration of 0.1% (w/v) the ER was 2.142, while the ER halved to 1.003 at 0.5% (w/v) and at 1.0% (w/v) the ER was 0.243. The change in ER values is possibly due to the concentration dependent inhibition of efflux in the presence of increasing Brij® 58 concentrations as seen in Figure 4.7. The resulting apparent increase in Rho123 transport in the AP-BL direction (as seen in Figures 4.4 and 4.6), is a direct result of P-gp related efflux inhibition.

4.3.1 Discussion

In a recent study conducted by Zhao *et al.* (2016:1526-1534) it was observed that Brij® 58 could potentially inhibit P-gp related efflux in compounds known to be P-gp substrates. No P-gp inhibitory effects were seen in compounds that were not P-gp substrates. The increase in the cumulative percentage transport they observed was not because of alteration of the tight junctions' structure, the authors concluded that paracellular transport was increased. It was confirmed by Zhang *et al.* (2016:832-843) that various types of Brij® inhibit P-gp. The concentration dependant reduction in ER in the presence of Brij® that is evident in Figure 4.7, is consistent with the data obtained in these previous studies, and it can be concluded that Brij® 58

inhibited the P-gp related efflux of the model compound, Rho123, and can potentially be used to increase transport of other P-gp substrates (Zhao *et al*., 2016:1526-1534; Zhang *et al*., 2016:832-843).

4.4 *In vitro* bidirectional transport of Rho123 in the presence of Cremophor® CO40

Polyoxyl 40 hydrogenated castor oil is a surfactant that has been identified as an inhibitor of the P-gp efflux transporter and/or cytochrome P450 3A (CYP3A). In the event that P-gp is inhibited by Cremophor® CO40, the transport of Rho123 ought to increase and the P-gp related efflux should be suppressed (Zhao *et al*., 2013:429). The bidirectional transport of Rho123 in the presence of three concentrations Cremophor® CO40 (0.1%, 0.5% and 1.0% (w/v)) was investigated and expressed as cumulative percentage transport.

The cumulative percentage transport of Rho123 in the presence of the various concentrations of Cremophor® CO40, in both the AP-BL and BL-AP directions, was plotted as a function of time in Figures 4.8 and 4.9, respectively.

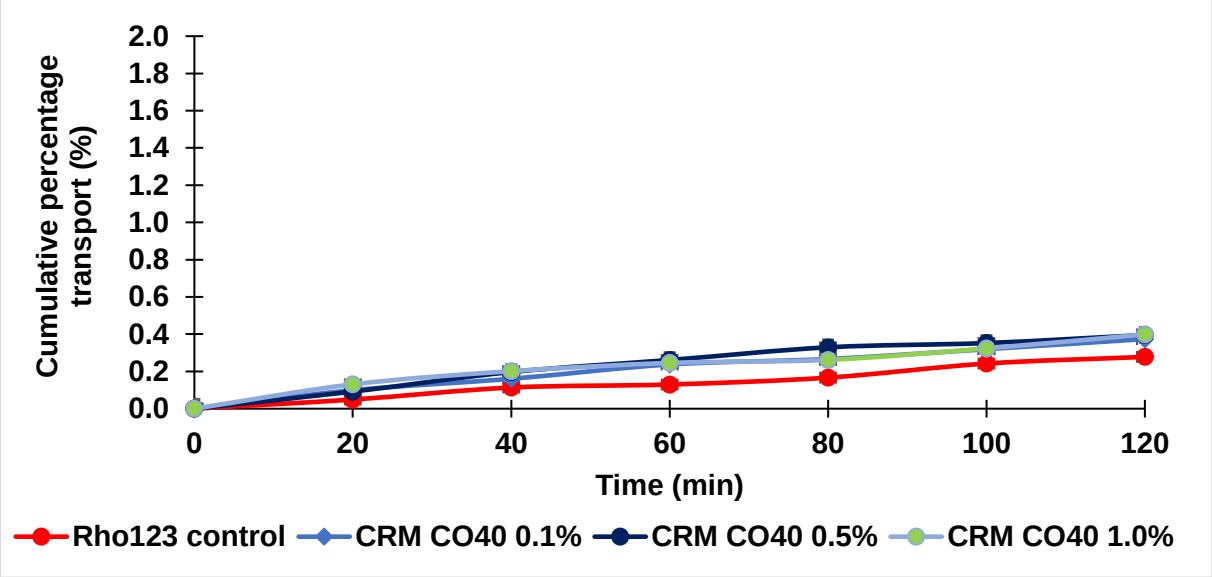

Figure 4.8: The cumulative percentage transport of Rho123 across excised porcine jejunum tissue in the apical to basolateral direction, plotted as a function of time, in the presence of 0.1% (w/v), 0.5% (w/v) and 1.0% (w/v) Cremophor® CO40

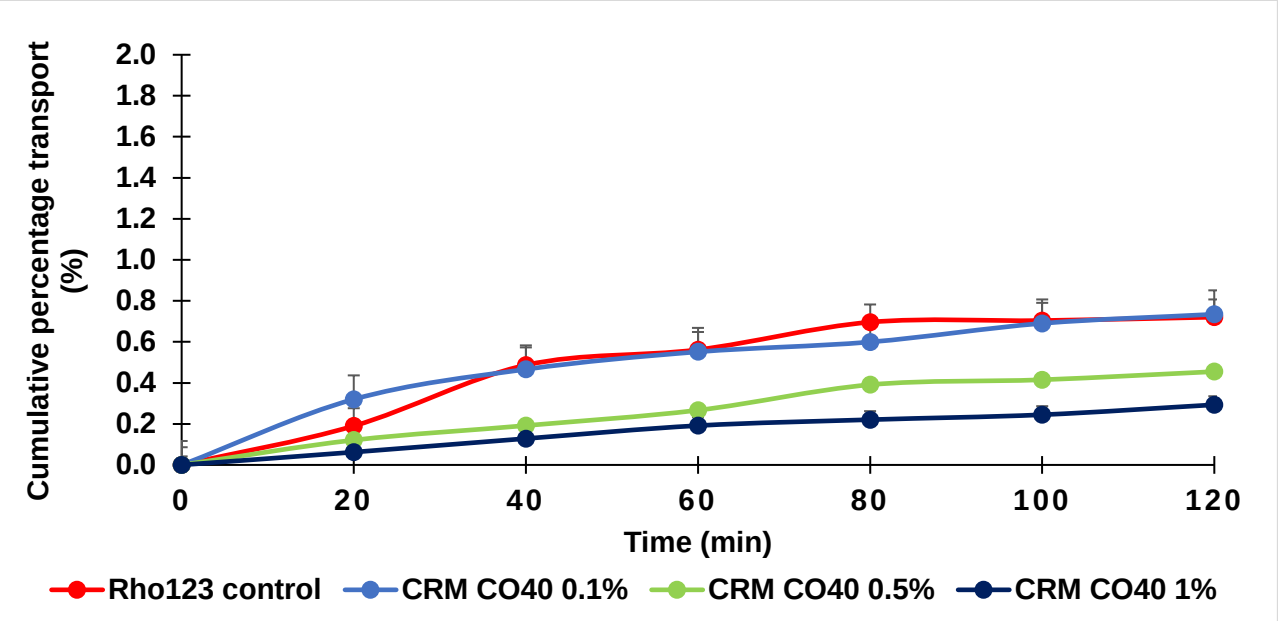

Figure 4.9: The cumulative percentage transport of Rho123 across excised porcine jejunum tissue in the basolateral to apical direction, plotted as a function of time, in the presence of 0.1% (w/v), 0.5% (w/v) and 1.0% (w/v) Cremophor® CO40

Although, a slight increase in Rho123 transport in the absorptive direction can be seen in Figures 4.8 and 4.10, in the presence of Cremophor® CO40 the cumulative percentage transport of Rho123 presented no statistically significant ($p > 0.05$) increase in the AP-BL direction at concentrations of 0.1% (w/v) ($p > 0.05$), 0.5% (w/v) ($p > 0.05$) or 1.0% (w/v) ($p > 0.05$).

Transport in the BL-AP direction yielded a statistically significant ($p < 0.05$) decrease in Rho123 transport in the presence of Cremophor®CO40 at concentrations of 0.1% (w/v), 0.5% (w/v) and 1.0% (w/v), where $p < 0.05$. The decrease in secretory transport suggests that Cremophor® CO40 inhibited efflux probably due to inhibiting P-gp.

The P_{app} values for the transport of Rho123 in the presence of the various concentrations of Cremophor® CO40 were calculated as seen in Addendum C (Table C.2), and is presented in Figure 4.10.

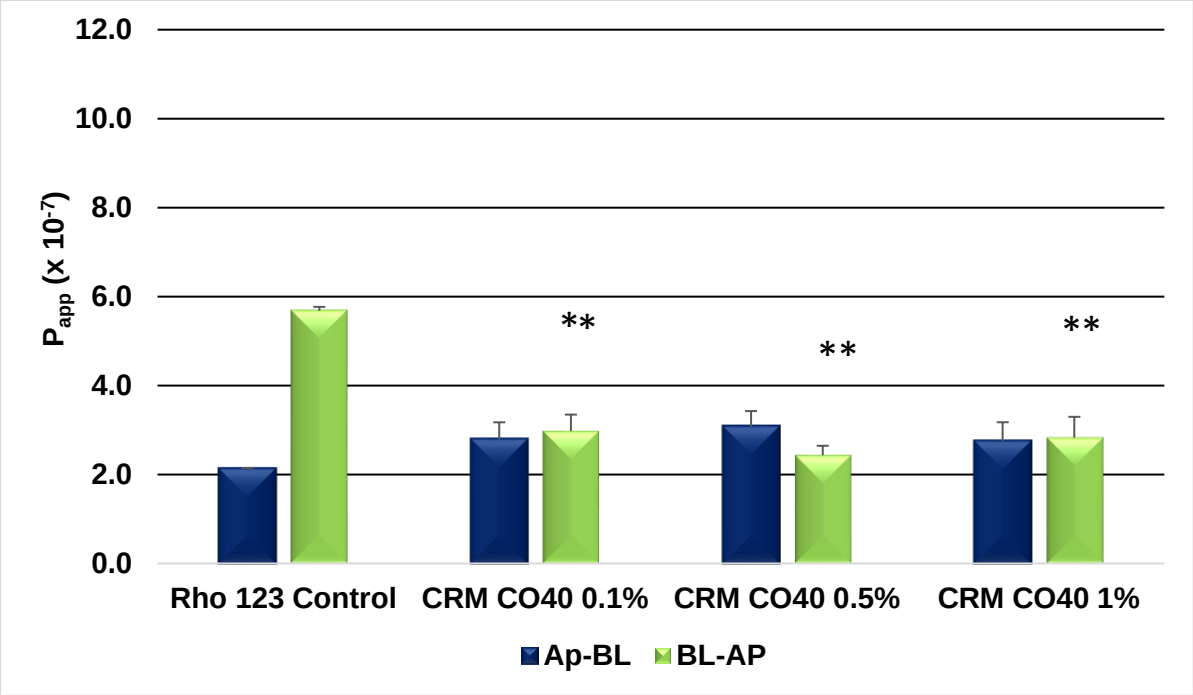

Figure 4.10: The mean P_{app} values of Rho123 transport in the presence of 0.1%, 0.5% and 1.0% (w/v) Cremophor® CO40 in the apical to basolateral and basolateral to apical direction. Statistical significance ($p < 0.05$) is indicated with an asterisk (*) and ($p < 0.01$) is indicated with a double asterisk (**)

Although not statistically significant, a slight increase in the P_{app} of Rho123 (AP-BL direction) in the presence of 0.1% (w/v), 0.5% (w/v) and 1.0% (w/v) Cremophor® CO40 can be seen in Figure 4.10. The P_{app} of Rho123 in the presence of 0.1% (w/v) Cremophor® CO40 increased with 0.76-fold, while 0.5% (w/v) and 1.0% (w/v) Cremophor®CO40 yielded a 0.69 and 0.77-fold increase, respectively.

A reduction in TEER for 0.1% w/v, 0.5% (w/v) and 1.0% (w/v) Cremophor® CO40 was recorded in the AP-BL direction, thus indicating the opening of tight junctions. This could result in an increase in the transport of P-gp substrates like Rho123, although the increase in P_{app} was not statistically significant.

A decrease in the P_{app} for the BL-AP was observed for all concentrations of Cremophor® CO40 ($p < 0.01$), as seen in Figure 4.10. The SD in Figures 4.10 and 4.8 was low, which shows good repeatability of Rho123 transport in the presence of Cremophor® CO40.

The ER for Rho123 in the presence of Cremophor® CO40 was calculated by means of the P_{app} values and Equation 2 (Chapter 3),and are presented in Figure 4.11.

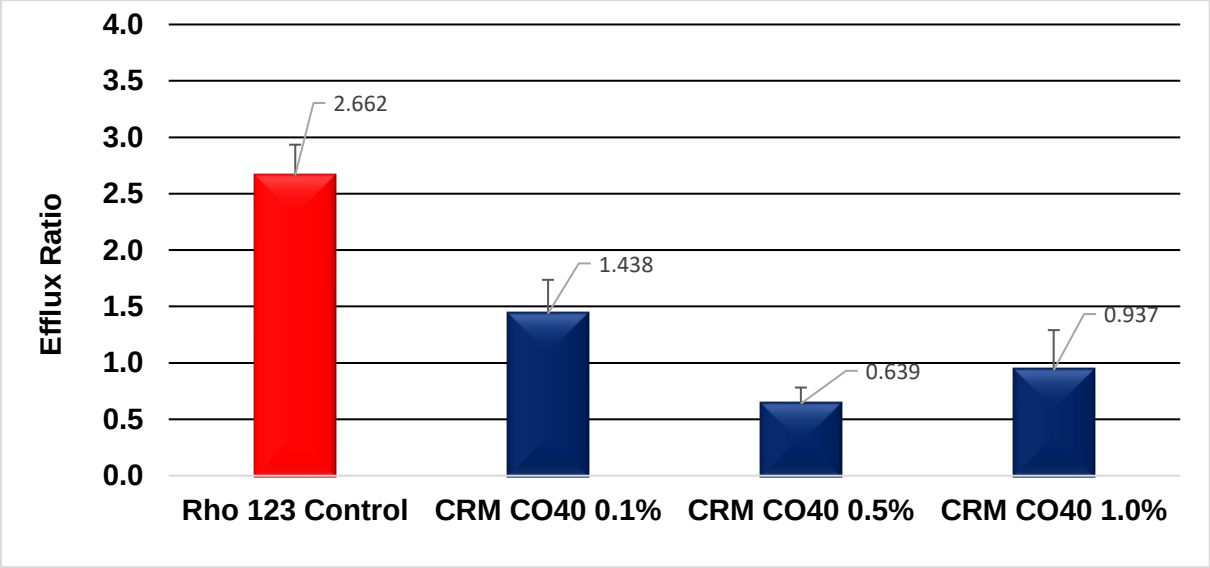

Figure 4.11: The efflux ratio values of Rho123 transport in the absence and presence of 0.1%, 0.5% and 1.0% (w/v) Cremophor® CO40

The ER in the presence of Cremophor® CO40 decreased in comparison to the Rho123 control group. At a concentration of 0.1% (w/v) the ER was 1.438, while the ER decreased to 0.639 at 0.5% (w/v) and at 1.0% (w/v) the ER was 0.937. The change in ER values is possibly due to the inhibition of efflux in the presence of increasing Cremophor® CO40 concentrations as seen in Figure 4.11. The resulting apparent increase in Rho123 transport in the AP-BL direction (as seen in Figure 4.8 and 4.10), is a direct result of P-gp related efflux inhibition.

4.4.1 Discussion

In a recent study, the absorption of fenofibrate in the presence of 2.0% (w/v), 15% (w/v) and 25% (w/v) Cremophor® CO40 was tested and an optimum increase in absorptive transport was seen at 15% (w/v), although the critical micelle concentration (CMC) of Cremophor® CO40 is 0.02% (w/v) (Berthelsen *et al*., 2015:1062-1071).

The micellar trapping theory claims that 'increasing surfactant concentrations above the CMC will increase the micellar solubilisation and decrease the amount of free fraction of drug (Rho123 in this case) available for intestinal permeation' (Miller *et al*., 2011:1848-1856; Dahan *et al*., 2012:244-251; Berthelsen *et al*., 2015:1062-1071). The micelle formation could therefore have

led to the limited permeation of Rho123 in the presence of Cremophor® CO40 in the apical to basolateral direction.

The results of this study suggest that Cremophor® CO40 inhibited P-gp and suppressed efflux, and as a result decreased the secretory transport. However, it is possible that due to the micellar formation on the apical side of the membrane, no significant increase in absorptive transport was observed.

4.5 *In vitro* transport Rho123 in the presence of Tween® 20

Polysorbate, commercially available as Tween®, has been known to improve the bioavailability of known P-gp substrate drugs by inhibiting their efflux (Zhang, 2009:551). In this study, the effect of various concentrations of Tween® 20 on the bidirectional transport of the model compound, Rho123, was studied. The bidirectional transport of Rho123 in the presence of 0.1% (w/v), 0.5% (w/v) and 1.0% (w/v) Tween® 20, over a period of 120 min, is presented in Figure 4.12 and 4.13.

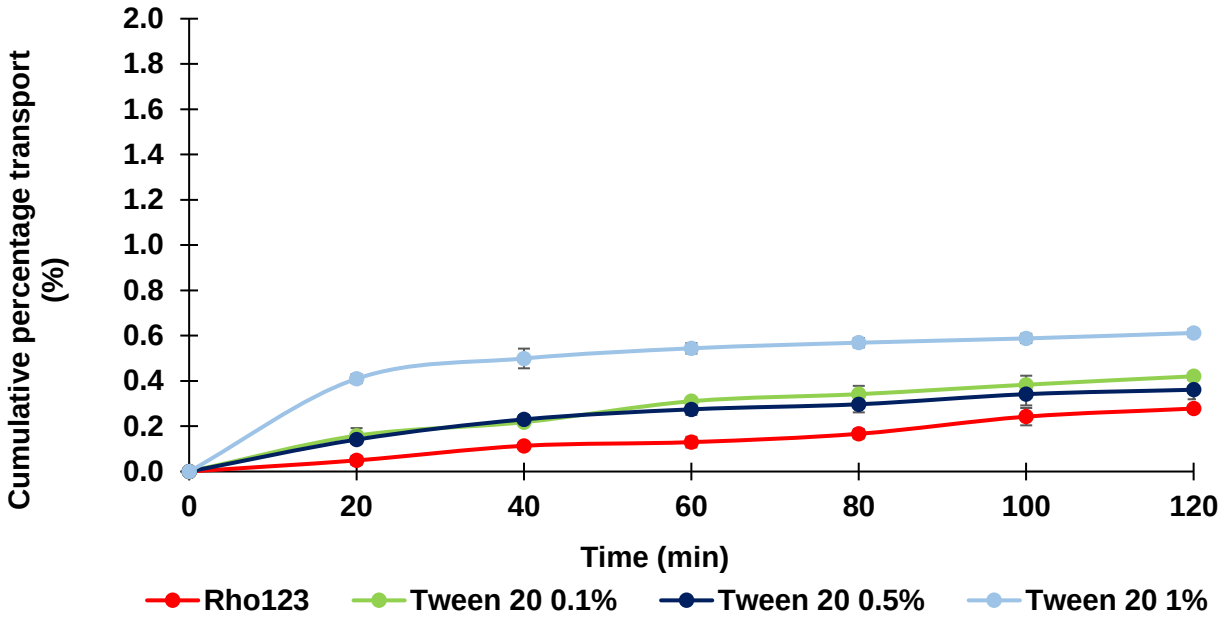

Figure 4.12: The cumulative percentage transport of Rho123 across excised porcine jejunum tissue in the apical to basolateral direction, plotted as a function of time, in the presence of 0.1% (w/v), 0.5% (w/v) and 1.0% (w/v) Tween® 20

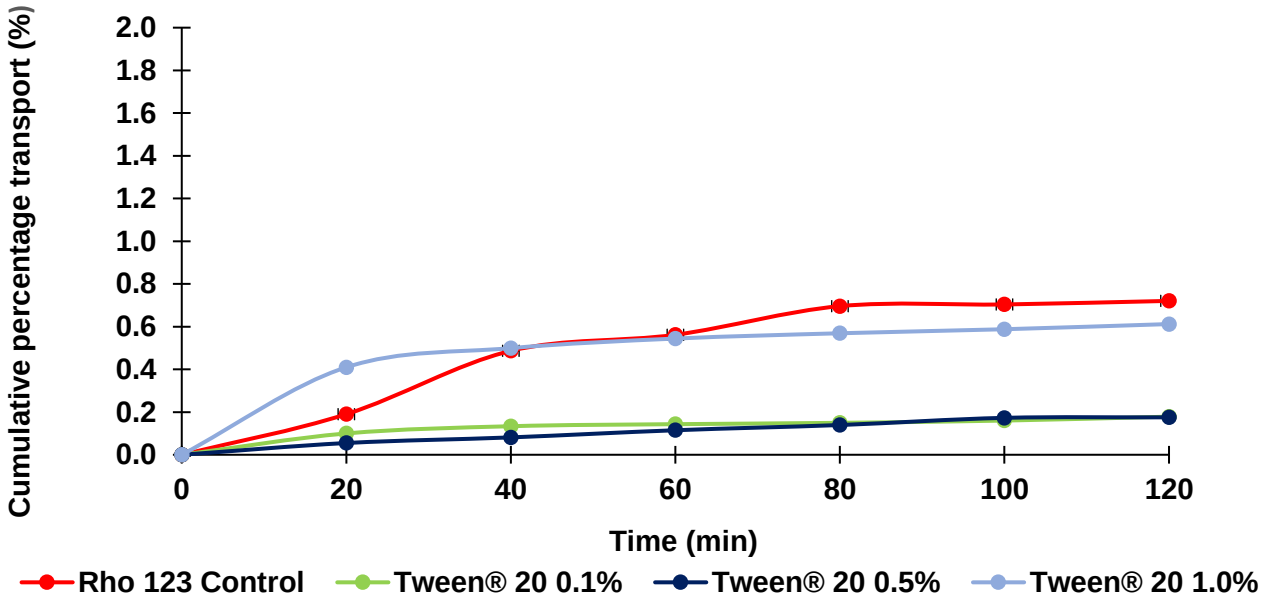

Figure 4.13: The cumulative percentage transport of Rho123 across excised porcine jejunum tissue in the basolateral to apical direction, plotted as a function of time, in the presence of 0.1% (w/v), 0.5% (w/v) and 1.0% (w/v) Tween®20

In comparison to the cumulative percentage transport of the control sample (Rho123 with no Tween®20), 0.1% (w/v), 0.5% (w/v) and 1.0% (w/v) Tween®20 yielded no statistically significant increase in the AP-BL transport of Rho123, as can be observed in Figure 4.12. The secretory (BL-AP) transport of Rho123 in the presence of 0.1% (w/v), 0.5% (w/v) and 1.0% (w/v) Tween®20 decreased in comparison to the Rho123 control group as seen in Figure 4.13.

The P_{app} values of the various concentrations of Tween® 20 were calculated as seen in Addendum C, and is represented in Figure 4.14.

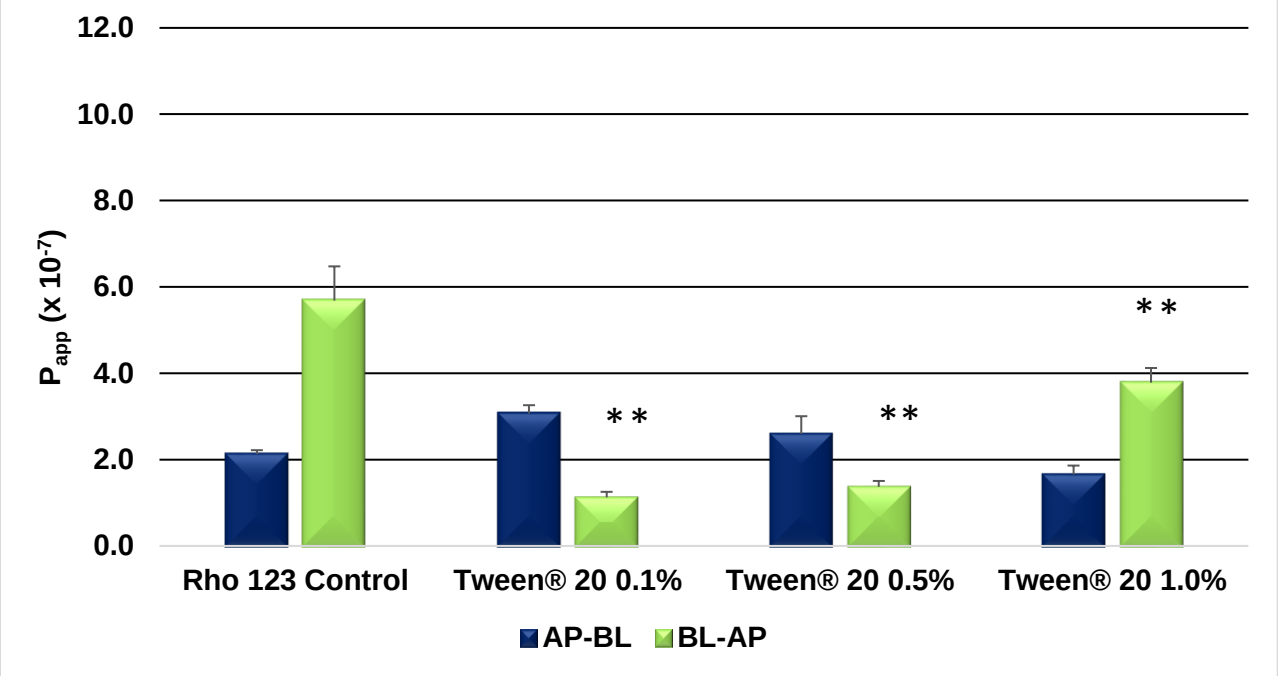

Figure 4.14: The mean P_{app} values of Rho123 transport in the presence of 0.1% (w/v), 0.5% (w/v) and 1.0% (w/v) Tween® 20 in the apical to basolateral and basolateral to apical direction. Statistical significance is indicated with an asterisk (*) where ($p < 0.05$) and with a double asterisk (**) where ($p < 0.01$)

Concentrations of 0.1% (w/v) and 0.5% (w/v) Tween® 20 mediated a slight increase in the P_{app} of Rho123 in the apical to basolateral direction, although not statistically significant, as seen in Figure 4.14.

Reduction in TEER values of 41.13 % for 0.1% (w/v) Tween® 20, 47.83% for 0.5% (w/v) Tween® 20 and 47.98% for 1.0% (w/v) Tween® 20 was recorded. The reduction in TEER values signifies the possible opening of tight junctions and should be associated with an increase in the transport of Rho123 in the apical to basolateral direction. Although an increase in the cumulative transport

of Rho123 in the apical to basolateral direction with an increase in Tween® 20 concentration is evident as seen in Figure 4.12, this increase in transport was, however not statistically significant.

In the BL-AP direction, a statistically significant decrease in the P_{app} of Rho123 was seen in the presence of 0.1%, 0.5% and 1.0% Tween® 20 ($p < 0.01$) as shown in Figure 4.14. A 5.06-fold decrease was seen at a concentration of 0.1% (w/v) Tween® 20, while a 4.15 and 1.50-fold decrease was observed at 0.5% (w/v) and 1.0% (w/v) Tween® 20, respectively.

The efflux ratios (ER) were calculated by means of the P_{app} values and Equation 2 (Chapter 3), and is represented in Figure 4.15.

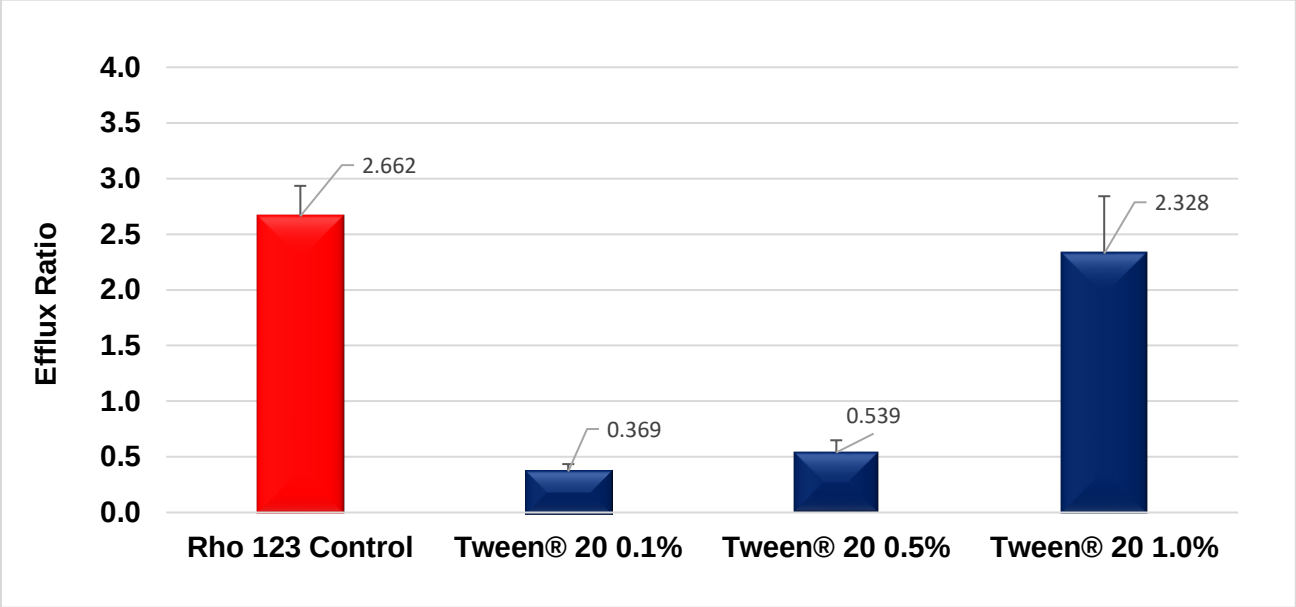

Figure 4.15: The efflux ratio values of Rho123 transport in the absence and presence of 0.1% (w/v), 0.5% (w/v) and 1.0% (w/v) Tween® 20

An inverse proportional relationship can be seen between the concentration and the resulting efflux inhibition as seen in Figure 4.15, where the lowest concentration (0.1% (w/v) Tween® 20 yielded the highest efflux inhibition. The resulting apparent increase in Rho123 transport in the AP-BL direction (as seen in Figure 4.12 and 4.14), is a direct result of P-gp related efflux inhibition.

4.5.1 Discussion

The CMC of Tween® 20 is 0.0074% (w/v) at a temperature range of 20-25°C, with an increase in CMC at temperatures of 37°C at which this experiment was conducted (As seen in Figure 4.14, the absorptive transport of Tween® 20 increased at the lowest concentration (0.1% (w/v)) and thereafter decreased as the concentration increased up to the highest concentration of 1.0% (w/v). In a study conducted by Al-Saraf *et al.* (2016:66-69), the absorption of doxorubicin, a P-gp substrate, was tested *in vitro* as well as *in vivo* in the presence of 0.025% (w/v) Tween® 20. The results concluded that Tween® 20 inhibited efflux and mediated an increase in the transport of doxrubicin across cell monolayers, but not *in vivo* across rat intestinal tissue. This suggested that the effect of Tween® 20 was solely based on the inhibition of efflux. It was indicated by Al-Saraf *et al.* (2016:66-69) that no previous studies showed an increase in AP-BL transport of a P -gp substrate in the presence of Tween® 20, although an increase was found in the study conducted by them. Following the questions of whether Tween® 20 increased or did not increase the absorption of doxorubicin *in vitro*, it is clear that, although not statistically significant ($p < 0.05$), Tween® 20 did increase the absorptive transport of Rho123 in this study slightly at 0.1% and 0.5% (w/v), and further investigation into the permeability altering effects of Tween® 20 is necessary. In this study Tween® 20 0.1% and Tween® 20 0.5% increased the absorptive concentration of Rho 123, but Tween® 20 1.0% decreased the absorptive concentration of the Rho123 indicating no efflux inhibition.

4.6 *In vitro* transport of Rho123 in the presence of Span® 20

Sorbitan monolaurate is a surfactant that is known to inhibit P-gp and consequently inhibit efflux, and therefore should decrease BL-AP transport and possibly increasing AP-BL transport (Bansal *et al*., 2009:1067-1074). The secretory and absorptive transport of Rho123 in the presence of 0.1% (w/v), 0.5% (w/v) and 1.0% (w/v) Span® 20 is represented as a percentage cumulative transport over a period of 120 min, and is illustrated in Figures 4.16 and 4.17, respectively.

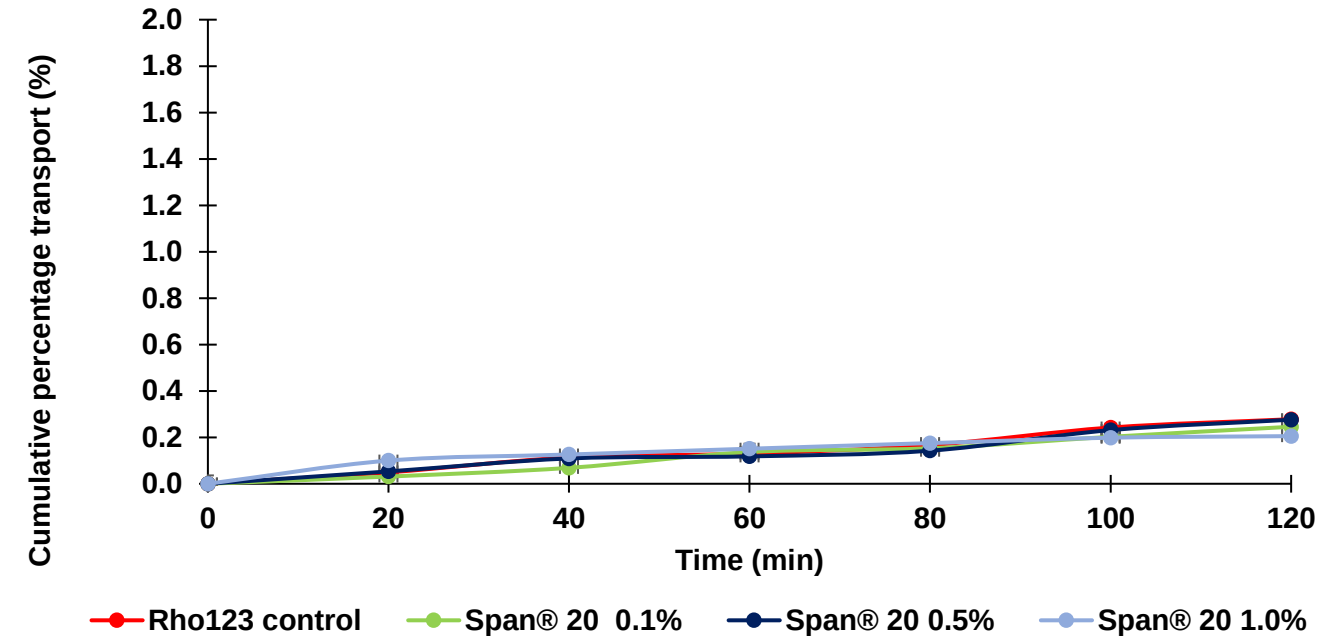

Figure 4.16: The cumulative percentage transport of Rho123 across excised porcine jejunum tissue in the apical to basolateral direction, plotted as a function of time, in the presence of 0.1% (w/v), 0.5% (w/v) and 1.0% (w/v) Span® 20

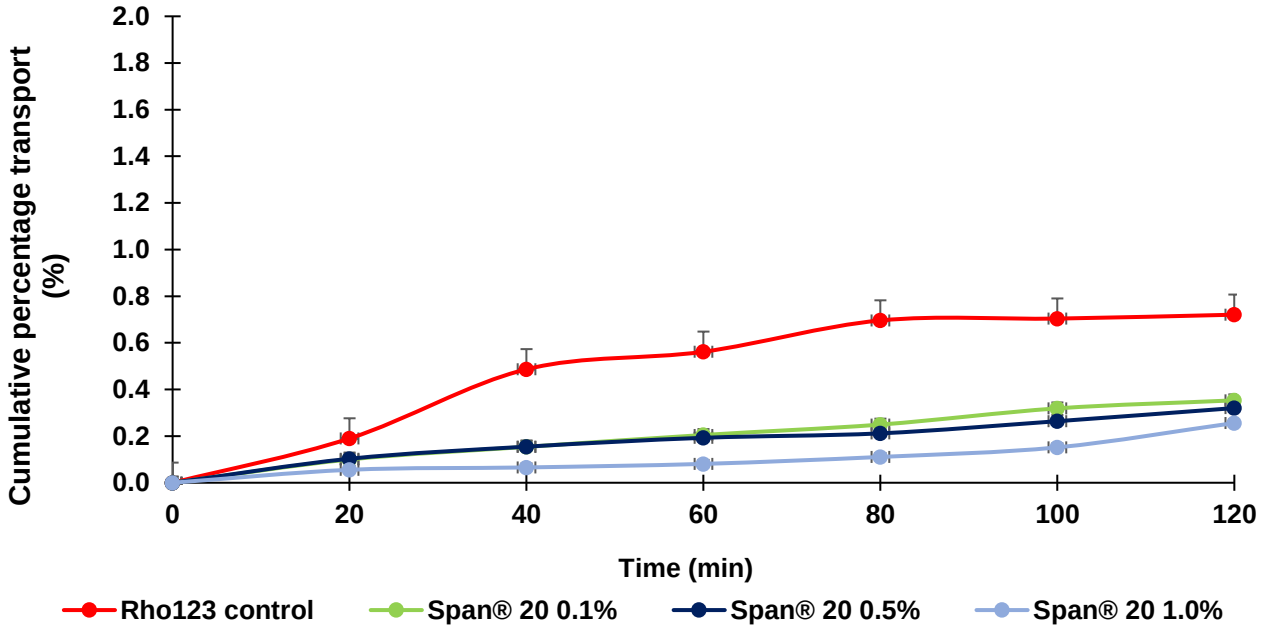

Figure 4.17: The cumulative percentage transport of Rho123 across excised porcine jejunum tissue in the basolateral to apical direction, plotted as a function of time, in the presence of 0.1% (w/v), 0.5% (w/v) and 1.0% (w/v) Span® 20

Rho123 yielded no statistically significant increase in absorptive (AP-BL) transport in the presence of Span® 20 at any of the concentrations ($p > 0.05$), as seen in Figures 4.16 and 4.18. On the contrary, the secretory transport (BL-AP) of Rho123 was decreased in a statistically significant manner ($p < 0.01$) in the presence of all of the Span® 20 concentrations (0.1% (w/v), 0.5% (w/v) and 1.0% (w/v)), as seen in Figures 4.17 and 4.18.

The P_{app} values of the various concentrations of Span® 20 were calculated as seen in Addendum C (Table C.2),and is presented in Figure 4.18.

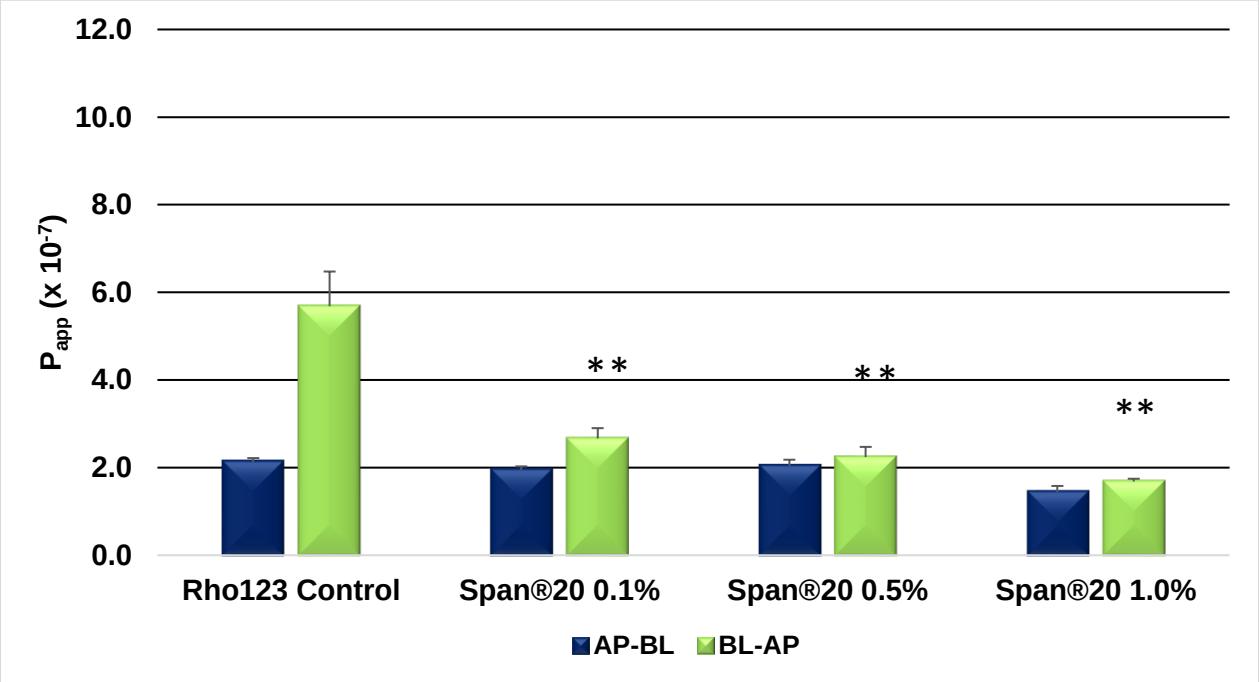

Figure 4.18: The mean P_{app} values of Rho123 transport in the presence of 0.1% (w/v), 0.5% (w/v) and 1.0% (w/v) Span® 20 in the apical to basolateral and basolateral to apical direction. Statistical significance is indicated with an asterisk (*) ($p < 0.05$) and with a double asterisk (**) ($p < 0.01$)

Span® 20 mediated no significant increase in the P_{app} of Rho123 in the apical to basolateral direction. The SD (as indicated by the error bars of Figure 4.18) is relatively small, which indicates that there is good repeatability.

An average TEER reduction of 51.43% ± 2.05 for 0.1% (w/v), 42.04% ± 4.54 for 0.5% (w/v) and 57.98% ± 1.70 for 1.0% (w/v) Span®20 was recorded. A reduction in TEER would theoretically lead to higher absorptive transport due to tight junctions opening, but Span® 20 is a highly viscous

surfactant that forms a dispersion when mixed with a water-like substance like KRB buffer, and this could have led to the lack of an increase in transport of Rho123 in the absorptive direction (Attwood, 2009:430).

The P_{app} of Rho123 in the basolateral to apical direction in the presence of Span® 20 indicated a statistically significant decrease ($p < 0.01$), in efflux as seen in Figure 4.18. Span®20 yielded a concentration dependent decrease in Rho123 transport in the basolateral to apical direction, with a 2.13-fold decrease at a 0.1% (w/v) concentration, a 2.54-fold decrease at a concentration of 0.5% (w/v) and the highest decrease can be seen at a concentration of 1.0% (w/v) yielding a 3.38-fold decrease.

The ER were calculated by means of the P_{app} values and Equation 2 (Chapter 3) and are represented in Figure 4.19.

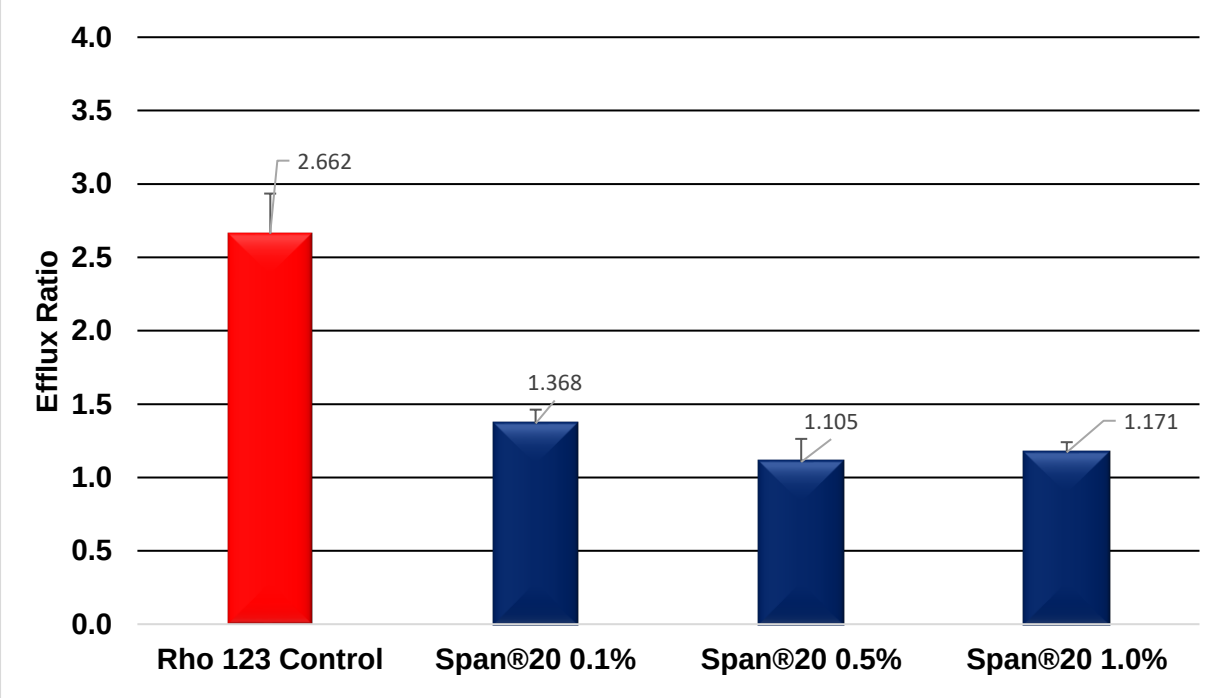

Figure 4.19: The efflux ratio values of Rho123 transport in the absence and presence of 0.1%, 0.5% and 1% (w/v) Span® 20.

The ER values according to Figure 4.19 demonstrates that the main mechanism of transport was active secretion (efflux) were the ER values >> 1 (refer to Section 4.2). Overall, Span® 20 showed a concentration dependent inhibition of Rho123 efflux as seen in Figure 4.19.

4.6.1 Discussion

In a study conducted in 2013, emulsification was used to evaluate the effect of surfactants on the permeability of Coenzyme Q10 (CoQ10) when orally administered to rats. The study concluded that Span® 20 had no significant effect on the permeation of CoQ10 when emulsified. The time necessary to reach maximum effect (t_{max}) was measured and the results showed that full effect was only reached after 4.180 h (Sato *et al.,* 2013:2016). In another study conducted on drug permeation through skin patches, the results concluded that at a concentration of 5.0% (w/v), Span® 20 did enhance the permeation of the active ingredient, 4-phenyl butanol (Lòpez *et* al., 2000:137). In the present study, Span® 20 showed no significant increase in absorption of Rho123, which could be the result of the Span® 20 concentration that was too low (0.1%, 0.5% and 1.0% (w/v)) to have any significant effect, or because the time of exposure was not sufficient for Span® 20 to affect the absorption of Rho123. At a HLB value of 8.6, a dispersion is formed that can lead to poor permeability of Span® 20 across the intestinal epithelia (Attwood., 2009:430). The decrease in Rho123 concentration in the presence of 1.0% (w/v) Span® 20 can be a result of the live tissue variability (Pietzonka *et al*., 2002; Westerhout *et al*., 2014:174).

Rho123 had a significant ($p < 0.01$) decrease in basolateral to apical transport at all concentrations Span® 20, thus illustrating that cumulative, concentration dependant P-gp related efflux inhibition took place while P-gp was inhibited. The data obtained in this study is in line with data found in literature, confirming that Span® 20 is a P-gp inhibitor and, therefore, inhibited P-gp related efflux (Bansal *et al*., 2009:1067-1074). A 3.38-fold decrease in Rho123 concentration was seen in at the highest concentration (1.0%) of Span® 20 used during this study.

4.7 *In vitro* transport of Rho123 in the presence of Sodium deoxycholate.

Sodium deoxycholate (NaDC) is a bile salt that has been used frequently in transport studies as a permeation enhancer. By interacting with the phospholipids in biological membranes, it can enhance drug absorption (Moghimipour *et al*., 2015:14456). The bi-directional transport of Rho123 in the presence of 0.1% (w/v), 0.5% (w/v) and 1.0% (w/v) sodium deoxycholate is presented as a percentage cumulative transport in the AP-BL and BL-AP direction, and was plotted as a function of time in Figures 4.20 and 4.21, respectively.

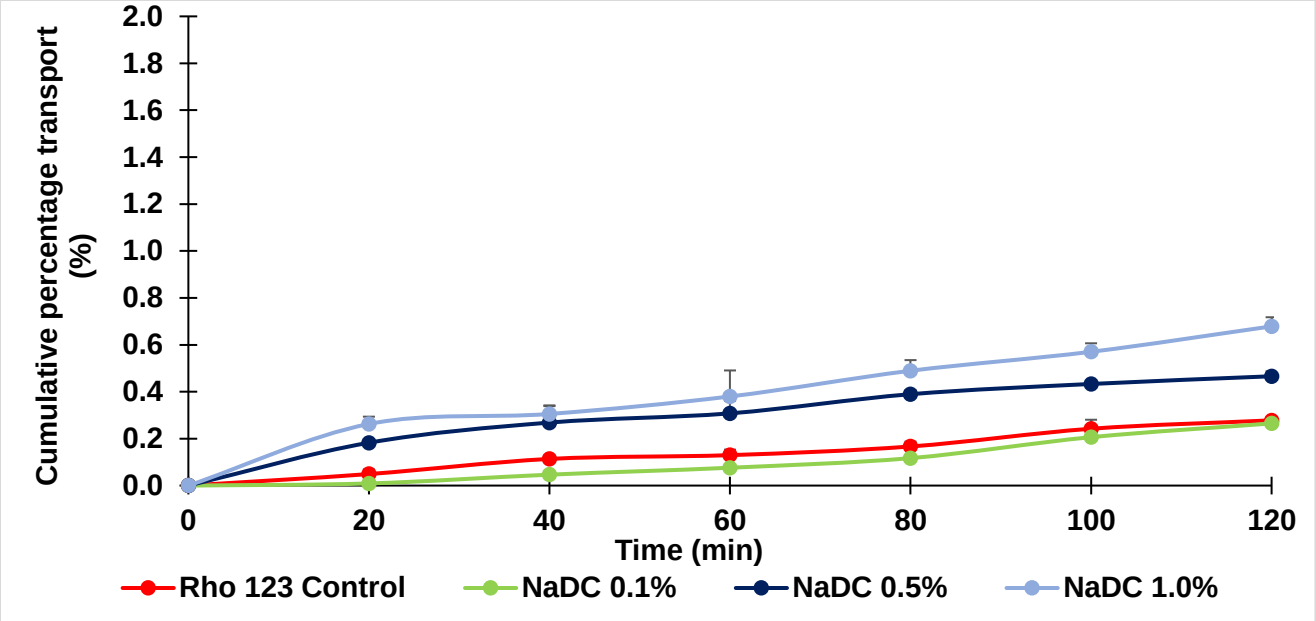

Figure 4.20: The cumulative percentage transport of Rho123 across excised porcine jejunum tissue in the apical to basolateral direction, plotted as a function of time, in the presence of 0.1% (w/v), 0.5% (w/v) and 1.0% (w/v) sodium deoxycholate

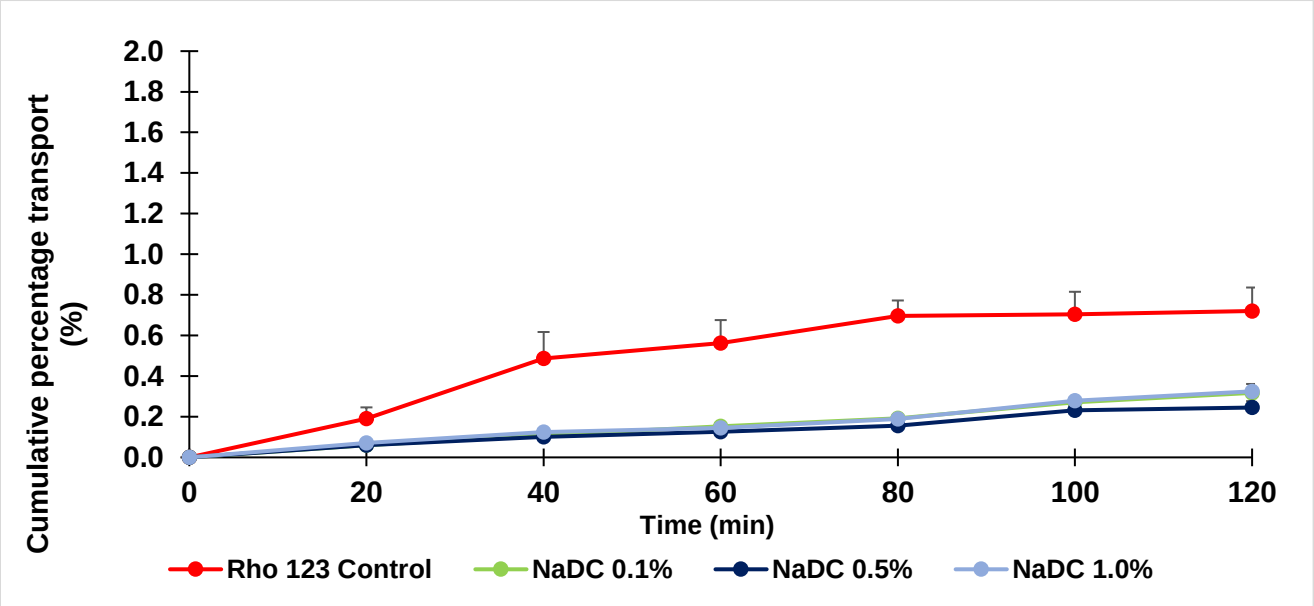

Figure 4.21: The cumulative percentage transport of Rho123 across excised porcine jejunum tissue in the basolateral to apical direction, plotted as a function of time, in the presence of 0.1% (w/v), 0.5% (w/v) and 1.0% (w/v) sodium deoxycholate

The presence of 0.1% (w/v) NaDC yielded no significant increase in Rho123 absorption in the AP-BL direction ($p > 0.05$), and although it is not statistically significant, a slight increase in Rho123 absorption can be seen at 0.5% (w/v) ($p > 0.05$). A statistically significant ($p < 0.01$) increase was seen at a concentration of 1.0% (w/v) NaDC as illustrated in Figures 4.20 and 4.22.

Rho123 transport in the BL-AP direction yielded a statistically significant decrease ($p = 0.000$) in the presence of 0.1% (w/v), 0.5% (w/v) and 1.0% (w/v) NaDC. The decrease in secretory transport of Rho123 is an indication that efflux and P-gp was inhibited in the presence of NaDC, as seen in Figure 4.21.

The P_{app} values of the various concentrations of sodium deoxycholate were calculated as seen in Addendum C, and is depicted in Figure 4.22.

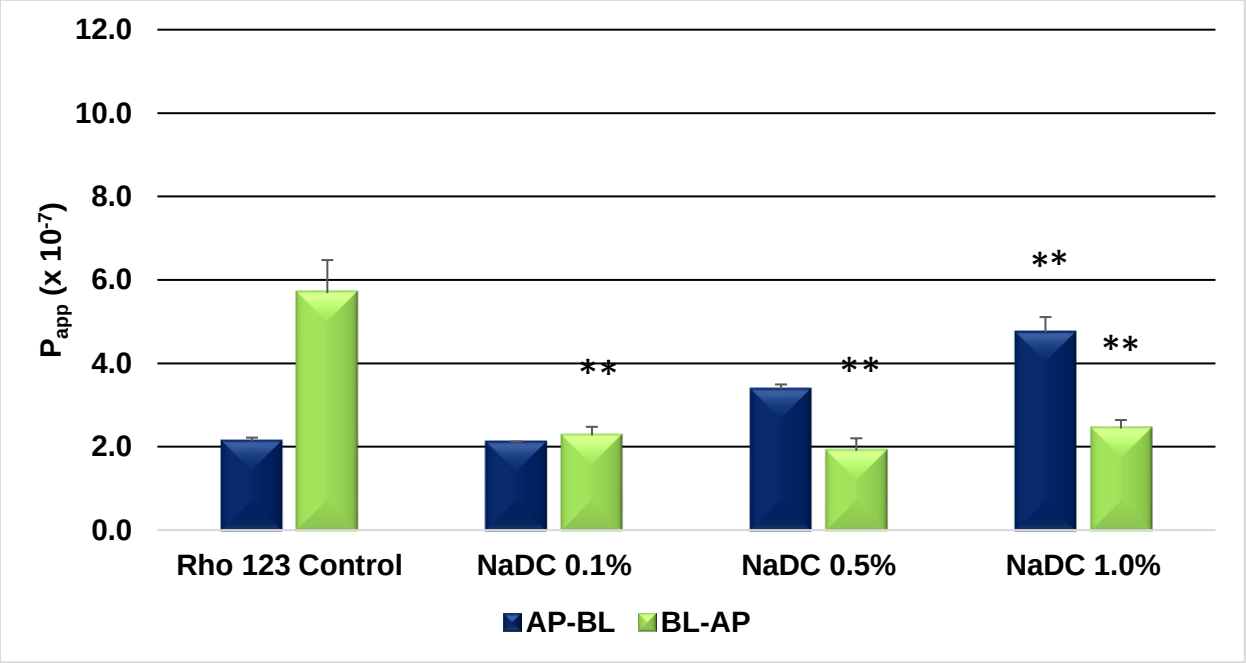

Figure 4.22 The mean P_{app} values of Rho123 transport in the presence of 0.1% (w/v), 0.5% (w/v) and 1.0% (w/v) sodium deoxycholate in the apical to basolateral and basolateral to apical direction. Statistical significance is indicated with an asterisk (*) where $p < 0.05$ and with a double asterisk (**) where $p < 0.01$

In the apical to basolateral direction a statistically significant increase (2.23-fold) in the P_{app} of Rho123 can be seen in the presence of 1.0% (w/v) NaDC. Although 0.5% NaDC yielded no statistically significant increase in the P_{app} of Rho123, there was still a 1.59-fold increase when

compared to the Rho123 control group, as seen in Figure 4.22. At a concentration of 0.1% NaDC no statistically significant increase in P_{app} of Rho123 was seen.

A reduction in TEER of 50.32% was seen at a concentration of 0.1% (w/v) NaDC, 40.48% for 0.5% (w/v) and 36.62% for 1.0% (w/v). The TEER reduction is an indication that tight junctions opened and the absorptive transport of Rho123 should then increase. In the present study, the TEER readings could have decreased as the concentration NaDC increased due to the possibility of compromised integrity caused by the bile salt. Further investigation on the effect of the bile salt on the membrane integrity is needed.

In the BL-AP direction, a 2.50-fold decrease in the P_{app} of Rho123 was seen for 0.1% (w/v) NaDC with a statistical significance of $p = 0.000$ (Figures 4.21 and 4.22). For 0.5% (w/v) and 1.0% (w/v) NaDC, a 2.99-fold and 2.33-fold decrease with statistical significance of $p = 0.000$ was observed.

The ER were calculated by means of the P_{app} values and Equation 2 (Chapter 3), and are presented in Figure 4.23.

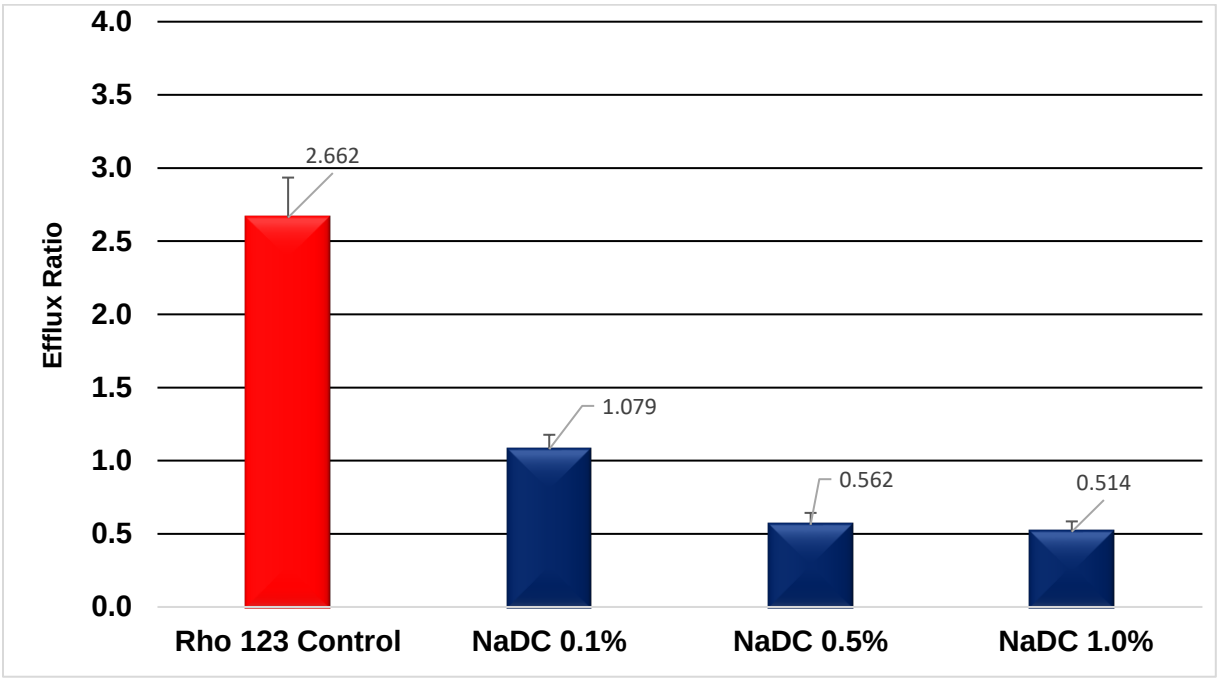

Figure 4.23: The efflux ratio values of Rho123 transport in the absence and presence of 0.1%, 0.5% and 1.0% (w/v) Sodium deoxycholate

The ER of Rho123 in the presence of various concentrations of NaDC clearly decreased when compared to that of the Rho123 control group alone. NaDC visibly mediated a concentration dependent inhibition of Rho123 efflux. From Figure 4.22 it is evident, although not statistically significant, an increase of Rho123 transport in the AP-BL direction for 0.5% (w/v) and 1.0% (w/v) NaDC and a decrease of Rho123 transport in the BL-AP direction resulting in a higher concentration of Rho123 on the basolateral side of the membrane indicating P-gp inhibition. While a statistically significant increase was seen at a concentration of 1.0% (w/v) NaDC. Efflux was evidently inhibited and the permeation of Rho123 in the presence of NaDC was enhanced.

4.7.1 Discussion

In literature, it is evident that NaDC has been known to enhance the absorption or epirubicin in the jejunum of rats at a concentration of 12 mM NaDC (Lo *et al*., 2000:665-672). In a study conducted by Sharma and associates (2005:884-893), a 4-fold increase was seen *in situ* at a concentration of 1% (w/v) NaDC (Maher *et al*., 2016:282). This data is consistent with the current findings of this study. NaDC has a CMC of 0.083% to 0.249% (w/v) (Maher *et al*., 2016:282). Concentrations above the CMC may lead to the formation of micelles which can cause variable absorption or lack of absorption as seen in the present study.

NaDC is known to cause perturbation in the epithelium of rat colon and Caco-2 cells which may change the membrane fluidity and consequently inhibit the activity of proteins such as P-gp (Lo *et al*., 2000:665-672). In the basolateral to apical direction the transport of Rho123 in the presence of NaDC decreased. This is an indication that, as mentioned before, P-gp and P-gp related efflux was inhibited. In the study conducted by Lo and associates (2000:665:672), they stated that, to their knowledge, it was the first study that indicated a decrease in basolateral to apical transport, contradictory to all the previous studies. Further investigation is necessary into this matter.

4.8 Conclusion

In conclusion, the transport of Rho123 in the presence of Brij® 58, Cremophor® CO40, Tween® 20, Span® 20 and sodium deoxycholate across porcine jejunum tissue was investigated. The results yielded a statistically significant ($p < 0.01$) increase in absorptive transport (AP-BL) of Rho123 in the presence of 0.5% (w/v) Brij® 58, 1.0% (w/v) Brij® 58 and 1.0% (w/v) NaDC. The increase is possibly as a result of the inhibition of P-gp. Micelle formation at concentrations above the CMC potentially caused lower absorption of Rho123 in the apical to basolateral direction in the presence of Cremophor® CO40 and NaDC. All the surfactants used, reduced the TEER as seen in Addendum C, which means that the surfactants possibly opened the tight junctions of the porcine intestinal tissue. The SD for the surfactants tested in the presence of a model compound Rho123 was low, indicating good repeatability. NaDC need further investigation as the bile salts could have possible effects on the membrane fluidity, although no statistically significant increase in cumulative percentage transport was seen at concentrations below 1.0% (w/v).

CHAPTER 5

FINAL CONCLUSIONS AND FUTURE RECOMMENDATIONS

Oral administration is by far the most preferred and most convenient method of drug administration with the highest level of patient compliance. Reason being that there is patient discomfort when using the parenteral or rectal route of administration, as well as a higher risk of infections associated with the parenteral route of administration. Excipients are added to active ingredients to create a pharmaceutical formulation that is easy to manufacture and easy to handle, keeping in mind aspects that may influence patient compliance. In the literature, excipients are thought to be inert, but recent findings have indicated that it may have altering effects on the permeability of active ingredients.

The aim of this study was to determine if selected surfactants (Brij® 58, Tween® 20, Span® 20, Cremophor® CO40 and sodium deoxycholate) could have altering effects on intestinal drug permeation. For this purpose, membrane permeability of a model compound, Rhodamine 123 (Rho123), at a concentration of 5 µM was evaluated across excised porcine jejunal tissue mounted in a Sweetana-Grass diffusion apparatus in the presence of various surfactant concentrations (0.1%, 0.5% and 1.0% (w/v). This was performed over a period of 120 min in two directions namely the apical to basolateral direction and the basolateral to apical direction. In addition, the study aimed to clarify the mechanism of interaction (e.g. modulation of efflux transporters or tight junctions) of the surfactants with the jejunal tissue. The cumulative percentage transport was calculated and plotted as a function of time. Subsequently, the P_{app} values and efflux ratios (ER) were calculated and presented in Chapter 4.

5.1 Final conclusions

The cumulative percentage transport of Rho123 in the presence of Brij® 58 in the apical to basolateral direction showed a concentration dependant increase in Rho123 transport, although only 0.5% and 1.0% w/v Brij® 58 showed a statistically significant increase. In the basolateral to apical direction a statistically significant decrease in Rho123 transport was seen at concentrations of 0.5% and 1.0% (w/v) Brij® 58. This indicates that Brij® 58 mediated inhibition of Rho123 efflux in a concentration dependent manner. A reduction of TEER was seen over the 120 min period indicating that tight-junctions probably opened.

Evaluation of Rho123 transport in the presence of Cremophor® CO40 showed no statistically significant effect on Rho123 transport in the apical to basolateral direction, possibly due to micelle formation on the apical side of the membrane. Another explanation could also be complex formation with Rho123. In the basolateral to apical direction a statistically significant decrease in Rho123 transport was seen at concentrations of 0.1%, 0.5% and 1.0% (w/v) Cremophor® CO40. A clear effect on the efflux transport of Rho123 could be seen, potentially due to the inhibition of P-gp, resulting in an inhibitory effect on efflux in the apical to basolateral direction. A reduction in TEER was also seen, thus possibly indicating that tight-junctions opened.

Tween® 20 had no statistically significant effect on Rho123 transport in the apical to basolateral direction at concentrations of 0.1%, 0.5% (w/v) although an increase was seen in Rho123 at concentration of 1.0% (w/v). In the basolateral to apical direction Rho123 transport decreased in a statistically significant manner in the presence of 1.0% (w/v) Tween® 20. This indicated that Tween® 20 caused a visible inhibition of Rho123 efflux in the basolateral to apical direction at concentration of 0.1% and 0.5% (w/v) although at a higher concentration of 1.0% (w/v) Rho123 indicated no efflux inhibition. Trans-epithelial electrical resistance was reduced which could be indicative that tight-junctions opened.

In the presence of Span® 20, no statistically significant increase in apical to basolateral transport was observed at concentrations of 0.1%, 0.5% and 1.0% (w/v) Rho123. Span® 20 is a viscous surfactant that possibly formed a dispersion when combined with Rho123. In the basolateral to apical direction, a statistically significant increase was seen at concentrations of 0.1%, 0.5% and 1.0% (w/v) Span® 20. This indicated that efflux of Rho123 was suppressed. Trans-epithelial electrical resistance was also reduced over a period of 120 min which indicated that tight junctions could have opened.

Sodium deoxycholate mediated a statistically significant increase in transport in the apical to basolateral direction at a concentration of 1.0% (w/v). Although not statistically significant, there was also a visible concentration dependent increase in the apical to basolateral transport of Rho123 at concentration of 0.5% (w/v). In the basolateral to apical direction a statistically significant inhibition of P-gp related efflux was seen at concentrations of 0.1%, 0.5% and 1.0% (w/v). Therefore, the increase in transport in the apical to basolateral direction could be attributed to the inhibition of P-gp related efflux in a concentration dependent manner.

To conclude, this study confirmed the hypothesis that excipients are not inert, and that surfactant-drug combinations could therefore have altering effects on the pharmacokinetics of the co-administered drug. The altered pharmacokinetics may cause unwanted side effects, but can also potentially be used to enhance drug permeation and absorption for drugs with low permeability.

5.2 Future Recommendations

This investigation into surfactant-drug pharmacokinetic interactions between Rho123 and various surfactants have led to a few aspects that need further investigation. It is recommended that future studies be structured to explore the following aspects:

- To study the interactions between Tween® 20 and Span® 20 and how the combination of these two surfactants will alter the permeation of Rho123.
- To characterise the mechanism of interaction between Rho123 and Cremophor® CO40, Tween® 20, Span® 20, and the how it affects efflux transporters like P-gp.
- To determine the pharmacokinetic interactions between surfactants and Rho123 at higher and lower concentration ranges.
- Determine if sodium deoxycholate have similar effects in models that have a thicker membrane, for example porcine buccal tissue, and if it has an effect on the membrane integrity.
- To explore the use of multifunctional excipients in pharmaceutical formulations, along with P-gp substrates to improve their absorption, and consequently the bioavailability of the active ingredients.
- Due to the wide variety of methods and animal models involved in *in vitro* studies, with variable absorption from the intestine, it is difficult to predict the outcome of the study *in vivo* solely based on the outcome of one *in vitro* model, therefore it is recommended to use different *in vitro* models with different animal tissues.
- Region specific transport across porcine intestinal tissue should be conducted to determine the influence of the surfactants on the duodenum, jejunum (proximal, medial and distal), ileum and possibly the colon.

BIBLIOGRAPHY

Alqahtani, S., Mohamed, LA. &Kaddoumi, A. 2013. Experimental models for predicting drug absorption and metabolism. *Expert Opinion on Drug Metabolism and Toxicology*, 9:1241-1254.

Al-Mohizea, A.M., Al-Jenoobi, F.I. & Alam, M.A. 2015. Rhodamine-123: A p-glycopotein marker complex with sodium lauryl sulfate. *Pakistan Journal of Pharmaceutical Sciences*, 28:617-622.

Al-Sabagh, A.M. 2002. The relevance HLB of surfactants on the stability of asphalt emulsion. Colloids and surfaces A*: Physicochemical and Engineering Aspects*, 204:73-83.

Al-Saraf, A., Holm, R. & Nielsen, C.U. 2016. Tween 20 increases intestinal transport of doxorubicin *in vitro* but not *in vivo*. *International Journal of Pharmaceutics,* 498:66-69.

Antunes, F., Andrade, F., Ferreira, D., Nielsen, H.M. & Sarmento, B. 2013. Models to predict intestinal absorption of therapeutic peptides and proteins. *Current Drug Metabolism*,14:4-20.

Ashford, M. 2007. Gastrointestinal tract- physiology and drug absorption. In Aulton's pharmaceutics: The design and manufacture, by Aulton, M.A. edited by Aulton M.E. Edinburgh: Churchill Livingstone - Elsevier. p 270-285.

Ashford, M. 2013. Gastrointestinal tract-physiology and drug absorption. In Aulton's pharmaceutics: The design and manufacture, by Aulton, M.A. edited by Aulton M.E. Philadelphia: Churchill Livingstone - Elsevier. p 298-306.

Attwood, D. 2009. Surfactants. In Modern pharmaceutics: Basic principles and systems. Edited by Florence, A.T, Siepmann, J. New York: Informa Healthcare. 5th Edition. p 423-430.

Aungst, B. J. 2012. Absorption enhancers: Applications and Advances. *American Association of Pharmaceutical Scientists Journal*, 14:10-18.

Balimane, P.V., Chong, S. & Morrison, R.A. 2000. Current methodologies used for evaluation of intestinal permeability and absorption. *Journal of Pharmacological and Toxicological Methods*, 44: 301-302.

Bansal, T., Jaggi, M., Khar, R.K. & Talegaonkar, S. 2009. Emerging significance of flavonoids as P-glycoprotein inhibitors in cancer chemotherapy. *Journal of Pharmacy and Pharmaceutical Sciences*, 12:46-78.

Barthe, L.W., Woodley, J. & Houin, G. 1999. Gastrointestinal absorption of drugs: methods and studies. *Fundamental and Clinical Pharmacology*, 13: 154-168.

Bergmann, H., Rogoll, D., Scheppach, W., Melcher., R. & Richling, E. 2009. The Ussing typer chamber model to study the intestinal transport and modulation of specific tight-junction genes using a colonic cell line. *Molecular Nutrition and Food Research Journal*, 53:1211-1225.

Berthelsen, R., Holm, R., Jacobsen, J., Kristensen, J., Abrahamsson, B. & Müllertz, A. 2015. Kolliphor surfactants affect solubilization and bioavailability of fenofibrate. Studies of *in vitro* digestion and absorption in rats. *Molecular Pharmaceutics,* 12:1062-1071.

Billany, M.R. 2007. Suspensions and emulsions. In Aulton's pharmaceutics: The design and manufacture of medicines, by Aulton, M.E. edited by Aulton M.E. Philadelphia: Churchill Livingstone- Elsevier. p 383-396.

Bock, U., Kottke, T. & Haltner, E. 2003. Validation of the Caco-2 monolayer system for determining the permeability of drug substances according to the Biopharmaceutics Classification system (BCS). (Unpublished)

Borchard, G., Luessen, H.L., De Boer, A.G., Verhoef, J.C., Lehr, C.M. & Junginger, H.E. 1996. The potential of mucoadhesive polymers in enhancing intestinal peptide drug absorption. III: Effects of chitosan-glutamate and carbomer on epithelial tight junctions *in vitro*. *Journal of Controlled Release,* 39: 131-138.

Buckley, S.T., Fischer, S.M., Fricker, G. & Brandl, M. 2012. In vitro models to evaluate the permeability of poorly soluble drug entities: Challenges and perspectives. *European Journal of Pharmaceutical Sciences*, 45:235-250.

Buggins, T.R., Dickinson, P.A. & Taylor, G. 2007. The effects of pharmaceutical excipients on drug disposition. *Advanced Drug Delivery Reviews*, 59:1482-1503.

Cabrera-Perez, M.A., Sanz, M.B., Sanjuan, V.M., Gonzales-Alvares, M. & Alvarez, I.G. 2016. Importance and applications of cell- and tissue-based *in vitro* models for drug permeability screening in early stages of drug development. *Concepts and Models for Drug Permeability Studies- Cell and Tissue Based in Vitro Culture Models*: 3-29.

Cao, X., Gibbs, S.T., Fang, L., Miller, H.A., Landowski, C.P., Shin, H.C., Lennernäs, H., Zhong, Y., Amidon, G.L., Yu, L.X. & Sun, D. 2006. Why is it challenging to predict intestinal drug

absorption and oral bioavailability in human using rat model. *Pharmaceutical Research* 23: 1675-1686.

Chan, L.M.S., Lowes, S., Hirst, B.H. 2004. The ABCs of drug transport in intestine and liver: efflux proteins limiting drug absorption and bioavailability. *European Journal of Pharmaceutical Sciences*, 21: 25-51.

Christiansen, A., Backensfeld, T., Denner, K. & Weitschies, W. 2011. Effects of non-ionic surfactants on cytochrome P450-mediated metabolism *in vitro*. *European Journal of Pharmaceutics and Biopharmaceutics, 78:166-172.*

Ćirin, D. M., Poša, M.M. & Krstonošić. 2012. Interactions between Sodium cholate or Sodium deoxycholate and nonionic surfactant (Tween 20 or Tween 60) in aqueous solution. *Industrial and Engineering Chemical Research,* 51:3670-3676.

Cornaire, G., Woodley, J., Hermann, P., Cloarec, A., Arellano, C. & Houin, G. 2004. Impact of excipients on the absorption of P-glycoprotein substrates *in vitro* and *in vivo*. *International Journal of Pharmaceutics*, 278:119-131.

Dahan, A. & Miller, J.M. 2012. The solubility-permeability interplay and its implications in formulation design and development for poorly soluble drugs. *American Association of Pharmaceutical Scientists Journal,* 14:244-251.

DeSesso, J.M. & Jacobson, C.F. 2001. Anatomical and physiological parameters affecting gastrointestinal absorption in humans and rats. *Food and Chemical Toxicology*, 39: 209-228.

Dimitrijevic, D., Shaw, A.J. & Florence, A.T. 2000. Effects of some non-ionic surfactants on transepithelial permeability in Caco-2 cells. *Journal of Pharmacy and Pharmacology*, 52:157-162.

Dixit, P., Jain, D.K. & Dumbwani, J. 2012. Standardisation of an *ex vivo* method for determination of intestinal permeability of drugs using everted rat intestine apparatus. *Journal of Pharmacology and Toxicology Methods* 65: 13-17.

Dos Santos, T., Lourenco, B.N., Coentro, J & Granja, P.L. 2015. Cell-based *in vitro* models for permeability studies. Consepts and models for drug permeability studies: Cell and tissue based *in vitro* culture models, edited by Sarmento, B. Kidlington: Woodhead publishing – Elsevier p410.

Fernandes, C.P., Mascarenhas, M.P., Zibetti F.M., Lima, B.G., Oliveira, R.P.R.F., Rocha, L. & Falcão, D.Q. 2013. HLB value, an important parameter for the development of essential oil phytopharmaceuticals. *The Brazilian Journal of Pharmacognosy*, 23:108-114.

Gamboa, J.M. & Leong, K.W. 2013. *In vitro* and *in vivo* models for the study of oral delivery of nanoparticles. *Advanced Drug Delivery Reviews*, 65:800-810

Gaush, C.R., Hard, W.L. & Smith, T.F. 1966. Characterization of an established line of canine kidney cells (MDCK). *Proceedings of the Society for Experimental Biology,*122: 931-935.

Goole, J., Lindley, D.J., Roth, W., Carl, S.M., Amighi, K., Kauffmann, J. & Knipp, G.T. 2010. The effects of excipients on transporter mediated absorption. *International Journal of Pharmaceutics*, 393:17-31.

García-Arieta, A. 2014. Interactions between active pharmaceutical ingredients and excipients affecting bioavailability: Impact on bioequivalence. *European Journal of Pharmaceutical Sciences*, 65:89-97.

Grass, G.M. & Sweetana, S.A. 1988. *In vitro* Measurement of gastrointestinal tissue permeability using a new diffusion cell. *Pharmaceutical Research,* 5: 372-376.

Gupta, V., Hwang, B.H., Doshi, N. & Mitragotri, S. 2013. A permeation enhancer for increasing transport of therapeutic macromolecules across the intestine. *Journal of Controlled Release,* 172:541-549.

Hamman, J.H., Enslin, G.M. & Kotzé, A.F. 2005. Oral delivery of peptide drugs: barriers and developments. *Biodrugs: Clinical Immunotherapeutics, Biopharmaceuticals and Gene Therapy*, 19:165-177.

Hanani, M. 2012. Lucifer Yellow – an angel rather than the devil. *Journal of Cellular and Molecular Medicine*, 16:22-31.

Hildalgo, I.J. 2001. Assessing the absorption of new pharmaceuticals. *Current Topics in Medicinal Chemistry*, 1: 385-401.

Hoffmann, E.K. 2001. The pump and leak steady-state concept with a variety of regulated leak pathways. *Journal of Membrane Biology ,*184;321-330.

International conference on harmonisation of technical requirements for registration of pharmaceuticals for human use (ICH). 2005. " Validation of analytical procedures: text and methodology Q2(R1). http://www.ich.org/fileadmin/Public_Web_Site/ICH_Products/Guidelines/Quality/Q2_R1/Step4/Q2_R1__Guideline.pdf Date of access 12 September 2016.

https://openwetware.org/wiki/Critical_micelle_concentration_(CMC). Date of access 26 September 2017.

Jackson, K., Young, K. & Pant, S. 2000. Drug-excipient interactions and their effect on absorption. *Pharmaceutical Science and Technology Today,* 3: 336-345.

Jain, C.P., Joshi, G., Kataria, U. & Patel, K. 2016. Enhanced permeation of an antiemetic drug from buccoadhesive tablets by using bile salts as permeation enhancers: Formulation characterization, *in vitro* and *ex vivo*, studies. *Scientia Pharmaceutica*, 84:379-392.

Junginger, H.E. & Verhoef, J.C. 1998. "Macromolecules as safe penetration enhancers for hydrophilic drugs: a fiction?" *Pharmaceutical Science and Technology Today* ,1: 370-376.

Kamerzell, T.J., Esfandiary, R., Joshi, S.B., Middaugh, C.R. & Volkin, D.B. 2011. Protein–excipient interactions: Mechanisms and biophysical characterization applied to protein formulation development. *Advanced Drug Delivery Reviews*, 63:1118-1159.

Kapoor, Y. & Chauhan, A. 2008. Drug and surfactant transport in cyclosporine A and brij 98 laden p-HEMA hydrogels. *Journal of Colloid and Interface Science*, 322:624-633

Kumar, A., Kishore, L., Kaur, N. & Nair, A. 2012. Method development and validation: Skills and tricks. *Chronicles of Young Scientists,* 3:3-11.

Le Ferrec, E., Chesne, C., Artursson, P., Braydeb, D., Fabre, G., Gires, P., Guillou, F., Rousset, M., Rubas, W. &Scarino, M.L. 2001. *In vitro* models of the intestinal barrier. Alternatives to animals, 29:649-668.

Lee, V.H.L. & Yamamoto, A. 1990. Penetration and enzymatic barriers to peptide and protein absorption. *Advanced Drug Delivery Reviews,* 4:171-207.

Legen, I., Salobir, M. & Kerč, J. 2005. Comparison of different intestinal epithelia as models for absorption enhancement studies. *International Journal of Pharmaceutics,* 291:183-188.

Lennernäs, H. 1998. Human intestinal permeability. *Journal of Pharmaceutical Sciences*, 87: 403-410.

Lennernäs, H. 2007. Animal data: The contributions of the Ussing chamber and perfusion systems to predict human oral drug delivery *in vivo. Advanced Drug Delivery Reviews,* 59: 1103-1120.

Lennernäs, H. 2014. Regional intestinal drug permeation: Biopharmaceutics and drug development. *European Journal of Pharmaceutical Sciences*, 57:333-341.

Linnankoski, J., Mäkelä, J., Palmgren, J., Mauriala, T., Vedin, C., Ungell, A-L., Lazorova, L.,Artursson, P., Urtti, A. & Yliperttula, M. 2010. Paracellular porosity and pore size of the human intestinal epithelium in tissue and cell culture models. *Journal of Pharmaceutical Sciences,* 99:2166-2175.

Lo, Y. & Huang, J. 2000. Effects of sodium deoxycholate and sodium caprate on the transport of epirubicin in human intestinal epithelial Caco-2 cell layers and everted gut sacs of rats. *Biochemical Pharmacology*, 59:665-672.

Loftsson, T. 2015. Excipient pharmacokinetics and profiling. *International Journal of Pharmaceutics*, 480: 48-84.

Lòpez, A., Llinares, F., Cortell, C. & Herráez, M. 2000. Comparative enhancer effects of Span®20 with Tween®20 and Azone® on the *in vitro* percutaneous penetrations of compounds with different lipophilicities. *International Journal of Pharmaceutics,* 202:133-140.

Mahato, R.I., Narang, A.S., Thoma, L. & Miller, D.D. 2003. Emerging trends in oral delivery of peptide and proteins. *Critical Reviews in Therapeutic Drug Carrier Systems,* 20: 153-214.

Maher, S., Mrsy, R.J. & Brayden, D.J. 2016. Intestinal permeation enhancers for oral peptide delivery. *Advance Drug Delivery Reviews,* 106:277-319.

Malik, N.A. 2016. Solubilization and interaction studies of bile salts with surfactants and drugs: a review. *Applied Biochemistry Biotechnology,* 179:201

Mayershon, M. 2009. Principles of drug absorption. In Modern pharmaceutics: Basic principles and systems. Edited by Florence, A.T, Siepmann, J. New York: Informa Healthcare. 5th Edition. p 658.

Miller, J., Beig, A., Krieg, B.J., Carr, R.A., Borchardt, T.B., Amidon, G.E., Amidon, G.L. & Dahan, A. 2011. The solubility-permeability interplay: mechanistic modelling and predictive application of the impact of mecellar solubilization on intestinal permeation. *Molecular Pharmaceutics,* 8:1848-1856.

Miyake, M., Koga, T., Kondo, S., Yoda, N., Emoto, C., Mukai, T. & Toguchi, H. 2017. Prediction of drug intestinal absorption in human using the Ussing chamber system: A comparison of intestinal tissues from animals and humans. *European Journal of Pharmaceutical Sciences*, 96:373-380.

Moghimipour, E., Abdulghani, A. & Handali, S. 2015. Absorption-enhancing effects of bile salts. *Molecules,* 20: 14451-14473.

Monte, M.J.; Marin, J.J.G.; Antelo, A.; Vazquez-Tato, J. 2009. Bile acids: Chemistry, physiology, and pathophysiology. *World Journal of Gastroenterology*, 15:804–816.

Nejdfors, P., Ekelund M., Jeppsson, B. & Weström, B.R. 2000. Mucosal *in vitro* permeability in the intestinal tract of the pig, the rat and man: species- and region-related differences. *Scandinavian Journal of Gastroenterology*, 5:501-507.

Neyfakh, A.A. 1988. Use of fluorescent dyes as molecular probes for the study of multidrug resistance. *Experimental Cell Research,* 174:168-176.

Nellans, H.N. 1991. Mechanism of peptide and protein absorption. (1) Paracellular intestinal transport: modulation of absorption. *Advanced Drug Delivery Reviews,* 7: 339-364.

Nunes,C., Silva, C, & Chaves, L. 2015. Tissue based *in vitro* and *ex vivo* models for intestinal permeability studies. Concepts and models for drug permeability studies. Cell and tissue based *in vitro culture models*, edited by Sarmento, B. Cambridge: Woodhead Publishing - Elsevier. p 203-230.

Ou, B., Hampsch-Woodill, M. & Prior, R.L. 2001. Development and validation of an improved oxygen radical absorbance capacity assay using fluorescein as the fluorescent probe. *Journal of Agricultural and Food Chemistry*, 49:4619-4626.

Panchagnula, R., Thomas N.S. 2000. Biopharmaceutics and pharmacokinetics in drug research. *International Journal of Pharmaceutics*, 201:131-150.

Pang, K.S. 2003. Modelling of intestinal drug absorption: roles of transporters and metabolic enzymes (for the Gillette review series). *Drug Metabolism and Disposition,*31(12):1507-1519.

Patterson, J.K., Lei, X.G.,Miller, D.D. 2008. The pig as an experimental model for elucidating the mechanisms governing dietary influence on mineral absorption. *Experimental Biology and Medicine*, 233: 651-664.

Pavek, P., Straud, F., Frendrich, Z., Sklenarova, H., Libra, A., Novotna, M., Kopecky, M., Nobilis, M. & Semecky, V. 2003. Examination of the functional activity of P-glycoprotein in the rat placental barrier using Rhodamine 123. *Journal of Pharmacological and Experimental Therapeutics,* 305:1239-1250.

Pelkonen, O., Boobis, A.R. & Gundert-remy, U. 2001. *In vitro* prediction of gastrointestinal absorption and bioavailability: an expert's meeting report. *European Journal of Clinical Pharmacology*, 57(9):621-629.

Pereira,C., Costa, J., Sarmento, B. & AraÚjo, F. 2015. Cell based *in vitro* models for intestinal permeability studies. Concepts and models for drug permeability studies. Cell and tissue based *in vitro culture models*, edited by Sarmento, B.. Cambridge: Woodhead Publishing - Elsevier. p 57-75.

Pietzonka, P., Walter, E., Duda-Johner, S., Langguth, P. & Merkle, H.P. 2002. Compromised integrity of excised porcine intestinal epithelium obtained from the abattoir affects the outcome of in vitro particle uptake studies. *European Journal of Pharmaceutical Sciences*, 15:39-47.

Pifferi, G. & Restani, P. 2003. The safety of pharmaceutical excipients. *Il Farmaco*, 58:541-550.

Pifferi, G., Santoro, P. & Pedrani, M. 1999. Quality and functionality of excipients. *Il Farmaco*, 54:1-14.

Rege, B.D., Kao, J.P.Y. & Polli, J.E. 2002. Effects of nonionic surfactants on membrane transporters in Caco-2 cell monolayers. *European Journal of Pharmaceutical Sciences*, 16:237-246.

Renukuntla, J., Vadlapudi, A.D., Patel, A., Boddu, S.H.S. & Mitra, A.K. 2013. Approaches for enhancing oral bioavailability of peptides and proteins. *International Journal of Pharmaceutics,* 447: 75-93.

Rozehnal, V., Nakaib, D., Hoepnera, U., Fischera, T., Kamiyamab, M., Takahashib, M., Yasudab, S. & Mueller, J. 2012. Human small intestinal and colonic tissue mounted in the Ussing chamber as a tool for characterising the intestinal absorption of drugs. *European Journal of Pharmaceutical Sciences*, 46: 367-373.

Rowland, M. & Tozer, T.N. 2011. *Clinical pharmacokinetics and pharmacodynamics*. 4th ed. Philadelphia: Lippincott Williams & Wilkins. P 839.

Shargel, L., Wu-Pong, S. & Yu, A.B.C. 2005. Applied biopharmaceutics and pharmacokinetics, 5th edition. New York: McGraw-Hill. p 892.

Sharma, P., Varma, M.V., Chawla, H.P. & Panchagnula, R. 2005. Absorption enhancement, mechanistic and toxicity studies of medium chain fatty acids, cyclodextrins and bile salts as peroral absorption enhancers. *Farmaco,* 60:884-893.

Shen, L., Guo, A. & Zhu, X. 2011. Tween surfactants: Absorption, self-organization, and protein resistance. *Surface Science*, 605: 494-499.

Silva, R., Vilas-Boas, V., Carmoa, H., Dinis-Oliveira, R.J., Carvalho, F., de Lourdes Bastos, M. & Remião, F. 2015. Modulation of P-glycoprotein efflux pump: induction and activation as a therapeutic strategy. *Pharmacology and Therapeutics*, 149: 1-123.

Singh, R. 2013. HPLC method development and validation – an overview. *Indian Journal of Pharmaceutical Education and Research*, 4:26-33.

Sjögren, E., Abrahamsson, B., Augustijns, P., Becker, D., Bolger, M. B., Brewster, M., Brouwers, J., Flanagan, T., Harwood, M., Heinen, C., Holm, R., Juretschke, H. P., Kubbinga, M., Lindahl, A., Lukacova, V., Munster, U., Neuhoff, S., Nguyen, M. A., Peer, A., Reppas, C., Hodjegan, A. R., Tannergren, C., Weitschies, W., Wilson, C., Zane, P., Lennernäs, H. & Langguth, P. 2014. *In vivo* methods for drug absorption - comparative physiologies, model selection, correlations with *in vitro* methods (IVIVC), and applications for formulation/API/excipient characterization including food effects. *European Journal of Pharmaceutical Sciences,* 57**:** 99-151.

Sjögren, E., Erikkson, J., Vedin, C., Breitholtz, K. & Hilgendorf, C. 2016. Excised segments of rat small intestine in Ussing chamber studies: A comparison of native and stripped tissue viability and permeability to drugs. *International Journal of Pharmaceutics*, 505: 361-368.

Sowmiya, M., Tiwari, A.K. & Saha, S.K. 2010. Fluorescent probe studies of micropolarity, premicellar and micellar aggregation of non-ionic brij surfactants. *Journal of Colloid and Interface Science*, 344:97-104.

Sugano, K., Kansy, M., Artursson, P., Avdeef, A., Bendels, S., Di, L., Ecker, G.F., Faller, B.,Fischer, H., Gerebtzoff, G., Lennernaes, H. & Senner, F. 2010. Coexistence of passive and carrier-mediated processes in drug transport. *Nature Reviews Drug Discovery,* 9:597-614.

Sweetana, S.A. & Grass, G.M. 1993. Apparatus for *in vitro* determination of substances across membranes, biological tissues, or cell cultures. (Patent: US 5183760) p9.

Tang, F., Ouyang, H., Yang, J.Z. & Borchardt, R.T. 2004. Bidirectional transport of Rhodamine 123 and Hoechst 33342, Fluorescence probes of the binding sites on P-glycoprotein, across MDCK-MDR1 cell monolayers. *Journal of Pharmaceutical Sciences,* 93:1185-1194.

Törnqvist, E., Annas, A., Granath, B., Jalkesten, E., Cotgreave, I. & Öberg, M. 2014. Strategic focus on 3R principles reveals major reductions in the use of animals in the pharmaceutical toxicity testing. *PLoS ONE,* 9:1-12

United States Pharmacopeial Convention. 2016a. Validation of compendial procedures. http://www.uspnf.com/uspnf/pub/index?usp=39&nf=34&s=0&officialOn=May%201,%202016 Date of access: 20 Jul. 2017.

Wahlang, B., Pawar, Y.B. & Bansal, A.K. 2011. Identification of permeability-related hurdles in oral delivery of curcumin using the Caco-2 cell model. *European Journal of Pharmaceutics and Biopharmaceutics*, 77:275-282.

Wang, S., Monagle, J., McNulty, C., Putnam, D, & Chen, H. 2004. Determination of P-glycoprotein inhibition by excipients and their combinations using an integrated high-throughput process. *Journal of Pharmaceutical Sciences*, 93: 2755-2767.

Ward, P.D., Tippin, T.K. & Thakker, D.R. 2000. Enhancing paracellular permeability by modulating epithelial tight junctions. *Pharmaceutical Science and Technology Today,* 3: 346-358.

Watanabe, E., Takahashi, M.& Hayashi, M. 2004. A possibility to predict the absorbability of poorly water-soluble drugs in humansbased on rat intestinal permeability assessed by an in vitro chamber method. *European Journal of Pharmaceutics and Biopharmaceutics*. 58: 659-66.

Wempe, M.F., Wright, C., Little, J.L., Lightner, J.W., Large, S.E., Caflisch, G.B., Buchanan, C.M., Rice, P.J., Wacher, V.J., Ruble, K.M. & Edgar, K.J. 2009. Inhibiting efflux with novel non-ionic surfactants: Rational design based on vitamin E TPGS. *International Journal of Pharmaceutics*, 370:93-102.

Werle, M. 2008. Natural and synthetic polymers as inhibitors of drug efflux pumps. *Pharmaceutical Research*, 25: 500-511.

Westerhout, J., Van de Steeg, E., Grossouw, D., Zeijdner, E.E., Krul, C.A.M. Verwei, M. & Wortelboer, H.M. 2014. A new approach to predict human intestinal absorption using porcine intestinal tissue and biorelevant matrices. *European Journal of Pharmaceutical Sciences*, 63: 167-177.

Yang, L.; Zhang, H.; Paul Fawcett, J.; Mikov, M.; Tucker, I.G. 2011. Effect of bile salts on the transport of morphine-6-glucuronide in rat brain endothelial cells. *Journal of Pharmaceutical Sciences*, 100:1516–1524.

Zhang, D. 2009. Polyoxyethylene Sorbitan Fatty acid Esters. In Handbook of pharmaceutical excipients, edited by Rowe, R.C., Sheskey, P.J., Quinn, M.E. Chicago: Pharmaceutical Press. p 549-553, 675-678.

Zhang, W., Li, Y., Zou, P., Wu, M., Zhang, Z. & Zhang, T. 2016. The Effects of Pharmaceutical excipients on gastrointestinal tract metabolic enzymes and transporters – an update. *American Association of Pharmaceutical Scientists Journal,* 18: 830-843.

Zhao, G., Huang, J., Xue, K., Si, L. & Li, G. 2013. Enhanced intestinal absorption of etoposide by self-microemulsifying drug delivery systerms: Roles of P-glycoprotein and cytochrome P450 3A inhibition. *European Journal of Pharmaceutical Sciences*, 50: 429-439.

Zhao, W., Uehera, S., Tanaka, K., Tadokoro, S., Kusamori, K., Katsumi, H., Sakane, T. & Yamamoto, A. 2016. Effects of polyoxyethylene alkyl ethers on the intestinal transport and absorption of rhodamine 123: a P-glycoprotein substrate by *in vitro* and *in vivo* studies. *Journal of Pharmaceutical Sciences*, 105:1526-1534.

Zurlo, J., Rudacille, D. & Goldberg, A.M. 1996. The three Rs: The Way Forward. *Environmental Health Perspectives*, 104:878-890.

ADDENDUM A : ETHICS APPROVAL FORM

NORTH-WEST UNIVERSITY
YUNIBESITI YA BOKONE-BOPHIRIMA
NOORDWES-UNIVERSITEIT

Private Bag X6001, Potchefstroom
South Africa 2520

Tel: (018) 299-4900
Faks: (018) 299-4910
Web: http://www.nwu.ac.za

Ethics Committee
Tel +27 18 299 4849
Email Ethics@nwu.ac.za

ETHICS APPROVAL OF PROJECT

The North-West University Research Ethics Regulatory Committee (NWU-RERC) hereby approves your project as indicated below. This implies that the NWU-RERC grants its permission that provided the special conditions specified below are met and pending any other authorisation that may be necessary, the project may be initiated, using the ethics number below.

Project title: Excised pig buccal and intestinal tissues as in vitro models for pharmacokinetic studies

Project Leader: Prof Sias Hamman

Ethics number: NWU-00025-15-A5
(Institution – Project Number – Year – Status)
Status: S = Submission; R = Re-Submission; P = Provisional Authorisation; A = Authorisation

Approval date: 2015-04-16 **Expiry date**: 2020-04-15

Special conditions of the approval (if any): None

General conditions:

While this ethics approval is subject to all declarations, undertakings and agreements incorporated and signed in the application form, please note the following:

- *The project leader (principle investigator) must report in the prescribed format to the NWU-RERC:*
  - *annually (or as otherwise requested) on the progress of the project,*
  - *without any delay in case of any adverse event (or any matter that interrupts sound ethical principles) during the course of the project.*
- *The approval applies strictly to the protocol as stipulated in the application form. Would any changes to the protocol be deemed necessary during the course of the project, the project leader must apply for approval of these changes at the NWU-RERC. Would there be deviated from the project protocol without the necessary approval of such changes, the ethics approval is immediately and automatically forfeited.*
- *The date of approval indicates the first date that the project may be started. Would the project have to continue after the expiry date, a new application must be made to the NWU-RERC and new approval received before or on the expiry date.*
- *In the interest of ethical responsibility the NWU-RERC retains the right to:*
  - *request access to any information or data at any time during the course or after completion of the project;*
  - *withdraw or postpone approval if:*
    - *any unethical principles or practices of the project are revealed or suspected,*
    - *it becomes apparent that any relevant information was withheld from the NWU-RERC or that information has been false or misrepresented,*
    - *the required annual report and reporting of adverse events was not done timely and accurately,*
    - *new institutional rules, national legislation or international conventions deem it necessary.*

The Ethics Committee would like to remain at your service as scientist and researcher, and wishes you well with your project. Please do not hesitate to contact the Ethics Committee for any further enquiries or requests for assistance.

Yours sincerely

Linda du Plessis

Digitally signed by Linda du Plessis
DN: cn=Linda du Plessis, o=NWU, Vaal Triangle Campus, ou=Vice-Rector: Academic, email=linda.duplessis@nwu.ac.za, c=US
Date: 2015.04.20 20:35:13 +02'00'

Prof Linda du Plessis
Chair NWU Research Ethics Regulatory Committee (RERC)

ADDENDUM B : DATA OBTAINED FROM RHODAMINE 123 VALIDATION

B1 Inter-day precision

Table B 1: Inter-day precision data obtained Day 1

Concentration (µM)	Repeats	Fluorescence (Fluorescent arbitrary units)	Recovery		
			(µM)	(%)	Average (%)
5	1	1370756158	5,01	100,21	101,56
	2	1394472254	5,1	101,94	
	3	1402411966	5,13	102,5	
2,5	1	687401319	2,51	100,5	99,69
	2	677045287	2,47	98,99	
	3	681060007	2,49	99,58	
0,0125	1	3524181	0,01	103,05	102,64
	2	3469147	0,01	101,44	
	3	3536930	0,01	103,43	
			Mean Recovery	101,30	
			SD	1,48	
			%RSD	1,46	

Table B 2 Inter-day precision data obtained Day 2

Concentration (µM)	**Repeats**	**Fluorescence (Fluorescent arbitrary units)**	**Recovery**		
			(µM)	**(%)**	**Average (%)**
5	1	1480158943	4.97	99.38	99.62
	2	1498958687	5.03	100.64	
	3	1472005855	4.94	98.83	
2,5	1	734019604	2.46	98.56	100.61
	2	743974868	2.50	99.90	
	3	769673172	2.58	103.35	
0,0125	1	3812735	0.01	102.39	100.20
	2	3726036	0.01	100.07	
	3	3653804	0.01	98.13	
			Mean Recovery	100.14	
			SD	1,65	
			%RSD	1,65	

Table B 3: Inter-day precision data obtained Day 3

Concentration (µM)	Repeats	Fluorescence (Fluorescent arbitrary units)	Recovery		
			(µM)	(%)	Average (%)
5	1	1598568747	5.17	103.39	101.77
	2	1539976747	4.98	99.60	
	3	1581828395	5.12	102.31	
2,5	1	761676150	2.46	98.53	99,39
	2	777829878	2.52	100.62	
	3	765423862	2.48	99.01	
0,0125	1	3836403	0.01	99.25	101.31
	2	3921821	0.01	101.46	
	3	3989452	0.01	103.21	
			Mean Recovery	100.82	
			SD	1.75	
			%RSD	1.73	

B2 Intraday precision and accuracy

Table B 4: Intraday precision data obtained Day 1: 11:00 am

Concentration (µM)	Repeats	Fluorescence (Fluorescent arbitrary units)	Recovery		
			(µM)	(%)	Average (%)
5	1	1659666688	5.06	101.22	101.28
	2	1680764800	5.13	102.50	
	3	1641487616	5.01	100.11	
3.75	1	1236405632	3.77	100.54	100.35
	2	1251038464	3.81	101.73	
	3	1214932352	3.70	98.79	
2.5	1	811237632	2.47	98.95	100.30
	2	826535744	2.52	100.81	
	3	829229632	2.53	101.14	
1.25	1	408992448	1.25	99.77	101.61
	2	414261376	1.26	101.06	
	3	426282656	1.30	103.99	
0.5	1	167228096	0.51	101.99	101.48
	2	164079824	0.50	100.07	
	3	167878744	0.51	102.38	
0.05	1	16821445	0.05	102.59	100.13
	2	16175234	0.05	98.65	
	3	16256531	0.05	99.14	
			Mean Recovery	100.86	
			SD	1,46	
			%RSD	1,45	

Table B 5 Intraday precision data obtained Day 1: 14:00pm

Concentration (µM)	Repeats	Fluorescence (Fluorescent arbitrary units)	Recovery		
			(µM)	(%)	Average (%)
5	1	1674406528	5.11	102.12	99.86
	2	1623846272	4.95	99.03	
	3	1614074240	4.92	98.44	
3.75	1	1254682624	3.83	102.02	101.84
	2	1265561216	3.86	102.91	
	3	1237166336	3.77	100.60	
2.5	1	814151872	2.48	99.30	100.47
	2	826627328	2.52	100.83	
	3	830465728	2.53	101.29	
1.25	1	417745280	1.27	101.91	100.53
	2	413499104	1.26	100.87	
	3	405078624	1.24	98.82	
0.5	1	161028840	0.49	98.21	98.70
	2	162623648	0.50	99.18	
	3	161867288	0.49	98.72	
0.05	1	16928424	0.05	103.24	103.15
	2	16945320	0.05	103.34	
	3	16869363	0.05	102.88	
			Mean Recovery	100.76	
			SD	1,74	
			%RSD	1,73	

Table B 6: Intraday precision data obtained Day 1: 18:00 pm

Concentration (µM)	Repeats	Fluorescence (Fluorescent arbitrary units)	Recovery		
			(µM)	(%)	Average (%)
5	1	1665092352	5.08	101.55	100.17
	2	1625161472	4.96	99.11	
	3	1637128576	4.99	99.84	
3.75	1	1263545088	3.85	102.74	103.56
	2	1278544768	3.90	103.96	
	3	1278544768	3.90	103.96	
2.5	1	823761152	2.51	100.48	100.03
	2	830981568	2.53	101.36	
	3	805644032	2.46	98.27	
1.25	1	425952864	1.30	103.91	101.30
	2	402681888	1.23	98.23	
	3	417131872	1.27	101.76	
0.5	1	164839696	0.50	100.53	99.64
	2	160582080	0.49	97.93	
	3	164718704	0.50	100.46	
0.05	1	16346328	0.05	99.69	99.93
	2	16474078	0.05	100.47	
	3	16334240	0.05	99.62	
			Mean Recovery	100.77	
			SD	1.88	
			%RSD	1.86	

B3 Limit of Detection (LOD) and Limit of Quantification (LOQ)

Table B 7 Data obtained from Rho123 concentrations pipetted in six fold to determine %RSD

Concentration (µM)	Repeats	Fluorescence (Fluorescent arbitrary units)	Recovery		
			(µM)	(%)	Average (%)
5	1	1407110044	4.94	98.70	100.83
	2	1409484331	4.94	98.87	
	3	1431152154	5.02	100.39	
	4	1475340340	5.17	103.49	
	5	1456409694	5.11	102.16	
	6	1445569050	5.07	101.40	
2.5	1	708441436	2.48	99.39	100.70
	2	714152299	2.50	100.19	
	3	722169882	2.53	101.31	
	4	718687924	2.52	100.82	
	5	709259934	2.49	99.50	
	6	734110490	2.57	102.99	
0.5	1	146124892	0.51	102.50	101.24
	2	141382075	0.50	99.17	
	3	148651466	0.52	104.27	
	4	143364865	0.50	100.56	
	5	142283709	0.50	99.80	
	6	144153000	0.51	101.12	
0.05	1	14626222	0.05	102.60	100.79
	2	14622395	0.05	102.57	
	3	14232358	0.05	99.83	
	4	13970522	0.05	98.00	
	5	14395710	0.05	100.98	
	6	14654983	0.05	102.80	
			Mean Recovery	100.98	
			SD	1.63	
			%RSD	1.62	

Table B 8: Rho123 standard range and the fluorescence of the background noise (Kreb's Ringer bicarbonate buffer) used to determine the LOD and LOQ

Concentration (µM)	Fluorescence (Fluorescent arbitrary units)	KRB Fluorescence (Fluorescent arbitrary units)
5	1407510936	269988
2.5	744470328	309011
0.5	164826668	271695
0.05	19217031.7	277154
0.005	2427760	259680
0.0005	6455331.67	295427
	SD	16675,28
	Slope	282379529,8
	LOD	0,000194874
	LOQ	0,000590527

ADDENDUM C : IN VITRO PERMEATION DATA OF RHODAMINE 123 ACROSS PORCINE JEJUNUM INTESTINAL TISSUE

Table C1: Apical to basolateral cumulative percentage transport of Rhodamine 123 across excised porcine jejunum tissue

Time (min)	Percentage transport: Chamber 1	Percentage transport: Chamber 2	Percentage transport: Chamber 3	Standard deviation (SD)	Mean percentage transport (%)
0	0,000	0,000	0,000	0,000	0,000
20	0,045	0,032	0,071	0,020	0,049
40	0,109	0,104	0,128	0,013	0,114
60	0,106	0,130	0,153	0,024	0,130
80	0,160	0,150	0,190	0,021	0,167
100	0,268	0,198	0,261	0,038	0,242
120	0,272	0,278	0,283	0,006	0,278
P_{app} ($x10^{-7}$)	2,197	2,031	2,162	0,088	

Table C2: Basolateral to apical cumulative percentage transport of Rhodamine 123 alone across excised porcine jejunum tissue

Time (min)	Percentage transport: Chamber 1	Percentage transport: Chamber 2	Percentage transport: Chamber 3	Standard deviation (SD)	Mean percentage transport (%)
0	0,000	0,000	0,000	0,000	0,000
20	0,239	0,202	0,129	0,056	0,190
40	0,631	0,452	0,377	0,131	0,487
60	0,685	0,541	0,460	0,114	0,562
80	0,777	0,625	0,685	0,077	0,696
100	0,829	0,615	0,668	0,111	0,704
120	0,854	0,647	0,661	0,116	0,721
P_{app} ($x10^{-7}$)	6,499	4,916	5,634	0.793	

Table C3: Apical to basolateral cumulative percentage transport of Rhodamine 123 in the presence of 0.1% (w/v) Brij® 58 across excised porcine jejunum tissue

Time (min)	Percentage transport: Chamber 1	Percentage transport: Chamber 2	Percentage transport: Chamber 3	Standard deviation (SD)	Mean percentage transport (%)
0	0.000	0.000	0.000	0.000	0.000
20	0.070	0.064	0.048	0.012	0.061
40	0.098	0.176	0.102	0.044	0.125
60	0.098	0.234	0.144	0.069	0.159
80	0.143	0.334	0.192	0.099	0.223
100	0.213	0.431	0.242	0.118	0.295
120	0.276	0.517	0.276	0.139	0.356
P_{app} ($x10^{-7}$)	1.937	4.085	2.184	1.175	

Table C4: Basolateral to apical cumulative percentage transport of Rhodamine 123 in the presence of 0.1% (w/v) Brij® 58 across excised porcine jejunum tissue

Time (min)	Percentage transport: Chamber 1	Percentage transport: Chamber 2	Percentage transport: Chamber 3	Standard deviation (SD)	Mean percentage transport (%)
0	0.000	0.000	0.000	0.000	0.000
20	0.417	0.295	0.248	0.087	0.320
40	0.625	0.415	0.360	0.140	0.466
60	0.752	0.476	0.427	0.175	0.551
80	0.767	0.545	0.486	0.148	0.599
100	0.854	0.590	0.627	0.143	0.690
120	0.874	0.693	0.637	0.124	0.735
P_{app} ($x10^{-7}$)	6.084	4.684	4.669	0.813	

Table C5: Apical to basolateral cumulative percentage transport of Rhodamine 123 in the presence of 0.5% (w/v) Brij® 58 across excised porcine jejunum tissue

Time (min)	Percentage transport: Chamber 1	Percentage transport: Chamber 2	Percentage transport: Chamber 3	Standard deviation (SD)	Mean percentage transport (%)
0	0.000	0.000	0.000	0.000	0.000
20	0.100	0.207	0.187	0.057	0.165
40	0.132	0.240	0.354	0.111	0.242
60	0.140	0.287	0.361	0.112	0.262
80	0.294	0.327	0.393	0.050	0.338
100	0.407	0.363	0.410	0.026	0.393
120	0.524	0.528	0.548	0.013	0.533
P_{app} ($x10^{-7}$)	3.923	3.315	3.556	0.306	

Table C6: Basolateral to apical cumulative percentage transport of Rhodamine 123 in the presence of 0.5% (w/v) Brij® 58 across excised porcine jejunum tissue

Time (min)	Percentage transport: Chamber 1	Percentage transport: Chamber 2	Percentage transport: Chamber 3	Standard deviation (SD)	Mean percentage transport (%)
0	0.000	0.000	0.000	0.000	0.000
20	0.137	0.105	0.121	0.016	0.121
40	0.176	0.207	0.192	0.015	0.192
60	0.263	0.261	0.267	0.009	0.267
80	0.407	0.375	0.391	0.016	0.391
100	0.447	0.378	0.415	0.035	0.415
120	0.478	0.450	0.455	0.021	0.455
P_{app} ($x10^{-7}$)	3.823	3.521	3.453	0.197	

Table C7: Apical to basolateral cumulative percentage transport of Rhodamine 123 in the presence of 1.0% (w/v) Brij® 58 across excised porcine jejunum tissue

Time (min)	Percentage transport: Chamber 1	Percentage transport: Chamber 2	Percentage transport: Chamber 3	Standard deviation (SD)	Mean percentage transport (%)
0	0.000	0.000	0.000	0.000	0.000
20	0.504	0.545	0.547	0.024	0.532
40	0.682	0.753	0.965	0.147	0.800
60	0.964	0.864	1.151	0.146	0.993
80	1.350	1.047	1.250	0.155	1.216
100	1.370	1.092	1.270	0.141	1.244
120	1.391	1.106	1.329	0.150	1.275
P_{app} ($x10^{-7}$)	10.990	7.867	9.560	1.563	

Table C8: Basolateral cumulative percentage transport of Rhodamine 123 in the presence of Brij® 58 across excised porcine jejunum tissue

Time (min)	Percentage transport: Chamber 1	Percentage transport: Chamber 2	Percentage transport: Chamber 3	Standard deviation (SD)	Mean percentage transport (%)
0	0.000	0.000	0.000	0.000	0.000
20	0.059	0.085	0.043	0.021	0.062
40	0.092	0.203	0.091	0.064	0.128
60	0.138	0.273	0.164	0.071	0.192
80	0.153	0.272	0.237	0.061	0.221
100	0.190	0.287	0.257	0.049	0.245
120	0.266	0.302	0.312	0.024	0.293
P_{app} ($x10^{-7}$)	1.877	2.306	2.522	0.328	

Table C9: Apical to basolateral cumulative percentage transport of Rhodamine 123 in the presence of 0.1% Cremophor® CO40 across excised porcine jejunum tissue

Time (min)	Percentage transport: Chamber 1	Percentage transport: Chamber 2	Percentage transport: Chamber 3	Standard deviation (SD)	Mean percentage transport (%)
0	0.000	0.000	0.000	0.000	0.000
20	0.157	0.078	0.063	0.050	0.099
40	0.193	0.194	0.094	0.058	0.161
60	0.276	0.279	0.158	0.069	0.237
80	0.302	0.314	0.185	0.071	0.267
100	0.358	0.373	0.228	0.080	0.319
120	0.408	0.383	0.330	0.040	0.374
P_{app} ($x10^{-7}$)	2.902	3.104	2.360	0.385	

Table C10: Basolateral to apical cumulative percentage transport of Rhodamine 123 in the presence of 0.1% Cremophor® CO40 across excised porcine jejunum tissue

Time (min)	Percentage transport: Chamber 1	Percentage transport: Chamber 2	Percentage transport: Chamber 3	Standard deviation (SD)	Mean percentage transport (%)
0	0.000	0.000	0.000	0.000	0.000
20	0.417	0.295	0.248	0.087	0.320
40	0.625	0.415	0.360	0.140	0.466
60	0.752	0.476	0.427	0.175	0.551
80	0.767	0.545	0.486	0.148	0.599
100	0.854	0.590	0.627	0.143	0.690
120	0.874	0.693	0.637	0.124	0.735
P_{app} ($x10^{-7}$)	2.673	2.851	3.393	0.375	

Table C11: Apical to basolateral cumulative percentage transport of Rhodamine 123 in the presence of 0.5% (w/v) Cremophor® CO40 across excised porcine jejunum tissue

Time (min)	Percentage transport: Chamber 1	Percentage transport: Chamber 2	Percentage transport: Chamber 3	Standard deviation (SD)	Mean percentage transport (%)
0	0.000	0.000	0.000	0.000	0.000
20	0.085	0.123	0.067	0.028	0.092
40	0.129	0.195	0.266	0.069	0.197
60	0.168	0.279	0.337	0.086	0.261
80	0.315	0.296	0.378	0.043	0.329
100	0.325	0.329	0.403	0.044	0.352
120	0.387	0.376	0.424	0.025	0.396
P_{app} ($x10^{-7}$)	3.052	2.743	3.438	0.348	

Table C12: Basolateral to apical cumulative percentage transport of Rhodamine 123 in the presence of 0.5% (w/v) Cremophor® CO40 across excised porcine jejunum tissue

Time (min)	Percentage transport: Chamber 1	Percentage transport: Chamber 2	Percentage transport: Chamber 3	Standard deviation (SD)	Mean percentage transport (%)
0	0.000	0.000	0.000	0.000	0.000
20	0.137	0.295	0.248	0.087	0.320
40	0.176	0.415	0.360	0.140	0.466
60	0.263	0.476	0.427	0.175	0.551
80	0.407	0.545	0.486	0.148	0.599
100	0.447	0.590	0.627	0.143	0.690
120	0.478	0.693	0.637	0.124	0.735
P_{app} ($x10^{-7}$)	2.612	2.491	2.197	0.213	

Table C13: Apical to basolateral cumulative percentage transport of Rhodamine 123 in the presence of 1.0% (w/v) Cremophor® CO40 across excised porcine jejunum tissue

Time (min)	Percentage transport: Chamber 1	Percentage transport: Chamber 2	Percentage transport: Chamber 3	Standard deviation (SD)	Mean percentage transport (%)
0	0.000	0.000	0.000	0.000	0.000
20	0.091	0.105	0.131	0.057	0.131
40	0.212	0.147	0.201	0.050	0.201
60	0.261	0.216	0.246	0.026	0.246
80	0.283	0.237	0.262	0.023	0.262
100	0.349	0.319	0.324	0.023	0.324
120	0.433	0.383	0.398	0.030	0.398
P_{app} ($x10^{-7}$)	2.902	3.104	2.360	0.385	

Table C14: Basolateral to apical cumulative percentage transport of Rhodamine 123 in the presence of 1.0% (w/v) Cremophor® CO40 across excised porcine jejunum tissue

Time (min)	Percentage transport: Chamber 1	Percentage transport: Chamber 2	Percentage transport: Chamber 3	Standard deviation (SD)	Mean percentage transport (%)
0	0.000	0.000	0.000	0.000	0.000
20	0.059	0.085	0.043	0.021	0.062
40	0.092	0.203	0.091	0.064	0.128
60	0.138	0.273	0.164	0.071	0.192
80	0.153	0.272	0.237	0.061	0.221
100	0.190	0.287	0.257	0.049	0.245
120	0.266	0.302	0.312	0.024	0.293
P_{app} ($x10^{-7}$)	2.673	2.851	3.393	0.375	

Table C15: Apical to basolateral cumulative percentage transport of Rhodamine 123 in the presence of 0.1% (w/v) Tween® 20 across excised porcine jejunum tissue

Time (min)	Percentage transport: Chamber 1	Percentage transport: Chamber 2	Percentage transport: Chamber 3	Standard deviation (SD)	Mean percentage transport (%)
0	0.000	0.000	0.000	0.000	0.000
20	0.098	0.091	0.110	0.009	0.100
40	0.129	0.134	0.138	0.005	0.134
60	0.141	0.137	0.152	0.008	0.143
80	0.145	0.142	0.162	0.011	0.150
100	0.149	0.152	0.180	0.017	0.160
120	0.164	0.173	0.199	0.018	0.179
P_{app} ($x10^{-7}$)	3.250	3.087	2.872	0.190	

Table C16: Basolateral to apical cumulative percentage transport of Rhodamine 123 in the presence of 0.1% (w/v) Tween® 20 across excised porcine jejunum tissue

Time (min)	Percentage transport: Chamber 1	Percentage transport: Chamber 2	Percentage transport: Chamber 3	Standard deviation (SD)	Mean percentage transport (%)
0	0.000	0.000	0.000	0.000	0.000
20	0.098	0.091	0.110	0.009	0.100
40	0.129	0.134	0.138	0.005	0.134
60	0.141	0.137	0.152	0.008	0.143
80	0.145	0.142	0.162	0.011	0.150
100	0.149	0.152	0.180	0.017	0.160
120	0.164	0.173	0.199	0.018	0.179
P_{app} ($x10^{-7}$)	1.019	1.086	1.268	0.129	

Table C17: Apical to basolateral cumulative percentage transport of Rhodamine 123 in the presence of 0.5% (w/v) Tween® 20 across excised porcine jejunum tissue

Time (min)	Percentage transport: Chamber 1	Percentage transport: Chamber 2	Percentage transport: Chamber 3	Standard deviation (SD)	Mean percentage transport (%)
0	0.000	0.000	0.000	0.000	0.000
20	0.157	0.125	0.141	0.016	0.141
40	0.217	0.221	0.253	0.019	0.230
60	0.277	0.249	0.299	0.025	0.275
80	0.284	0.270	0.338	0.036	0.297
100	0.304	0.323	0.398	0.050	0.342
120	0.319	0.362	0.403	0.042	0.361
P_{app} ($x10^{-7}$)	2.202	2.559	3.021	0.411	

Table C18: Basolateral to apical cumulative percentage transport of Rhodamine 123 in the presence of 0.5% (w/v) Tween® 20 across excised porcine jejunum tissue

Time (min)	Percentage transport: Chamber 1	Percentage transport: Chamber 2	Percentage transport: Chamber 3	Standard deviation (SD)	Mean percentage transport (%)
0	0.000	0.000	0.000	0.000	0.000
20	0.047	0.042	0.076	0.018	0.055
40	0.099	0.059	0.087	0.021	0.081
60	0.116	0.102	0.127	0.012	0.115
80	0.151	0.122	0.144	0.015	0.139
100	0.169	0.182	0.167	0.008	0.173
120	0.170	0.187	0.168	0.010	0.175
P_{app} ($x10^{-7}$)	1.349	1.514	1.247	0.135	

Table C19: Apical to basolateral cumulative percentage transport of Rhodamine 123 in the presence of 1.0% (w/v) Tween® 20 across excised porcine jejunum tissue

Time (min)	Percentage transport: Chamber 1	Percentage transport: Chamber 2	Percentage transport: Chamber 3	Standard deviation (SD)	Mean percentage transport (%)
0	0.000	0.000	0.000	0.000	0.000
20	0.133	0.138	0.138	0.003	0.124
40	0.220	0.196	0.196	0.014	0.184
60	0.237	0.197	0.197	0.023	0.210
80	0.239	0.204	0.204	0.021	0.216
100	0.244	0.207	0.207	0.021	0.220
120	0.263	0.235	0.235	0.016	0.256
P_{app} ($x10^{-7}$)	1.718	1.718	1.718	0.206	

Table C20: Basolateral to apical cumulative percentage transport of Rhodamine 123 in the presence of 1.0% (w/v) Tween® 20 across excised porcine jejunum tissue

Time (min)	Percentage transport: Chamber 1	Percentage transport: Chamber 2	Percentage transport: Chamber 3	Standard deviation (SD)	Mean percentage transport (%)
0	0.000	0.000	0.000	0.000	0.000
20	0.508	0.402	0.320	0.094	0.410
40	0.595	0.526	0.378	0.111	0.499
60	0.625	0.584	0.424	0.106	0.544
80	0.627	0.610	0.470	0.086	0.569
100	0.641	0.622	0.501	0.076	0.588
120	0.653	0.647	0.536	0.066	0.612
P_{app} ($x10^{-7}$)	3.775	4.124	3.446	0.339	

Table C21: Apical to basolateral cumulative percentage transport of Rhodamine 123 in the presence of 0.1% (w/v) Span® 20 across excised porcine jejunum tissue

Time (min)	Percentage transport: Chamber 1	Percentage transport: Chamber 2	Percentage transport: Chamber 3	Standard deviation (SD)	Mean percentage transport (%)
0	0.000	0.000	0.000	0.000	0.000
20	0.067	0.007	0.019	0.032	0.031
40	0.115	0.060	0.030	0.043	0.069
60	0.205	0.085	0.120	0.061	0.137
80	0.218	0.094	0.147	0.062	0.153
100	0.245	0.161	0.202	0.042	0.202
120	0.247	0.256	0.234	0.011	0.246
P_{app} ($x10^{-7}$)	2.005	1.854	1.981	0.081	

Table C22: Basolateral to apical cumulative percentage transport of Rhodamine 123 in the presence of 0.1% (w/v) Span® 20 across excised porcine jejunum tissue

Time (min)	Percentage transport: Chamber 1	Percentage transport: Chamber 2	Percentage transport: Chamber 3	Standard deviation (SD)	Mean percentage transport (%)
0	0.000	0.000	0.000	0.000	0.000
20	0.123	0.096	0.080	0.022	0.100
40	0.186	0.141	0.134	0.028	0.154
60	0.246	0.196	0.173	0.037	0.205
80	0.289	0.218	0.241	0.037	0.249
100	0.335	0.269	0.352	0.044	0.319
120	0.345	0.349	0.366	0.011	0.353
P_{app} ($x10^{-7}$)	2.612	2.460	2.923	0.236	

Table C23: Apical to basolateral cumulative percentage transport of Rhodamine 123 in the presence of 0.5% (w/v) Span® 20 across excised porcine jejunum tissue

Time (min)	Percentage transport:	Percentage transport:	Percentage transport:	Standard deviation	Mean percentage transport (%)
0	0.000	0.000	0.000	0.000	0.000
20	0.075	0.044	0.040	0.019	0.053
40	0.111	0.105	0.111	0.003	0.109
60	0.124	0.107	0.124	0.010	0.118
80	0.134	0.120	0.174	0.028	0.143
100	0.231	0.227	0.236	0.005	0.231
120	0.265	0.280	0.282	0.009	0.276
P_{app} ($x10^{-7}$)	1.890	2.042	2.177	0.144	

Table C24: Basolateral to apical cumulative percentage transport of Rhodamine 123 in the presence of 0.5% (w/v) Span® 20 across excised porcine jejunum tissue

Time (min)	Percentage transport: Chamber 1	Percentage transport: Chamber 2	Percentage transport: Chamber 3	Standard deviation (SD)	Mean percentage transport (%)
0	0.000	0.000	0.000	0.000	0.000
20	0.116	0.096	0.096	0.012	0.103
40	0.179	0.147	0.139	0.021	0.155
60	0.234	0.155	0.190	0.040	0.193
80	0.267	0.159	0.210	0.054	0.212
100	0.314	0.220	0.258	0.047	0.264
120	0.320	0.308	0.333	0.013	0.320
P_{app} ($x10^{-7}$)	2.414	1.975	2.331	0.233	

Table C25: Apical to basolateral cumulative percentage transport of Rhodamine 123 in the presence of 1.0% (w/v) Span® 20 across excised porcine jejunum tissue

Time (min)	Percentage transport: Chamber 1	Percentage transport: Chamber 2	Percentage transport: Chamber 3	Standard deviation (SD)	Mean percentage transport (%)
0	0.000	0.000	0.000	0.000	0.000
20	0.092	0.084	0.124	0.019	0.053
40	0.125	0.115	0.138	0.003	0.109
60	0.144	0.170	0.140	0.010	0.118
80	0.159	0.200	0.166	0.028	0.143
100	0.189	0.207	0.200	0.005	0.231
120	0.198	0.209	0.209	0.009	0.276
P_{app} ($x10^{-7}$)	1.376	1.602	1.348	1.319	

Table C26: Basolateral to apical cumulative percentage transport of Rhodamine 123 in the presence of 1.0% (w/v) Span® 20 across excised porcine jejunum tissue

Time (min)	Percentage transport: Chamber 1	Percentage transport: Chamber 2	Percentage transport: Chamber 3	Standard deviation (SD)	Mean percentage transport (%)
0	0.000	0.000	0.000	0.000	0.000
20	0.080	0.043	0.043	0.021	0.056
40	0.091	0.053	0.053	0.022	0.066
60	0.105	0.069	0.069	0.020	0.081
80	0.140	0.081	0.111	0.030	0.111
100	0.159	0.163	0.133	0.016	0.152
120	0.265	0.260	0.244	0.011	0.256
P_{app} ($x10^{-7}$)	1.678	1.748	1.620	0.064	

Table C27: Apical to basolateral cumulative percentage transport of Rhodamine 123 in the presence of 0.1% (w/v) Sodium deoxycholate (NaDC) across excised porcine jejunum tissue

Time (min)	Percentage transport: Chamber 1	Percentage transport: Chamber 2	Percentage transport: Chamber 3	Standard deviation (SD)	Mean percentage transport (%)
0	0.000	0.000	0.000	0.000	0.000
20	0.004	0.006	0.018	0.007	0.009
40	0.047	0.042	0.051	0.004	0.047
60	0.075	0.069	0.084	0.008	0.076
80	0.124	0.116	0.111	0.006	0.117
100	0.205	0.210	0.203	0.003	0.206
120	0.261	0.262	0.272	0.006	0.265
P_{app} ($x10^{-7}$)	2.113	2.121	2.085	0.019	

Table C28: Basolateral to apical cumulative percentage transport of Rhodamine 123 in the presence of 0.1% (w/v) Sodium deoxycholate across excised porcine jejunum tissue

Time (min)	Percentage transport: Chamber 1	Percentage transport: Chamber 2	Percentage transport: Chamber 3	Standard deviation (SD)	Mean percentage transport (%)
0	0.000	0.000	0.000	0.000	0.000
20	0.028	0.041	0.036	0.007	0.060
40	0.090	0.109	0.108	0.011	0.109
60	0.128	0.176	0.137	0.026	0.153
80	0.152	0.203	0.202	0.029	0.192
100	0.208	0.259	0.272	0.034	0.272
120	0.266	0.309	0.277	0.022	0.318
P_{app} ($x10^{-7}$)	2.042	2.435	2.338	0.019	

Table C29: Apical to basolateral cumulative percentage transport of Rhodamine 123 in the presence of 0.5% (w/v) NaDC across excised porcine jejunum tissue

Time (min)	Percentage transport: Chamber 1	Percentage transport: Chamber 2	Percentage transport: Chamber 3	Standard deviation (SD)	Mean percentage transport (%)
0	0.000	0.000	0.000	0.000	0.000
20	0.180	0.176	0.191	0.008	0.183
40	0.303	0.188	0.315	0.070	0.269
60	0.319	0.250	0.355	0.053	0.308
80	0.385	0.375	0.408	0.017	0.390
100	0.425	0.431	0.444	0.009	0.433
120	0.456	0.451	0.491	0.022	0.466
P_{app} ($x10^{-7}$)	3.246	3.424	3.461	0.115	

Table C30: Basolateral to apical cumulative percentage transport of Rhodamine 123 in the presence of 0.5% (w/v) NaDC across excised porcine jejunum tissue

Time (min)	Percentage transport: Chamber 1	Percentage transport: Chamber 2	Percentage transport: Chamber 3	Standard deviation (SD)	Mean percentage transport (%)
0	0.000	0.000	0.000	0.000	0.000
20	0.064	0.055	0.060	0.004	11.502
40	0.111	0.082	0.109	0.016	23.026
60	0.112	0.111	0.154	0.024	34.559
80	0.139	0.136	0.193	0.032	46.078
100	0.221	0.202	0.270	0.035	57.575
120	0.243	0.215	0.278	0.032	69.091
P_{app} ($x10^{-7}$)	2.240	2.645	2.426	0.203	

Table C31: Apical to basolateral cumulative percentage transport of Rhodamine 123 in the presence of 1.0% (w/v) NaDC across excised porcine jejunum tissue

Time (min)	Percentage transport: Chamber 1	Percentage transport: Chamber 2	Percentage transport: Chamber 3	Standard deviation (SD)	Mean percentage transport (%)
0	0.000	0.000	0.000	0.000	0.000
20	0.269	0.290	0.228	0.031	0.262
40	0.339	0.311	0.267	0.036	0.305
60	0.506	0.336	0.297	0.111	0.380
80	0.541	0.472	0.455	0.045	0.489
100	0.593	0.529	0.589	0.036	0.570
120	0.646	0.668	0.722	0.039	0.679
P_{app} ($x10^{-7}$)	4.663	4.420	5.142	0.367	

Table C32: Basolateral to apical cumulative percentage transport of Rhodamine 123 in the presence of 1.0% (w/v) NaDC alone across excised porcine jejunum tissue

Time (min)	Percentage transport: Chamber 1	Percentage transport: Chamber 2	Percentage transport: Chamber 3	Standard deviation (SD)	Mean percentage transport (%)
0	0.000	0.000	0.000	0.000	0.000
20	0.079	0.078	0.056	0.013	0.071
40	0.125	0.111	0.136	0.012	0.124
60	0.154	0.130	0.153	0.014	0.146
80	0.203	0.179	0.185	0.012	0.189
100	0.266	0.287	0.286	0.011	0.279
120	0.296	0.366	0.314	0.036	0.325
P_{app} ($x10^{-7}$)	2.240	2.645	2.426	0.203	

ADDENDUM D: TRANS-EPITHELIAL ELECTRICAL RESISTANCE MEASUREMENTS

Table D1: Apical to basolateral TEER measurements across excised porcine intestinal tissue in the presence of Rho123 alone

	Rho123	
	0 min	**120min**
Cell 1	55	38
Cell 2	67	42
Cell 3	58	39
Mean	60.00	39.67
TEER reduct.	33.88	

Table D2: Basolateral to apical TEER measurements across excised porcine intestinal tissue in the presence of Rho123 alone

	Rho123	
	0 min	**120min**
Cell 1	42	28
Cell 2	38	26
Cell 3	52	34
Mean	44.00	29.33
TEER reduct.	33.34	

Table D3: Apical to basolateral TEER measurements across excised porcine intestinal tissue in the presence of 0.1%, 0.5% and 1.0% (w/v) Brij® 58

	Brij®58 0,1%		**Brij®58 0,5%**		**Brij®58 1%**	
	0 min	**120min**	**0 min**	**120 min**	**0 min**	**120 min**
Cell 1	43	22	75	42	33	28
Cell 2	41	28	67	24	37	30
Cell 3	42	29	89	30	34	22
Mean	42,00	26,33	77,00	32,00	34,67	26,67
TEER reduct.	38,10		58,44		22,86	

Table D4: Basolateral to apical TEER measurements across excised porcine intestinal tissue in the presence of 0.1%, 0.5% and 1.0% (w/v) Brij® 58.

	Brij®58 0,1%		**Brij®58 0,5%**		**Brij®58 1%**	
	0 min	**120min**	**0 min**	**120 min**	**0 min**	**120 min**
Cell 1	56	40	50	29	56	29
Cell 2	48	33	49	28	51	31
Cell 3	58	32	40	30	54	38
Mean	54,00	35,00	46,33	29,00	53,67	32,67
TEER reduct.	35,19		37,41		39,13	

Table D5: Apical to basolateral TEER measurements across excised porcine intestinal tissue in the presence of 0.1%, 0.5% and 1.0% (w/v) Cremophor® CO40

	CRM CO40 0,1%		**CRM CO40 0,5%**		**CRM CO40 1%**	
	0 min	**120min**	**0 min**	**120 min**	**0 min**	**120 min**
Cell 1	53	28	47	29	53	21
Cell 2	66	36	46	28	58	30
Cell 3	67	32	45	30	54	28
Mean	62,00	32,00	46,00	29,00	55,00	26,33
TEER reduct.	48,39		36,96		52,12	

Table D6: Basolateral to apical TEER measurements across excised porcine intestinal tissue in the presence of 0.1%, 0.5% and 1.0% (w/v) Cremophor® CO40.

	CRM CO40 0,1%		**CRM CO40 0,5%**		**CRM CO40 1%**	
	0 min	**120min**	**0 min**	**120 min**	**0 min**	**120 min**
Cell 1	60	42	67	30	53	32
Cell 2	55	35	62	26	67	34
Cell 3	51	46	65	28	62	26
Mean	55,33	41,00	64,67	28,00	60,67	30,67
TEER reduct.	25,90		56,70		49,45	

Table D7: Apical to basolateral TEER measurements across excised porcine intestinal tissue in the presence of 0.1%, 0.5% and 1.0% (w/v) Tween® 20

	Tween®20 0,1%		Tween®20 0,5%		Tween®20 1%	
	0 min	**120min**	**0 min**	**120 min**	**0 min**	**120 min**
Cell 1	38	26	60	32	59	30
Cell 2	44	22	52	30	54	27
Cell 3	42	25	49	22	60	33
Mean	41,33	24,33	53,67	28,00	57,67	30,00
TEER reduct.	41,13		47,83		47,98	

Table D8: Basolateral to apical TEER measurements across excised porcine intestinal tissue in the presence of 0.1%, 0.5% and 1.0% (w/v) Tween® 20.

	Tween®20 0,1%		Tween®20 0,5%		Tween®20 1%	
	0 min	**120min**	**0 min**	**120 min**	**0 min**	**120 min**
Cell 1	71	39	58	22	65	30
Cell 2	68	32	54	23	48	21
Cell 3	59	27	53	26	49	24
Mean	66,00	32,67	55,00	23,67	54,00	25,00
TEER reduct.	50,51		56,97		53,70	

Table D9: Apical to basolateral TEER measurements across excised porcine intestinal tissue in the presence of 0.1%, 0.5% and 1.0% (w/v) Span® 20

	Span®20 0,1%		Span®20 0,5%		Span®20 1%	
	0 min	**120min**	**0 min**	**120 min**	**0 min**	**120 min**
Cell 1	61	26	45	23	63	31
Cell 2	58	31	52	34	63	27
Cell 3	56	28	56	27	53	28
Mean	58,33	28,33	51,00	28,00	59,67	28,67
TEER reduct.	51,43		45,10		51,96	

Table D10: Basolateral to apical TEER measurements across excised porcine intestinal tissue in the presence of 0.1%, 0.5% and 1.0% (w/v) Span® 20.

	Span®20 0,1%		Span®20 0,5%		Span®20 1%	
	0 min	**120min**	**0 min**	**120 min**	**0 min**	**120 min**
Cell 1	48	30	56	27	60	22
Cell 2	56	27	49	30	58	26
Cell 3	52	33	52	34	51	23
Mean	52,00	30,00	52,33	30,33	56,33	23,67
TEER reduct.	42,31		42,04		57,99	

Table D11: Apical to basolateral TEER measurements across excised porcine intestinal tissue in the presence of 0.1%, 0.5% and 1.0% (w/v) sodium deoxycholate

	NaDC®20 0,1%		NaDC®20 0,5%		NaDC®20 1%	
	0 min	**120min**	**0 min**	**120 min**	**0 min**	**120 min**
Cell 1	52	26	39	29	45	27
Cell 2	50	27	43	22	49	31
Cell 3	53	24	44	24	48	32
Mean	51,67	25,67	42,00	25,00	47,33	30,00
TEER reduct.	50,32		40,48		36,62	

Table D12: Basolateral to apical TEER measurements across excised porcine intestinal tissue in the presence of 0.1%, 0.5% and 1.0% (w/v) Sodium deoxycholate

	NaDC®20 0,1%		NaDC®20 0,5%		NaDC®20 1%	
	0 min	**120min**	**0 min**	**120 min**	**0 min**	**120 min**
Cell 1	45	29	43	26	52	26
Cell 2	38	33	46	31	50	27
Cell 3	45	27	39	32	52	32
Mean	42,67	29,67	42,67	29,67	51,33	28,33
TEER reduct.	30,47		30,47		44,81	